Optimizing Mobile Application Performance through Network Infrastructure Aware Adaptation

by

Qiang Xu

A dissertation submitted in partial fulfillment
of the requirements for the degree of
Doctor of Philosophy
(Computer Science and Engineering)
in the University of Michigan
2013

To my family.

ACKNOWLEDGEMENTS

I would like to appreciate many people who helped me during this time. Without them, it would be impossible for me to complete the dissertation.

First, I would like to thank my advisor Prof. Z. Morley Mao, who has broad interests in networking systems, routing protocols, mobile and distributed systems, and network security. Working with her, I not only have learned how to develop professional research skills in mobile networking but also have deepened my research interests in other system areas. It is my great pleasure to work with Morley in past 4.5 years. I appreciate Prof. Jason Flinn, Prof. Robert Dick, and Dr. Feng Qian for serving on my thesis committee. They have provided valuable comments and suggestions for refining my dissertation.

I would also like to thank my mentors: Alexandre Gerber, Jeffrey Pang, Sanjeev Mehrotra, Jin Li, Yong Liao, and Stanislav Miskovic, along with other researchers in these collaborations: Ming Zhang, Paramvir Bahl, Yi-Min Wang, Jeffrey Erman, Shobha Venkataraman, Mario Baldi, and Antonio Nucci. They have shared their great knowledge and experience to help me shape research problems and address challenges.

My life in Michigan has been wonderful because of many colleagues and friends. I would like to thank Ying Zhang, Xu Chen, Feng Qian, Zhiyun Qian, Yudong Gao, Junxian Huang, Birjodh Tiwana, Ni Pan, Zhaoguang Wang, Mark Gordon, Sanae Rosen, Thomas Andrews, Yihua Guo, Mehrdad Moradi, Haokun Luo, Qi Chen, Yuanyuan Zhou, Ashkan Nikravesh, Yunjing Xu, Timur Alperovich, Lujun Fang, Li Qian, and Jie Yu. There is a special thank you to my roommate Wen Chen for the encouragement during tough days.

Finally, the help from my wife, Jinhua Quan, is tremendous. She is always a source of love and encouragement. I have been very fortunate to have so many wonderful people around since I was born. I dedicated this dissertation to all of them.

TABLE OF CONTENTS

LIST OF FIGURES

LIST OF TABLES

ABSTRACT

Optimizing Mobile Application Performance through Network Infrastructure Aware Adaptation

by

Qiang Xu

Chair: Z. Morley Mao

Encouraged by the fast adoption of mobile devices and the widespread deployment of mobile networks, mobile applications are becoming the preferred “gateways” connecting users to networking services. Although the CPU capability of mobile devices is approaching that of off-the-shelf PCs, the performance of mobile networking applications is still far behind. One of the fundamental reasons is that most mobile applications are unaware of the mobile network specific characteristics, leading to inefficient network and device resource utilization. Thus, in order to improve the user experience for most mobile applications, it is essential to dive into the critical network components along network connections including mobile networks, smartphone platforms, mobile applications, and content partners. We aim to optimize the performance of mobile network applications through network-aware resource adaptation approaches. Our techniques consist of the following four aspects: (i) revealing the fundamental infrastructure characteristics of cellular networks that are distinctive from wireline networks; (ii) isolating the impact of important factors on user perceived performance in mobile network applications;

(iii) determining the particular usage patterns of mobile applications; and (iv) improving the performance of mobile applications through network aware adaptations.

CHAPTER I

INTRODUCTION

Due to the emergence of smartphones and the ubiquitous wireless network deployment, smartphone user experience has been significantly enriched in recent years. However, the performance of mobile network applications is still far behind our expectation despite the rapid increase in the computational capabilities with more powerful processors and multi-core designs for mobile platforms. One of the fundamental reasons is that many mobile applications are unaware of or do not fully understand the mobile network specific characteristics, leading to inefficient resource utilization, which often results in performance bottlenecks eventually. **In order to effectively adapt mobile networking applications to cellular network conditions, in this thesis, we investigate the unique cellular network characteristics that are fundamentally different from the wireline Internet's, determine the impact of such characteristics on application performance, and eventually leverage such knowledge to optimize mobile application designs.**

To achieve the goal, it is essential to dive into all the critical network components along end-to-end network connections including the content partner, the mobile network, the smartphone platform, the application implementation, and the usage pattern. First, the current routing of cellular network traffic is quite restricted, as it must traverse a rather limited number (e.g., 4–6) of infrastructure gateways, which is in sharp contrast to wireline Internet traffic. Such centralized infrastructure directly affects the network performance and application design. Second, the on-device networking performance is highly variable, affected by a multitude of factors including channel quality, radio resource allocation, cellular network infrastructure, etc. Therefore, decomposing the impact of individual network components is an essential step towards improving the performance of smartphone applications from the perspectives of users, developers, network operators, and smartphone vendors. Third, unlike desktop applications assuming network resource always desirable, mobile applications have to apply performance adaptation techniques to accommodate performance variation. As cellular networks have very unique characteristics in performance and infrastructure, these techniques have to be aware of such factors. Fourth, as applications are known to be diverse, before we can invent sophisticated performance optimization techniques, a prerequisite is the knowledge of application behaviors and usage patterns.

Accordingly, our techniques consist of the following four thrusts as shown in Figure 1.1: (i) revealing the fundamental infrastructure characteristics of cellular networks that are distinctive from wireline networks; (ii) identifying the important factors that affect the user perceived performance of mobile network applications; (iii) determining the particular usage patterns of mobile applications; and (iv) developing performance adaptation techniques to optimize the performance of mobile applications accordingly. We will introduce each of the four thrusts respectively in the following.

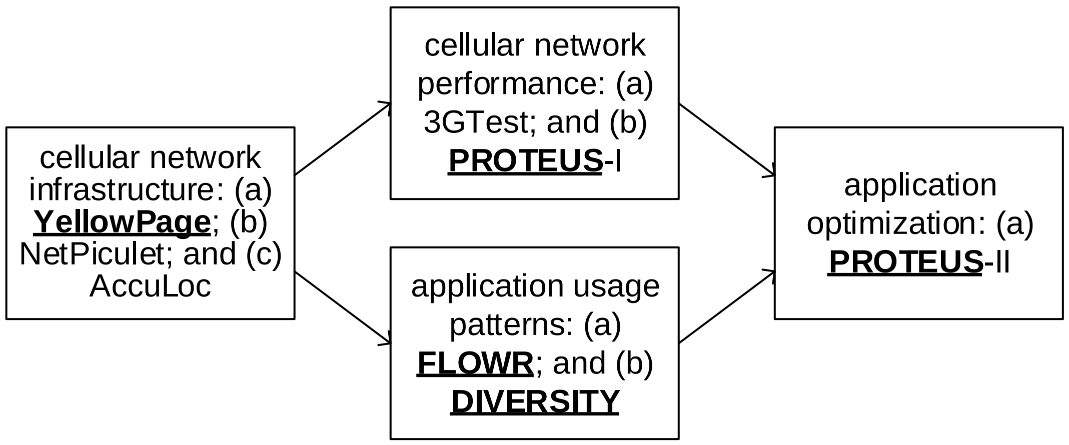

cellular network infrastructure: (a) **YellowPage**; (b) NetPiculet; and (c) AccuLoc
cellular network performance: (a) 3GTest; and (b) **PROTEUS**-I
application usage patterns: (a) **FLOWR**; and (b) **DIVERSITY**
application optimization: (a) **PROTEUS**-II

Figure 1.1: Task breakdown. YellowPage [120], NetPiculet [110, 91], AccuLoc [119], MobiPerf [62], PROTEUS [121], FLOWR [118], and DIVERSITY [122] are the projects inside the four major thrusts. PROTEUS -I and PROTEUS -II are two phases of PROTEUS.

1.1 Revealing Fundamental Cellular Characteristics

Cellular data networks have not been explored much by the research community to explain the dynamics of cellular IP addresses despite the growing popularity of their usage. Some infrastructure characteristics of cellular networks are distinct from the Internet counterpart, such as network topology, routing design, address allocation, middlebox behavior, and DNS resolution. Understanding the impact of cellular network infrastructure is one of the first steps in identifying the bottlenecks inside cellular networks. We performed the first comprehensive analysis to characterize the cellular data network infrastructure in 2010 [120], i.e., YellowPage, explored the challenge faced by cellular network operators of localizing performance measurements in the hierarchical infrastructure of cellular networks in 2011 [119], i.e., AccuLoc, implemented the first tool that unveils cellular NAT and firewall policies in 2011 and 2012 [110, 91], i.e., NetPiculet.

In YellowPage, we concluded among other previously little known results that the current routing of cellular data traffic is quite restricted, as it must traverse a rather limited number (e.g., 4–6) of infrastructure gateways, which is in sharp contrast to wireline Internet traffic. Such a significant difference could demand new provisioning support for mobile applications.

In NetPiculet, we designed and implemented a measurement tool for accurately and efficiently identifying middlebox policies in cellular networks. We released NetPiculet in January 2011 and collected enough measurements for 107 cellular network operators over the world. In the long run, NetPiculet is highly valuable to provide visibility into opaque cellular network policies and expose their impact as networks and applications continue to evolve.

In AccuLoc, we developed a system for network operators to localize performance measurements to lower aggregation levels such as cell sectors, cell sites, and RNCs. Applying AccuLoc in performance anomaly detection, we achieved both the lowest false positive and negative compared with the solutions based on other forms of clustering. We believe that our work can be an important utility for cellular operators for the purpose of performance monitoring, network maintenance, and anomaly detection.

1.2 Decomposing the Impact of Cellular Characteristics

Unlike the traditional network applications running on PCs, whose performance is mostly constrained by the wired network, network application performance on smartphones with limited physical resources also heavily depends on factors including the hardware and the software on the phone as well as the quality and load of wireless link. Isolating the impact on smartphone application performance due to each of such factors is important for cellular network operators, smartphone vendors, and application developers to optimize applications for better user perceived experiences.

In 2009 and 2010, we developed a systematic methodology for comparing this performance along several key dimensions such as carrier networks, device capabilities, and server configurations. To ensure a fair and representative comparison, we implemented MobiPerf (a.k.a. 3GTest), a cross-platform measurement tool installed by more than 300K users from all over the world. Running MobiPerf, a user can have the knowledge of his smartphone's networking properties, such as field test results, UDP and TCP benchmark performance, HTTP benchmark performance, and much more. Our analysis based on MobiPerf's measurements provides insights into how network operators and smartphone vendors can improve 3G or cellular networks and mobile devices, and how content providers can optimize for mobile devices.

1.3 Identifying the Usage Patterns of Mobile Applications

The rapid adoption of mobile devices is dramatically changing the access to various networking services, i.e., rather than browsers, mobile applications are becoming the preferred "gateways" connecting users to the Internet. Despite the increasing importance of applications as gateways to network services, we have a much limited understanding of how, where, and when they are used compared to traditional web services, particularly at scale.

Identifying application usage patterns at scale is not straightforward because applications are indistinguishable as they are communicating predominantly over HTTP. In 2012, we developed FLOWR (i.e., Flow Recognition System) that identifies the applications originating the real-time network flows in mobile networks without supervised learning effort [118].

The goal of FLOWR is to identify mobile network applications. In 2011, we undertook a first step in identifying the usage patterns of smartphone network applications [122], i.e., DIVERSITY. We studied smartphone network applications from the angle of their spatial and temporal prevalence, locality, and correlation. We believe that our findings on the diverse usage patterns of smartphone applications in spatial, temporal, user, device dimensions will motivate future work in the mobile community.

1.4 Optimizing Applications via Network-Aware Adaptation

The rapid adoption of mobile devices is resulting in the migration of real-time communication (RTC) applications from desktop machines to mobile devices. To adapt and deliver good performance, RTC applications require accurate estimations of short-term network performance metrics, e.g., loss rate, one-way delay, and throughput. However, the wide variation in mobile cellular network performance makes them running on these networks problematic. To address this issue, various performance adaptation techniques have been proposed, but one common problem of such techniques is that they only adjust application behavior reactively after performance degradation is visible. Thus, proactive adaptation based on accurate short-term, fine-grained network performance prediction can be a preferred alternative that benefits RTC applications. Since 2011, we have started to investigate the predictability of cellular network performance [121]. We observed that forecasting the short-term performance in cellular networks is possible in part due to the channel estimation scheme on the device and the radio resource scheduling algorithm at the base station. Thus, we developed a system interface called PROTEUS, which passively collects current network performance, such as throughput, loss, and one-way delay, and then uses regression trees to forecast future network performance. We demonstrated how PROTEUS can be integrated with RTC applications to significantly improve the perceptual quality.

1.5 Thesis Organization

To summarize, this is my thesis that: **we (i) reveal the unique characteristics of cellular networks in terms of network infrastructure, network management, and resource allocation; (ii) evaluate the impact of such unique characteristics on mobile application performance, and (iii) develop performance adaptation techniques accordingly to improve mobile application performance.**

This dissertation is structured as follows. In §II, we provide sufficient background of cellular network infrastructure. §III introduces our work YellowPage identifying the routing restriction issue in cellular networks. §IV proposes FLOWR for network operators to classifying mobile traffic into applications and characterizes the usage patterns of mobile networking applications. §V describes the proposal of PROTEUS to adapt mobile applications to cellular networks. The previous related studies are summarized in §VI. §VII concludes the dissertation.

CHAPTER II

BACKGROUND

In this chapter, we introduce the necessary background knowledge of cellular networks emphasizing on the fundamental cellular network infrastructure, network management, and resource allocation.

2.1 Cellular Network Hierarchy

Despite the differences among cellular technologies, a cellular data network is usually divided into two parts, the radio access network (RAN) and the core network. The RAN contains the infrastructure differences supporting 2G technologies (e.g., GPRS, EDGE, 1xRTT, etc.), 3G technologies (e.g., UMTS, EV-DO, HSPA, etc.), and 4G ones (e.g., WiMAX, LTE, etc.), but the structure of the core network does not differ across 2G, 3G, and 4G technologies.

Figure 2.1 illustrates the internal of a typical cellular network taking a UMTS network as an example. The RAN architecture, which allows the connectivity between user handsets and the core network, consists of the base station and the radio network controller (RNC). Across various cellular technologies, the exact names of base stations and RNCs differ, e.g., the base station is named as the base transceiver station (BTS) in GPRS, EDGE, 1xRTT, and EV-DO networks, and Node B in UMTS and HSPA networks, as shown in Table 2.1, but their

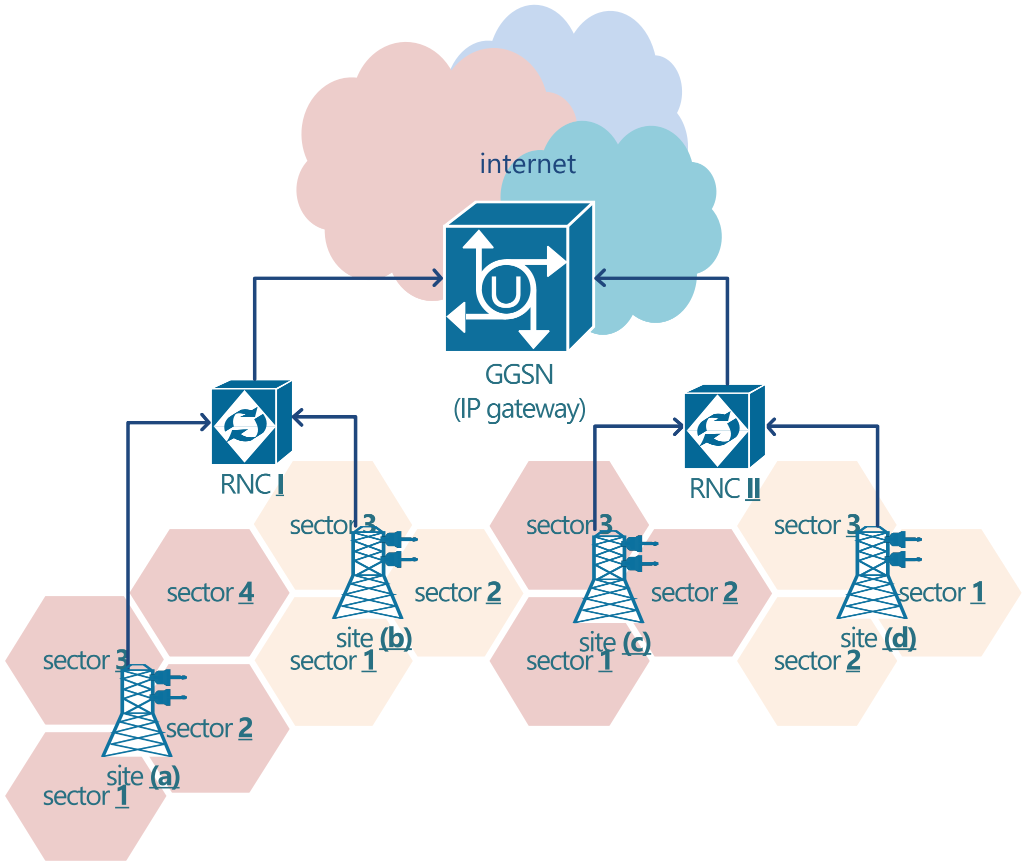

Figure 2.1: Cellular network infrastructure, applicable to 2G, 3G, and 4G networks. The terminology variation is included in Table 2.1.

functionalities are roughly the same. In WiMAX and LTE networks, there is no more intermediate controlling node as BSC or RNC. This infrastructure change has the advantage of a simpler network architecture and allows better performance because end-to-end path between the mobile device and the Internet is shortened.

The core network, which is shared by 2G, 3G, and 4G RANs, is comprised of the IP gateway connecting the RAN and the Internet. In GPRS, EDGE, UMTS, and HSPA networks, to start a data session, a user first communicates with its local SGSN that delivers its traffic to a GGSN. The SGSN requests the DNS server for the GGSN via the user's access point name (APN). Once the GGSN is determined, the communication between the SGSN and the GGSN is tunneled, so the GGSN is

	2G		3G		4G	
	GPRS,EDGE	1xRTT	UMTS,HSPA	EV-DO	WiMAX	LTE
cell site (base station)	BTS	BTS	Node B	BTS	BS	eNodeB
RNC	BSC	BSC	RNC	BSC		
GSN	SGSN,GGSN	PDSN	SGSN,GGSN	PDSN	ASN-GW	SGW,PGW

Table 2.1: Terminology of network elements in various cellular technologies.

the first outbound IP hop and is followed by multiple hops such as NATs and firewalls within the core network. Serving as the IP gateway for the connected cellular device, the GGSN is responsible for IP address assignment, IP pool management, address mapping, QoS, authentication, etc. [21], An 1xRTT or EV-DO network has a very similar architecture except that the Packet Data Serving Node (PDSN) serves as a combination of the SGSN and the GGSN. Similarly in WiMAX networks, an access service network gateway (ASN-GW) combines the functions of the SGSN and the GGSN. In LTE network, a serving gateway (SGW) acts as the mobility anchor for the handovers across eNodeBs as well as routing and forwarding data plane traffic, and the packet data network gateway (PGW) behaves as the first outbound IP hop.

2.2 Cellular Network Mobility Management

As depicted in Figure 2.1, a cellular network is hierarchical. At the root of the network is the GGSN. In practice, there are multiple GGSNs, but they are located in only a handful of locations (to introduce in §III). At the leaves are mobile devices, which are connected to the cellular network in a particular cell sector. Each base station has multiple cell sectors, one for each antenna attached to its cell tower. Typically these point in different directions and/or operate on different frequencies. Base stations send their data traffic to RNCs, which forward traffic to SGSNs, which, in turn, send the traffic to GGSNs. The GGSN sends and receives traffic from the Internet.

An important characteristic of cellular networks is that IP traffic sent by mobile devices is tunneled to the GGSN using lower layer 3GPP tunneling protocols. As a consequence, none of the intermediate nodes in the cellular network can directly inspect the sent IP packets and a mobile device's IP address is "anchored" to the GGSN, regardless of where it moves in the network. This characteristic ensures that the mobile device can maintain its IP address (and thus, its IP connections) even as it is mobile.

The tunnel between the SGSN and the GGSN is called the PDP Context, and it uses the GPRS Tunneling Protocol (GTP) (GTP-U to carry data traffic and GTP-C for signaling control messages. When a mobile device first connects to the UMTS network, the PDP Context that carries its IP traffic is set up. At this point, the originating cell sector and RNC is reported to the GGSN via GTP-C protocol. When a mobile device moves to a different sector, the path that its data takes through the cellular network changes.[1] RNCs manage the operation of handovers when a mobile device moves from one sector to another (e.g., by coordinating base stations and other RNCs). However, to avoid unnecessary signaling overhead, the change of cell sectors is not reported to the higher in the hierarchy. Thus, the GGSN is not informed that a mobile device has moved unless the SGSN in its network path changes. This can occur for two reasons: (i) it moves far enough away that the SGSN changes (typically into a different metro area); or (ii) the device changes between technologies, e.g., 3G, 2G, WiFi, or vice versa. This scenario typically occurs if a device moves from 3G/4G areas that cover primary urban and suburban areas to 2G/3G areas that cover less populated areas.

[1] In practice, a device can be connected to multiple nearby sectors at the same time. This set of sectors, typically 1 to 4 in size, is called the active set. While all sectors in the active set coordinate to receive uplink data sent by the device, only one, the serving cell, transmits downlink data to the device at a given time. This is typically the sector with the highest signal-to-noise ratio.

2.3 Cellular Network Resource Allocation

In cellular networks, a mobile device estimates the channel quality through the perceived signal-to-noise ratio of the pilot signal from the base station in every time slot, e.g., 1.67ms for EV-DO. The device determines the modulation and coding scheme (i.e., DRC) from the channel quality and reports back to the base station. Depending on the channel quality, the base station allocates time slots via proportional fair scheduling to fairly allocate radio resource while maximizing the overall radio resource utilization [22].

To precisely understand how the proportional fair scheduler works, let $\mathtt{W[n]}$ denote the exponentially averaged throughput at time slot $\mathtt{n}$ which is computed from $\mathtt{W[n]}=(1-\alpha)\cdot\mathtt{W[n-1]}+\alpha\cdot\mathtt{I[n-1]}\cdot\mathtt{C[n-1]}$, where $\mathtt{I[\cdot]}$ is the indicator function on whether the user is served in a given time slot, $\mathtt{C[\cdot]}$ is the function of channel quality report, and α is the discount factor controlling the aggressiveness for the base station switching time slots across users [72]. The proportional fair scheduler allocates time slot $\mathtt{n}$ to a user with the maximum value of $\frac{\mathtt{C[n]}}{\mathtt{W[n]}}$ to balance serving between the device with the best channel quality and the device consuming the most resources.

The average duration of staying in a DRC is hundreds to thousands of time slots for stationary devices and tens of time slots for moving devices [75]. Moreover, a device spends a large fraction of time in one dominant DRC, indicating the presence of a dominant channel condition [75]. Thus, the number of continuous time slots that a device can occupy is decided by $\frac{1}{\mathtt{W[n]}}$, which is affected by the discount factor α. To encourage a device to access a time slot in time [43] and to occupy enough continuous time slots to efficiently deliver a non-trivial amount of data, α is usually set to a small value (e.g., 0.001) [63]. This allows a device to occupy the order of $\approx\frac{1}{\alpha}=1000$ time slots, which means that a device can occupy the channel with the same DRC on the order of ≈1.67s. Since the network performance on a wireless link between the device and base station is largely a function of the channel condition and the DRC value, we expect that it should be possible to predict network performance on a similar time scale, i.e., 1.67s. Note that we expect the presence of network predictability in other variants of 3G or 4G networks as well due to the consistent utilization of proportional fair scheduling and channel quality report scheme [69].

CHAPTER III

CELLULAR INFRASTRUCTURE DISCOVERY

To achieve the thesis goal of effectively adapting mobile networking applications to cellular networks, we first explore the characteristics of cellular network infrastructure. The characteristics of cellular networks can be significantly different from those of the wireline Internet. One example is the locality of IP addresses. On the Internet, IP addresses indicate to some degree the identity and location of end-hosts. IP-based geolocation is widely used in different types of network applications such as content customization and server selection. Using IP addresses to geolocate wireline end-hosts is known to work reasonably well despite the prevalence of NAT, since most NAT boxes consist of only a few hosts [37]. However, one recent study [28] exposed very different characteristics of IP addresses in cellular networks, i.e., cellular IP addresses can be shared across geographically very disjoint regions within a short time duration. This observation suggests that cellular IP addresses do not contain enough geographic information at a sufficiently high fidelity. Moreover, it implies only a few IP gateways may exist for cellular data networks, and that IP address management is much more centralized than that for wireline networks, for which tens to hundreds of Points of Presence (PoPs) are spread out at geographically distinct locations.

Cellular data networks have not been explored much by the research community to explain the dynamics of cellular IP addresses despite the growing popularity of their use. The impact of the cellular architecture on the performance of a diverse set of smartphone network applications and cellular users has been largely overlooked. We perform the first comprehensive characterization study of the cellular data network infrastructure to explain the diverse geographic distribution of cellular IP addresses, and to highlight the key importance of the design decisions of the network infrastructure that affect the performance, manageability, and evolvability of the network architecture. Understanding the current architecture of cellular data networks is critical for future improvement.

Since the observation of the diversity in the geographic distribution of cellular IP address in the previous study [28] indicates that there may exist very few cellular IP data network gateways, identifying the location of these gateways becomes the key for cellular infrastructure characterization in our study. The major challenge is exacerbated by the lack of openness of such networks. We are unable to infer topological information using existing probing tools. For example, merely sending traceroute probes from cellular devices to the Internet IP addresses exposes mostly private IP addresses along the path within the UMTS architecture. In the reverse direction, only some of the IP hops outside the cellular networks respond to *traceroute* probes.

To tackle these challenges, instead of relying on those cellular IP hops, we use the geographic coverage of cellular IP addresses to infer the placement of IP gateways following the intuition that those cellular IP addresses with the same geographic coverage are likely to have the same IP allocation policy, i.e., they are managed by the same set of gateways. To obtain the geographic coverage, we use two distinct data sources (i.e., YellowPage and MobiPerf) and devise a systematic approach for processing the data reconciling potential conflicts, combined with other data obtained via simple probing and passive data analysis.

One key contribution of our work is the measurement methodology for characterizing the cellular network infrastructure, which requires finding the relevant address blocks, locating them, and clustering them based on their geographic coverage. This enables the identification of IP gateways within cellular data networks, corresponding to the first several outbound IP hops used to reach the rest of the Internet. We draw parallels with many past studies in the Internet topology characterization, such as Rocketfuel [102] characterizing ISP topologies, while our problem highlights additional challenges due to the lack of publicly available information and the difficulties in collecting relevant measurement data. We enumerate our key findings and major contributions below.

- We comprehensively characterize the cellular network infrastructure for four major U.S. carriers including both UMTS and EV-DO networks by clustering their IP addresses based on their geographic coverage. Our technique relies on the device-side IP behavior easily collected through our lightweight measurement tool instead of requiring any proprietary information from network providers. Our characterization methodology is applicable to all cellular access technologies (2G, 3G, or 4G).
- We observe that the traffic for all four carriers traverses through only 4–6 IP gateways, each encompassing a large geographic coverage, implying the sharing of address blocks within the same geographic area. This is fundamentally different from wireline networks with more distributed infrastructure. The restricted routing topology for cellular networks creates new challenges for applications such as CDN service.
- We perform the first study to examine the geographic coverage of local DNS servers and discussed in depth its implication on content server selection. We observe that although local DNS servers provide coarse-grained approximation for users' network location, for some carriers, choosing content servers based on local

DNS servers is reasonably accurate for the current cellular infrastructure due to restricted routing in cellular networks.

- We investigate the performance in terms of end-to-end delay for current content delivery networks and evaluated the benefit of placing content servers at different network locations, i.e., on the Internet or inside cellular networks. We observe that pushing content close to GGSNs can potentially reduce the end-to-end latency by 50% excluding the variability from air interface. Our observation strongly encourages CDN service providers to place content servers inside cellular networks for better performance.

The rest of this chapter is organized as follows. §3.1 explains the high-level solution to discover IP gateways in cellular infrastructure and the main methodology in the data analysis and the data sets studied. The results in characterizing cellular data network infrastructure along the dimensions of IP address, topology, local DNS server, and routing behavior are covered in §3.2. We discuss the implications of these results in §3.3 and summarize in §3.4 with key observations and insights.

3.1 Determining IPs' Geographic Coverage

Identifying GGSNs in the cellular infrastructure is the key to explain the geographically diverse distribution of cellular addresses discovered by the recent study [28]. GGSNs serve as the gateway between the cellular and the Internet infrastructure and thus play an essential role in determining the basic network functions, e.g., routing and address allocation. We leverage the geographic coverage of cellular addresses to infer the placement of GGSNs, assuming that prefixes sharing similar IP behaviors are likely to have the same IP allocation policy, i.e., they are managed by the same GGSN. Considering geographic coverage as one type of IP behaviors, we cluster prefixes based on the feature of geographic

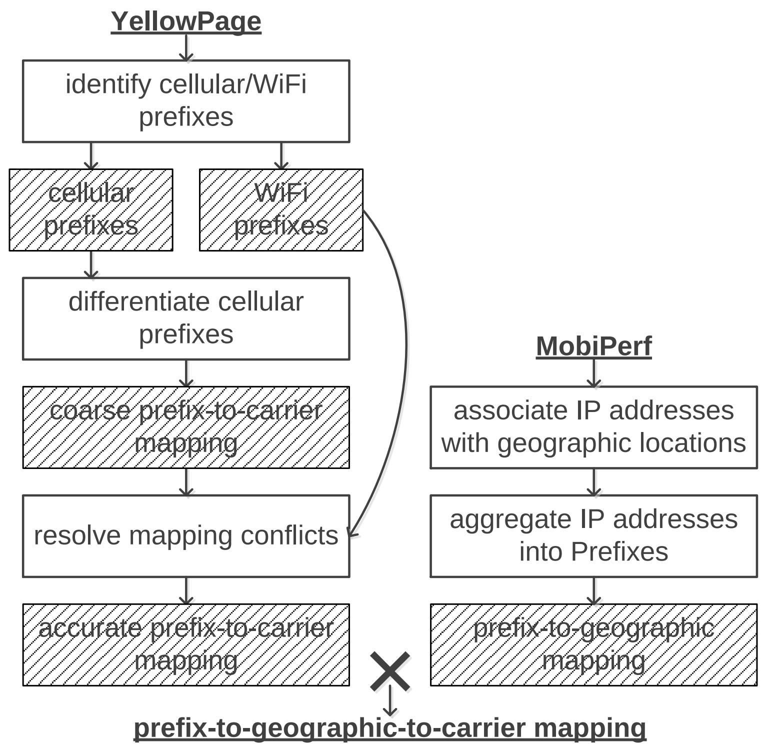
YellowPage
identify cellular/WiFi prefixes
cellular prefixes
WiFi prefixes
differentiate cellular prefixes
coarse prefix-to-carrier mapping
resolve mapping conflicts
accurate prefix-to-carrier mapping
MobiPerf
associate IP addresses with geographic locations
aggregate IP addresses into Prefixes
prefix-to-geographic mapping
prefix-to-geographic-to-carrier mapping

Figure 3.1: Workflow for determining IPs' geographic coverage. The boxes filled with patterns correspond to intermediate data (i.e., mapping tables), manipulated by processing operations (i.e., the white boxes).

coverage, and infer the placement of GGSNs according to the prefix clusters that we generated.

As depicted by Figure 3.1, to get the geographic location of cellular IP addresses, we leverage a popular location search service whose server logs public IP address and GPS location of users (i.e., YellowPage). We use the mobile service log to generate prefix-to-geographic-coverage mappings. In order to identify cellular addresses and to further differentiate different cellular providers, we also deploy a measurement tool for mainstream smartphone OSes to build a database (i.e., MobiPerf) for prefix-to-carrier mappings. They provide the ground truth for determining the cellular provider who owns a certain IP address block. By correlating prefix-carrier mappings with prefix-geographic coverage mappings, we can obtain the prefix-to-geographic-coverage-to-carrier mappings for clustering.

Once the clustering is finished, we validate the clustering results via three independent ways: clustering using the mobile application log, identifying the placement of local DNS servers in cellular networks, and classifying *traceroute* paths. Based on our findings during clustering and validation, we investigate implications of the cellular infrastructure on content delivery service for mobile users.

In §3.1.1, we introduce the datasets of YellowPage and MobiPerf, and in §3.1.2, we detail our methodology for identifying cellular addresses and cellular providers. Note that we design our methodology to be generally applicable for any data cellular network technologies (2G, 3G, and 4G), and particularly from the perspective of data requirement. Any mobile data source that contains IP addresses, location information, and network carrier information can be used for our purpose of characterizing the cellular data network infrastructure. Based on our experience of deploying smartphone applications, it is not difficult to collect such data.

3.1.1 Datasets

The first data set used is from server logs associated with a popular location search service for mobile users [18]. We refer to this data source as YellowPage. It contains the IP address, the timestamp, and the GPS location of mobile devices. The GPS location is requested by the application and is measured from the device. The data set ranges from August 2009 until September 2010, containing several million records. This comprehensive data set covers 16,439 BGP prefixes, 121,567 /24 address blocks from 1,862 AS numbers. However, YellowPage does not differentiate the carrier for each record. Later we discuss how to map YellowPage's records to corresponding cellular carriers or WiFi networks with the help of MobiPerf's prefix-to-carrier table in §3.1.2. Users of the search service may also use WiFi besides cellular networks to access the service.

operator	3G technology	% of records	# AS numbers	# of BGP prefixes	# of /24 address blocks
AT&T	UMTS	43.34%	1	54	16,288
T-Mobile	UMTS	7.09%	1	12	41
Verizon	EV-DO	1.51%	2	202	15,590
Sprint	EV-DO	1.22%	1	172	11,205
*	-	100%	1,862	16,439	121,567

Table 3.1: Statistics of YellowPage (August 2009 – September 2010).

Table 3.1 shows the breakdown of the records among the four major U.S. cellular providers for YellowPage. 43.34% of all the records in YellowPage are mapped to AT&T due to the disproportionate popularity of the service among different mobile users. Despite this bias, we still find sufficient information to characterize the other three major carriers. 46.71% of YellowPage is from WiFi users, and 0.13% is from cellular carriers besides the four major carriers. Note that one cellular carrier may be mapped to more than one AS number (ASN), e.g., Verizon corresponds to more than one ASN.

The long-term and nation-wide YellowPage is the major data source that we rely on to map cellular prefixes to their geographic coverage after we aggregate cellular IP addresses to prefixes based on RouteViews BGP update announcements [17].

platform	# of users	# of carriers	# of BGP prefixes	# of /24 address blocks	# of AS numbers
iPhone	25K	- [1]	5.2(1.8)K	10.8(2.8)K	1.2K(268)
Android	28K	278(36)[2]	2.7(1.1)K	7.3(3.1)K	720(179)
WM	9K	516(66)	1.6(0.5)K	5.7(3.5)K	545(121)
other	63K	571(87)	7.6(2.9)K	23(9.3)K	1.5K(387)

[1] On iPhone OS, we cannot tell the serving carrier.
[2] Numbers inside parentheses refer to the U.S. users only.

Table 3.2: Statistics of MobiPerf (September 2009 – October 2010).

The second main data source of our analysis comes from an application that we have widely deployed on three popular smartphone platforms: iPhone OS, Android, and Windows Mobile (WM). We refer to this data source as MobiPerf, with the basic statistics shown in Table 3.2. The application is freely available for mobile users to download for the purpose of evaluating and diagnosing their networks from which we can collect common network characteristics such as the IP address, the carrier name, the local DNS server, and the outbound *traceroute* path. The hashed unique device ID provided by the smartphone application development API allows us to distinguish devices while preserving user privacy. Our application also asks users for access permission for their GPS location. So far, this application has already been executed more than 143,700 times on 62,600 distinct devices. MobiPerf covers about the same time period as YellowPage: from September 2009 till October 2010. Given that the application is used globally, we observe a much larger number of carriers, many of which are outside the U.S. Note that this method of collecting data provides some ground truths for certain data which is unavailable in YellowPage, e.g., IP addresses associated with cellular networks instead of Internet end-points via WiFi network can be accurately identified because of the API offered by those mobile OSes.

set	# of BGP prefixes	% in YellowPage	% in MobiPerf
YellowPage $\cup$ MobiPerf	453	-	-
YellowPage $\cap$ MobiPerf	259	99.97%	98.96%
$\in$ YellowPage,$\notin$ MobiPerf	181	0.03%	-
$\in$ MobiPerf,$\notin$ YellowPage	13	-	1.04%

Table 3.3: Cross overlap between YellowPage and MobiPerf.

Characterizing the overlap between our two data sources helps us estimate the effectiveness of using MobiPerf to identify the carrier name of YellowPage's cellular prefixes. Moreover, a significant overlap can confirm the representativeness of both YellowPage and MobiPerf on cellular IP addresses as those two data sources are collected independently. We first compare the overlap between YellowPage and MobiPerf's records in the U.S. in terms of number of prefixes within the four carriers as shown in Table 3.3. Although YellowPage and MobiPerf do not overlap much in terms of number of prefixes, e.g., 181 prefixes in YellowPage are excluded by

MobiPerf, in terms of number of records the overlap is still significant due to the disappropriate usage of prefixes, i.e., overlapped prefixes contribute to the majority. 99.97% of YellowPage's records are covered by the prefixes shared by both YellowPage and MobiPerf. Therefore, we have high confidence in identifying the majority of cellular addresses based on MobiPerf. In addition, the big overlap indicates that both data sources are likely to represent the cellular IP behavior of active users well.

3.1.2 Operating Datasets to Identify IPs' Geographic Coverage

One important general technique we adopt in this work, commonly used by many measurement studies, is to intelligently combine multiple data sources to resolve conflicts and improve accuracy of the analysis. This is necessary as each data source alone has certain limitations and is often insufficient to provide conclusive information.

Correlating YellowPage and MobiPerf allows us to tell based on the IP address whether each record in YellowPage is from cellular or WiFi networks and recognize the correct carrier names for those cellular records. Under the assumption that a longest matching prefix is entirely assigned to either a cellular network or an Internet wireline network, the overall idea for correlating YellowPage and MobiPerf depicted by Figure 3.1 is as follows. Both data sources directly provide the IP address information: Each record in YellowPage contains the GPS location information reported by the device allocated with the cellular IP address; while MobiPerf contains the carrier names of those cellular IP addresses. We first map IP addresses in both data sets into their longest matching prefixes obtained from routing table data of RouteViews. After mapping cellular IP addresses into prefixes, we have a prefix-to-location table from YellowPage and a prefix-to-carrier table from MobiPerf. Note that the prefix-to-location mapping is not one-to-one mapping because one IP address can be present at multiple locations over time. Combining these two tables results in a prefix-to-carrier-to-location table, which is used to infer the placement of GGSNs after further clustering discussed later.

We believe that cellular network address blocks are distinct from Internet wireline host IP address blocks for ease of management. To share address blocks across distinct network locations requires announcing BGP routing updates to modify the routes for incoming traffic, affecting routing behavior globally. Due to the added overhead, management complexity, and associated routing disruption, we do not expect this to be done in practice and thus assume that a longest matching prefix is either assigned to cellular networks or Internet wireline networks. That is why we map the IP addresses in both data sets to their longest matching prefixes.

One issue in Figure 3.1 still requires additional consideration, i.e., building the prefix-to-carrier mapping via MobiPerf. We expect MobiPerf to provide the ground truth for differentiating IP addresses from cellular networks and identifying the corresponding carriers of cellular IP addresses. Each record in MobiPerf contains the network type, i.e., cellular vs. WiFi, reported by APIs provided by the OS. The carrier name is only available on Android and Windows Mobile due to the API limitation on iPhone OS. After mapping IP addresses to their longest matching BGP prefixes, we can build a table mapping from the BGP prefix to the carrier name for Android and Windows Mobile separately. Although we cannot have a prefix-to-carrier table from iPhone OS, we do not expect that IP allocation differentiates towards device types.

3.2 Inferring GGSNs from IPs' Geographic Coverage

As mentioned in §3.1, discovering the placement of GGSNs is the key to understanding the cellular infrastructure, explaining the diverse geographic distribution of cellular addresses. This illuminates the important characteristics of cellular network infrastructure that affect performance, manageability, and evolvability. We leverage the information of the geographic coverage of cellular address blocks to infer the placement of each GGSN because those address blocks sharing the similar geographic coverage are likely managed by the same GGSN. In this section, we (i) identify the geographic coverage of the cellular prefixes in YellowPage; (ii) cluster those prefixes according to the similarity of their geographic coverage; and (iii) infer the placement of GGSNs from the different types of clusters. To validate the clustering results we present three validation techniques based on MobiPerf, DNS request logs from a DNS authoritative server, and `traceroute` probing respectively.

3.2.1 Clustering IPs

On the Internet, an IP address can often provide a good indication of geolocation, albeit perhaps only at a coarse-grained level, as shown by numerous previous work on IP-based geolocation [87, 56, 67, 117]. however, for cellular networks, it is uncertain due to a lack of clear association of IP addresses with physical network locations, especially given the observed highly dynamic nature of IP addresses assigned to a mobile device [28]. In this section, we derive geographic coverage of cellular address blocks in YellowPage to study the allocation properties of cellular IP addresses. We have previously described our methodology on how to identify cellular addresses and their corresponding carriers in §3.1: by aggregating IP addresses to prefixes, we can identify the presence of a prefix at different physical locations based on the GPS information in YellowPage.

As discussed in §3.1, we expect that address blocks with similar geographic coverage are likely be subjected to similar address allocation policy. From our data sets, we do observe similarity of geographic coverage present across address

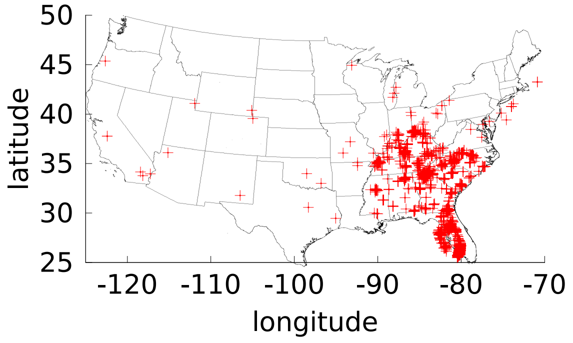

(a) AT&T's /24 address block #22.

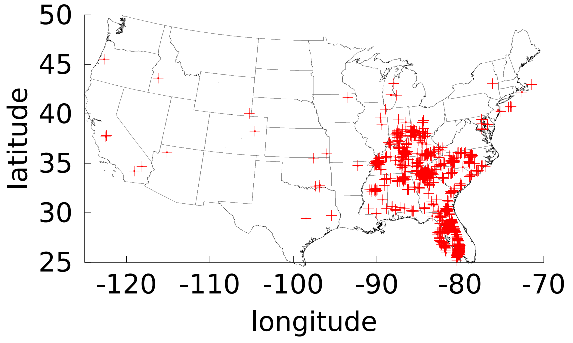

(b) AT&T's /24 address block #5.

Figure 3.2: Similarity of IPs' geographic coverage (AT&T).

blocks. In Figure 3.2, both /24 address blocks 22 and 5 from AT&T have more records in the southeast region of the U.S.. The geographic coverage of these two prefixes is clearly different from the distribution of all AT&T's addresses in YellowPage shown in Figure 3.5, which is influenced by the population density as well as AT&T's user base. Moreover, we confirm and further investigate the observation in study [28] that a single prefix can be observed at many distinct locations, clearly illustrating that the location property of cellular addresses differs significantly from that of Internet wireline addresses. The large geographic coverage of these /24 address blocks also indicates that users from both Florida and Georgia are served by the same GGSN within this region.

We intend to capture the similarity in geographic coverage through clustering to better understand the underlying network structure. Also, to verify our initial assumption that carriers do not aggregate their internal routes, we repeat the clustering for /24 address blocks instead of for BGP prefixes by aggregating addresses into /24 address blocks. If cellular carriers do aggregate their internal routes, the number of clusters based on /24 address blocks should be larger than that based on BGP prefixes.

The logical flow to systematically study the similarity of geographic coverage is as follows. Firstly, we quantify the geographic coverage. By dividing the entire U.S.

continent into N tiles, we assign each prefix a N-dimension feature vector, each element corresponding to one tile and the number of records located in this tile from this prefix. As a result, the normalized feature vector of each prefix is the probability distribution function (PDF) of the girds where this prefix appears. Secondly, we cluster prefixes based on their normalized feature vectors using the bisect K-means algorithm for each of the four carriers. The choice of N, varying from 15 to 150 does not affect the clustering results, this is because the geographic coverage of each cluster is so large that the clustering results are insensitive to the granularity of the tile size.

The process of clustering prefixes consists of two steps: (i) pre-filtering prefixes with very few records; and (ii) tuning the maximum tolerable average sum of squared error (SSE) of bisect K-means. We present the details next.

3.2.1.1 Pre-filtering the prefixes with few Records

Before clustering, we perform pre-filtering to exclude prefixes with very few records so that the number of clusters would not be inflated due to data limitations. Note that aggressive pre-filtering may lead to losing too many records in YellowPage.

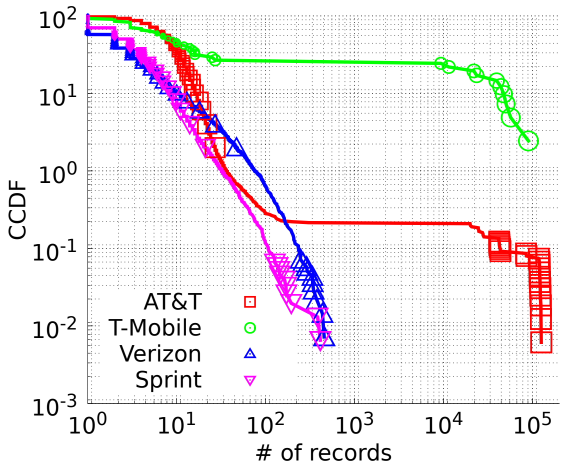

Figure 3.3: Number of records of individual prefixes in YellowPage dataset.

One intuitive way to filter out those prefixes is to set a threshold on the minimum number of records that a prefix must have. However, the effectiveness of this pre-filtering depends on the distribution of the number of records of prefixes. We plot the complementary cumulative distribution function (CCDF) of the number of records of prefixes in Figure 3.3. All the four carriers have bi-modal distributions on the number of records of prefixes, implying that we can easily choose the threshold without losing too many records. In our experiments, we choose a threshold for each prefix to be 1% of its carrier's records.

3.2.1.2 Tuning the SSE in bisect K-means algorithm

To compare the similarity across prefixes and further cluster them we use the bisect K-means algorithm [106] which automatically determines the number of clusters with only one input parameter, i.e., the maximum tolerable SSE. In each cluster, consisting of multiple elements, the SSE is the average distance from the element to the centroid of the cluster. A smaller value of SSE generates more clusters. The clustering quality is determined by the geographic coverage similarity of the prefixes within a cluster, which is measured by the SSE.

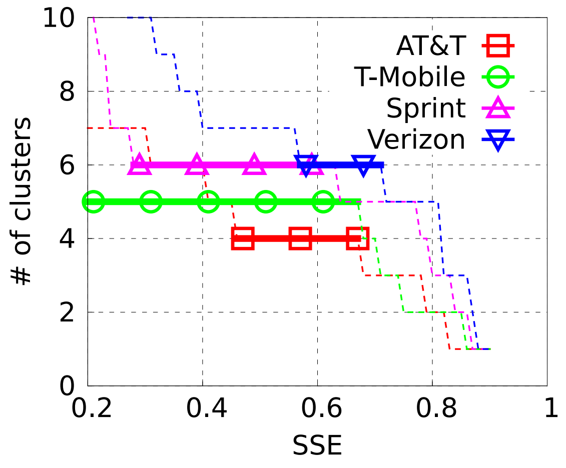

Figure 3.4: Tuning the input SSE in bi-sect K-means clustering.

Figure 3.4 depicts how the SSE, as a measure of the quality of clustering, affects the number of clusters generated for the four carriers. We vary the choice of SSE from 0.01 to 0.99 with increment 0.01. Since there may be multiple stable numbers of clusters, we select the one with the largest range of SSE values. For example, the number of clusters for AT&T is 4 instead of 3 because it covers $[0.45,0.67]$ when the number is 4 while it only covers $[0.68,0.78]$ when the number is 3. From Figure 3.4, we can also observe that every carriers has an obvious longest SSE range that results in a stable number of clusters, indicating that (i) the geographic coverage across prefixes in the same cluster is very similar; and that (ii) the geographic coverage of the prefixes across clusters is very different.

3.2.1.3 Interpreting the clustering results

carrier	thre.	# of prefixes	SSE	# of clusters	(% of records)[# of prefixes]
AT&T	500,300	20,35	0.6,0.5	4,4	(28,19,27,26)[6,5,5,4], (18,24,25,27)[11,8,8,8]
T-Mobile	500,300	11,11	0.5,0.5	5,5	(10,14,40,19,17)[1,2,3,2,2], (10,14,40,17,19)[1,2,3,2,2]
Verizon	500,50	63,245	0.5,0.5	6,6	(28,24,10,7,9,19)[17,11,8,7,6,14], (50,24,3,3,12,5)[130,59,11,11,23,11]
Sprint[1]	100,100	155,177	0.7,0.2	6,10	(30,10,13,22,9,14)[28,25,28,28,22,24], (32,6,6,11,6,7,9,4,4,8,4) [27,23,16,16,12,14,11,8,7,7,10]

[1]Sprint's clusters based on /24 address blocks are different from those based on BGP prefixes, which indicates the existence of internal routing

Table 3.4: Clustering parameters and results on both BGP prefixes and /24 address blocks. Separated by a ",", the first item in a cell refers to BGP's and the second item refers to /24's.

We address the problems of pre-filtering and tuning SSE for bisect k-means clustering in the last two sections. Table 3.4 shows the parameters we used in pre-filtering and clustering and the clustering results. Aggressive filtering does not happen as every carrier contains at least 99% of the original records after pre-filtering. For AT&T, T-Mobile, and Verizon, comparing the clustering at the BGP prefix level vs. the /24 address block level, we do not observe any difference in the number of the clusters generated and the cluster that every address block belongs to. Unlike AT&T, T-Mobile, and Verizon, Sprint does have finer-grained clusters based on its /24 address blocks. We observe that some Sprint's prefix-level clusters are further divided into smaller clusters at the level of /24 address blocks. These results answer our previous question on the existence of internal route aggregation. Since no internal route aggregation observed for AT&T, T-Mobile, and Verizon, BGP prefixes are sufficiently fine-grained to characterize the properties of address blocks. For Sprint, although the clustering based on /24 address blocks is finer-grained, it does not affect our later analysis. We have applied the clustering on YellowPage's records month by month as well, but we do not see any different numbers of clusters for these 4 carriers.

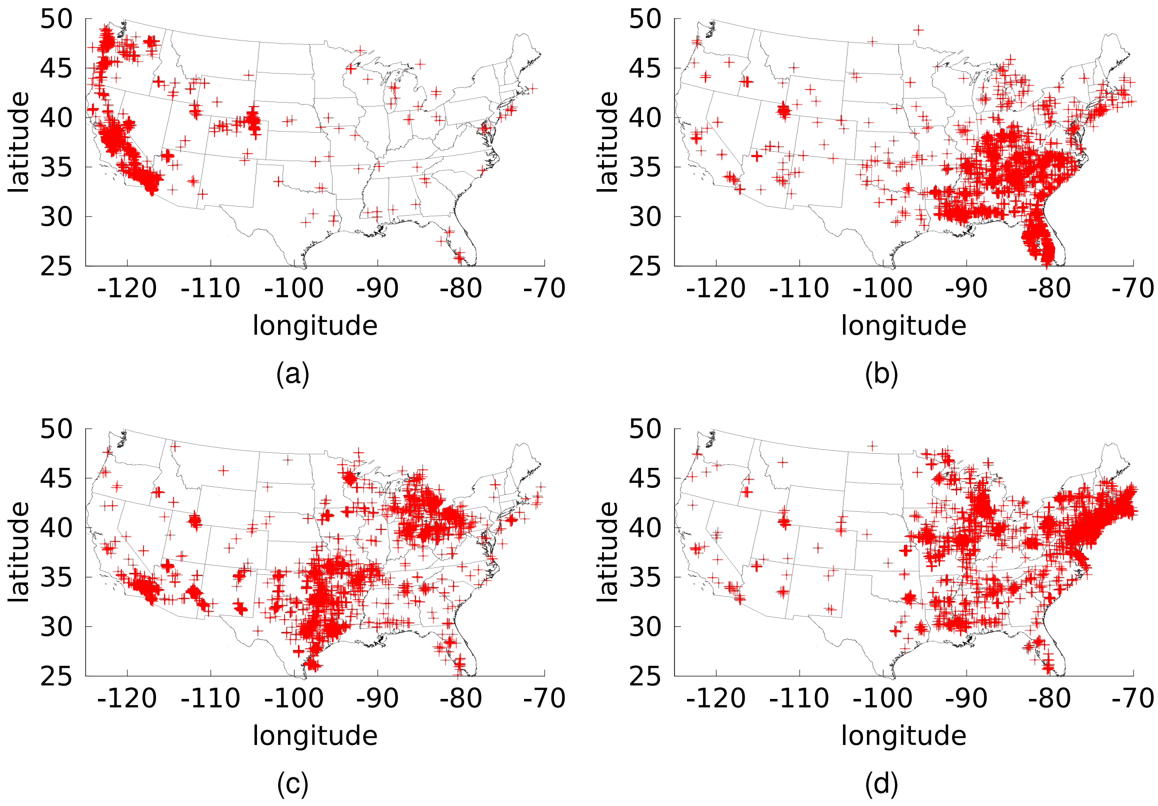

Figure 3.5: Geographic coverage of individual GGSN clusters (AT&T).

Figure 3.5 shows the geographic coverage of each AT&T's cluster, from the perspective of the U.S. mainland ignoring Alaska and Hawaii, illustrating the diversity across clusters as well as the unexpected large geographic coverage of every single cluster. Note that each cluster consists of prefixes with similar geographic coverage. Each AT&T's cluster has different geographic spread and center, i.e., Cluster 1 mainly covers the western, Cluster 2 mainly covers the southeastern, Cluster 3 mainly covers the southern and the mid-eastern, which are two very disjoint geographic areas, and Cluster 4 mainly covers the eastern. However, note that the clusters are not disjoint in its geographic coverage, i.e., overlap exists among clusters although those clusters have different geographic centers. For example, comparing Figure 3.5(b) and 3.5(d), we can observe that Cluster 2 and Cluster 4 overlap in the northeast region.

We further quantify the overlap among clusters at tile level. Given a tile, based on all the records located in this tile, we count how many records are from each prefix. Since we know which cluster each prefix belongs to, we can calculate the fraction of records for each tile contributed by different clusters. As a result, for each tile overlapped by multiple clusters, we have a probability distribution function (PDF) on the cluster covering this tile. Based on the PDF, we can calculate the Shannon entropy for each tile. For example, four clusters have 300, 700, 600, and 400 records at tile X respectively, then the PDF for tile X is $[0.3, 0.7, 0.6, 0.4]$ whose Shannon entropy is $-0.3\lg 0.3 - 0.7\lg 0.7 - 0.6\lg 0.6 - 0.4\lg 0.4$. Smaller values of the entropy reflect smaller overlapping degree, e.g., if all the records for a tile are from the same cluster, the tile has an entropy of $-\infty$. Given the number of clusters is N, the theoretical maximum entropy for a tile is $\lg N$.

Figure 3.6 draws the CDF of the entropy of the tile. We can observe that overlap at tile level is quite common for all four carriers, e.g., AT&T's median entropy value close to 1 means that the records in the corresponding tiles are evenly divided by two clusters. We conjecture two reasons for the overlap. The first reason is due to load balancing. Because of user mobility, the regional load variation can be high.

Higher overlapping degree is better for maintaining service quality. Moreover, in the extreme case if one cluster has a failure, the overlap can increase the reliability of the cellular infrastructure by shifting the load to adjacent clusters. Another reason is that users commute across the boundary of adjacent clusters. For example, a user in YellowPage gets an IP address at a region covered by one cluster, subsequently moves to a nearby region covered by another cluster while still maintaining the data connection. This will result in records showing the overlap between the first and the second cluster in adjacent regions.

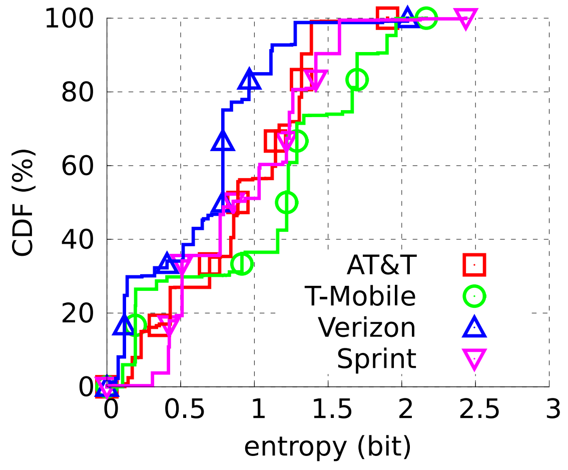

Figure 3.6: Overlap degree across GGSN clusters.

Figure 3.7 shows the clustering results for all four carriers. Although we have already noticed the overlap among clusters in Figure 3.5, we are still interested in the dominant geographic coverage of each cluster by assigning every tile to its dominant cluster by majority voting. We make the following observations:

- All 4 carriers we studied appear to cover the entire U.S. with only a handful of clusters (4–6), each covering a large geographic area, differing significantly from the Internet backbone design.
- There appears to be some “outlier” cases with sparse presence for each cluster in addition to consistent load balancing patterns. We conjecture that this is caused by limited choice of GGSNs for a small set of devices that use a special set of APNs to

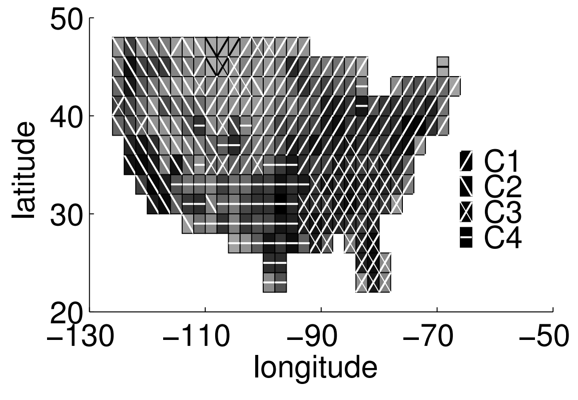

(a) AT&T.

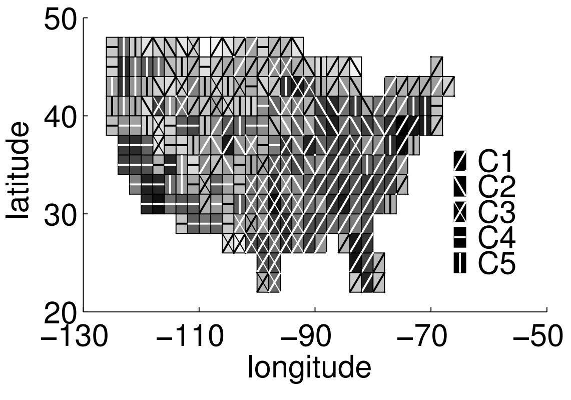

(b) T-Mobile.

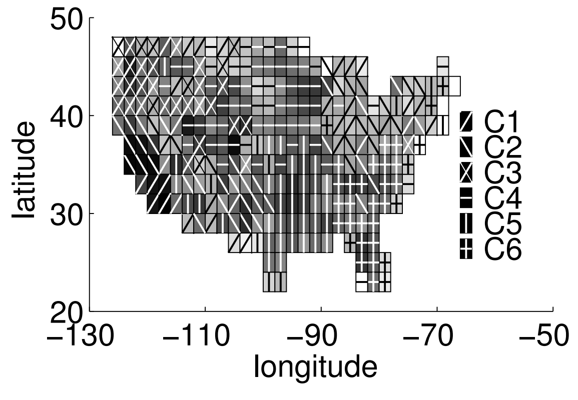

(c) Verizon.

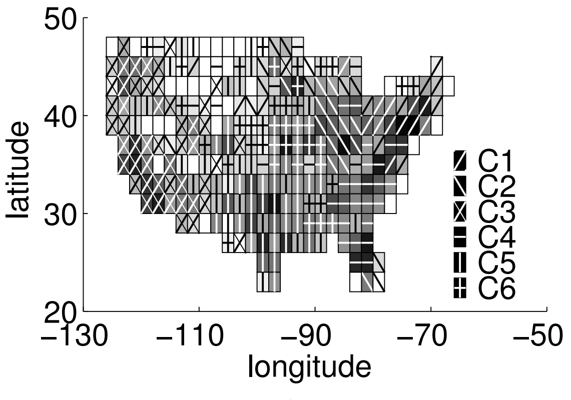

(d) Sprint.

Figure 3.7: Four major carriers' GGSN clusters (AT&T, T-Mobile, Verizon, and Sprint).

which not all GGSNs are available for use.

- Besides those "outliers", overlap among clusters commonly exists at many locations, e.g., the geographic area around Michigan is clearly covered by three of four AT&T's clusters. We believe the overlap is due to load balancing and user mobility.
- Clusters do not always appear to be geographically contiguous. There are clearly cases where traffic from users are routed through clusters far away instead of the closest one, e.g., AT&T's Cluster 3 covers both the Great Lake area and the Southern region. We believe this is due to SGSNs performing load balancing of traffic across GGSNs in different data centers.
- The clustering for /24 address blocks is the same as that for BGP prefixes for AT&T,

T-Mobile, Verizon confirming that there is no internal route aggregation performed by their cellular IP networks. However, Sprint has finer-grained clustering for /24 address blocks than that for visible BGP prefixes. Despite this observation, its number of clusters for /24 address blocks is only 10 which is still very limited.

In our analysis, we discover that the infrastructure of cellular networks differs significantly from the infrastructure of wireline networks. The cellular networks of all four carriers exhibit only very few types of geographic coverage. As we expected, the type of geographic coverage reflects the placement of IP gateways. Since the GGSN is the first IP hop, we can conclude the surprisingly restricted IP paths of cellular data network. This network structure implies that routing diversity is limited in cellular networks, and that content delivery service (CDN) cannot deliver content very close to cellular users as each cluster clearly covers large geographic areas.

3.2.2 Validating GGSN Clusters

We validate the clustering result in three independent ways: clustering using MobiPerf's records, identifying the placement of local DNS servers in cellular networks, and classifying *traceroute* paths.

3.2.2.1 Via YellowPage

Although the size of MobiPerf is much smaller than that of YellowPage, we can still use MobiPerf to validate the clustering results obtained from YellowPage. We repeat the clustering on the prefixes with more than 100 records from the MobiPerf. Besides, we repeat the clustering on different types of device, i.e., Android, iPhone, and WM based on MobiPerf's records. The clustering results are consistent with those of YellowPage in terms of the number of clusters and the cluster that each prefix belongs to. Moreover, all the observations from YellowPage listed in §3.2.1 consistently apply to MobiPerf.

3.2.2.2 Via local DNS server

The configuration of the local DNS infrastructure is essential to ensure good network performance. Besides performance concerns, local DNS information is often used for directing clients to the nearest cache server expected to have the best performance. This is based on the key assumption that clients tend to be close to their configured local DNS servers, which may not always hold [100]. In this work, we perform the first study to examine the placement and configuration of the local DNS servers relative to the cellular users and the implication of the local DNS configuration of cellular users on mobile content delivery. It is particularly interesting to study the correlation between the local DNS server IP and the device's physical location. Since DNS servers are expected to be placed at the same level as IP gateways, i.e., GGSNs, we expect to see similar clusters of cellular local DNS servers based on the geographic coverage.

To collect a diverse set of local DNS server configurations, we resort to our MobiPerf application by having the client send a specialized DNS request for a unique but nonexistent DNS name which embeds the device identifier and the timestamp (`id_timestamp_example.com`) to a domain (`example.com`) where we have access to the DNS request logs on the authoritative DNS server. The device identifier, `id_timestamp`, is used for correlating the corresponding entry in the MobiPerf's log which stores the information such as the GPS information, the IP address, etc. The timestamp ensures that the request is globally unique so that it is not cached. This is a known technique used in previous studies for recording the association between clients and their local DNS servers [79]. Since most DNS servers operate in the iterative mode, from the authoritative DNS server, we can observe the formatted incoming DNS requests from local DNS servers.

We summarize our results in Table 3.5. The four carriers appear to have different policies for configuring local DNS servers. All the local DNS servers of

carrier	# of user	# of records	# of LDNS	# of clusters
AT&T	289	384	12	4
T-Mobile	574	1045	4	1
Verizon	704	884	12	3
Sprint	122	142	15	3

Table 3.5: Statistics of local DNS discovery.

AT&T across the country fall into one /19 address block. T-Mobile altogether only has four distinct DNS IP addresses within two different /24 address blocks, although it has four GGSN clusters. This implies that T-Mobile's local DNS servers are unlikely located directly at cellular network gateways, as a single /24 prefix usually constitutes the smallest routing unit. For Verizon, we observe 12 local DNS server IP addresses within 3 different /24 address blocks. This indicates that, just like T-Mobile's clusters, Verizon's clusters share local DNS servers as well, since Verizon has more clusters than the /24 address blocks of its local DNS servers. For Sprint, we observe 15 IP addresses of local DNS servers in 12 /24 address blocks.

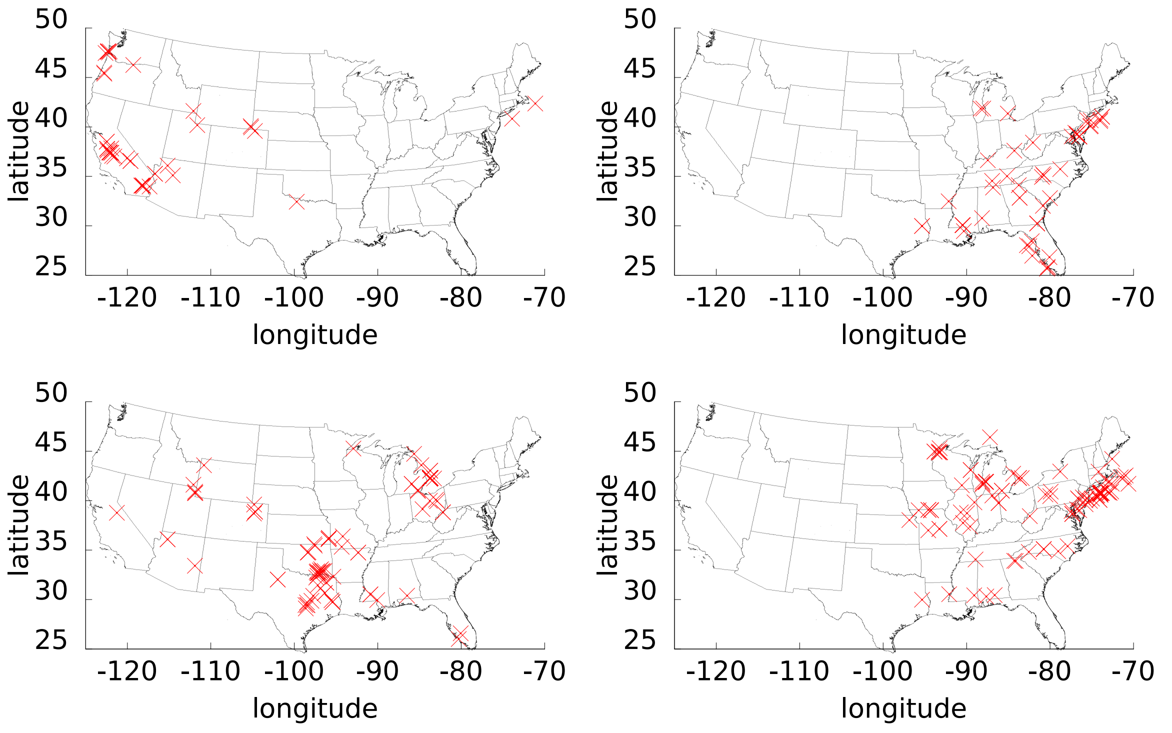

Figure 3.8: Geographic clusters based on local DNS resolvers (AT&T).

For each carrier, we cluster its local DNS servers based on their geographic coverage without any other prior knowledge and show the results in Figure 3.8. Comparing the clusters based on the local DNS servers with previous clustering based on prefixes in §3.2.1, we observe that AT&T's clusters for local DNS servers match very well with the clusters for address blocks (shown in Figure 3.8). AT&T's users sharing the same local DNS server IP belong to the same cluster based on cellular prefixes. This serves as another independent validation for previous clustering. T-Mobile's users across the U.S. all share the same four local DNS servers, while Verizon's and Sprint's clusters based on local DNS servers are "one-to-many" mapped to their clusters based on address blocks, indicating that their local DNS servers are shared across multiple clusters as well.

On the current Internet, local DNS-based server selection is widely adopted by commercial CDNs. For AT&T, Verizon, Sprint since their local DNS servers are ”one-to-one” or ”one-to-many” mapped to GGSNs, server selection based on local DNS servers cannot be finer-grained than the GGSN level. For T-Mobile, server selection can be even worse because all T-Mobile's local DNS servers are used across the entire U.S.

3.2.2.3 Via *traceroute* probing

Since the clusters created based on cellular prefixes should correspond to the prefixes serving clients within the same network location, we use bi-directional *traceroute* to further validate this. For the inbound direction, for each prefix of these four carriers in YellowPage, we run traceroute on 5 *PlanetLab* nodes at geographically distinct locations within the U.S. to one IP address in this prefix for four days. We make the following observations.

- Stability of *traceroute* paths at IP level: All traceroute paths obtained from our experiments are found to be very stable without any change at DNS or IP level.

- Stability of *traceroute* paths at the prefix level: To the same prefix, the last 5 visible hops in the *traceroute* path from different *PlanetLab* nodes are consistently the same.
- Similarity of *traceroute* paths to prefixes in the same cluster: For AT&T, Verizon, and Sprint, prefixes in the same bisect K-means cluster share the same *traceroute* path at DNS or IP level validating their geographic proximity. For T-Mobile, each prefix has a distinct traceroute path, making validation more challenging.
- Location correlation between *traceroute* paths and the cluster's region: For some AT&T's, T-Mobile's, Verizon's clusters, we can infer the GGSN locations from the DNS name of the hops along the path; while for others there is insufficient information to determine router locations. Table 3.6 shows for the last inferred location along the inbound *traceroute* path to some clusters with location information inferred from router DNS names. They all agree with the geographic coverage of these clusters.

carrier	cluster	coverage	DNS key word	location
AT&T	1	west	WA	WA
	2	southeast	GA	GA
	3	south	DLSTX	Dallas, TX
T-Mobile	1	middle	CHI	Chicago, IL
	2	southeast	FL	FL
	3	southeast	ATLGA	Atlanta, GA
	4	west	TUSTIN	Tustin, CA
	5	south	DLSTX	Dallas, TX
Verizon	1	east	CLE	Cleveland, OH
	2	west	SCL	Salt Lake City, UT
	3	northwest	SEA	Seattle, WA
	4	middle	AURORA	Aurora, CO
	5	south	HOU	Houston, TX
	6	east	NEWARK	Newark, NJ

Table 3.6: GGSN locations inferred from *traceroute* paths.

Similar to the inbound direction, the outbound *traceroute* can validate the clustering to some degree. MobiPerf application runs ICMP traceroute from the device to an Internet server. Assigning the outbound *traceroute* path to the prefix, we have the following observations:

- For all four carriers, their *traceroute* paths in the same cluster have the same path pattern, i.e., the sequence of IP addresses or the sequence of address blocks are the same. All clusters are "one-to-one" or "one-to-many" mapped to *traceroute* path patterns, so each cluster has very different traceroute patterns from the others.
- The prefixes in the same AT&T's cluster always go through the same set of IP addresses, while for T-Mobile, Verizon, and Sprint, their prefixes in the same cluster always go through the same set of /24 address blocks. Therefore we can always tell a prefix's corresponding cluster based on the IP addresses or the /24.

3.3 Impact of the Routing Restriction due to GGSNs

Based on the previous characterization of cellular data network infrastructure, we highlight the key impact of cellular infrastructure by examining its implication on content delivery networks from the perspectives of content placement and server selection.

3.3.1 Content Placement

On today's Internet, CDN plays an important role of reducing the latency for accessing web content. The essential idea behind CDN is to serve users from nearby CDN servers that replicate the content from the origin server located potentially far away. By characterizing the cellular infrastructure, we have observed that the current restrictive cellular topology route all traffic through only a handful GGSNs. Therefore, no matter how close to a CDN server the user is, the content still has to go through the GGSN before reaching the destination. The possible reasons for such a restrictive topology design by routing all traffic through GGSNs include simplicity and ease of management, e.g., billing and accounting.

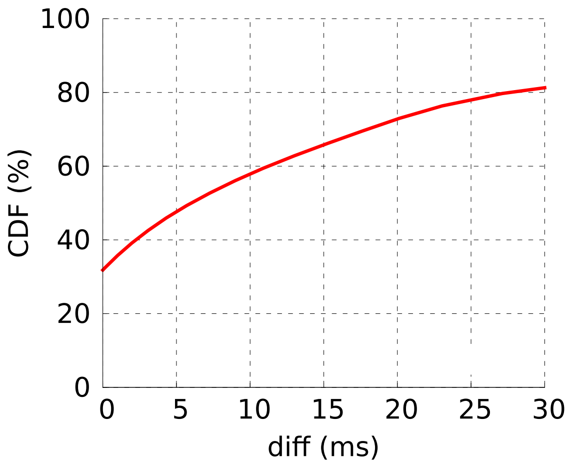

(a) the minimum global vs. the GGSN.

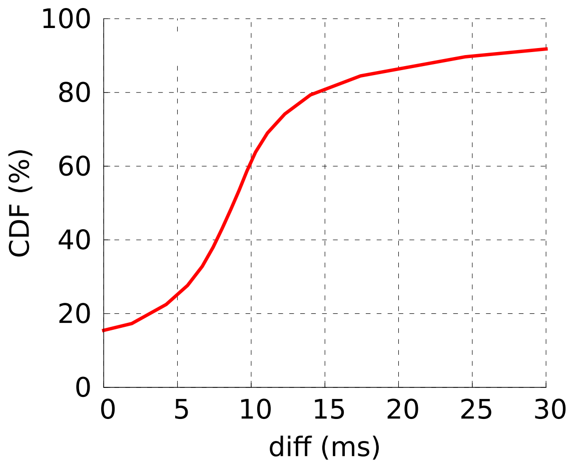

(b) the physically local vs. the GGSN.

Figure 3.9: Latency to GGSNs against landmark servers.

Furthermore, it is also easy to enforce policies for security and traffic management. This certainly has negative implication on content delivery.

It is not simple to adapt an existing CDN service, e.g., *Akamai* and *Limelight*, directly to cellular networks due to routing restrictions. One possible alternative is deploying CDN servers within cellular networks to be closer to end users so that the traffic does not have to go through GGSNs to reach the content on the Internet. There has been some startup effort of placing boxes between the RNC and the SGSN to accelerate data delivery and lighten data traffic growth [16], but this design brings additional challenges to management due to the increased number of locations traffic can terminate. Without the support of placing CDN servers inside cellular core networks, placing them close to GGSNs becomes a quick solution for now, and this solution is clearly limited due to the property of the GGSN serving a large geographic region of users.

In MobiPerf's application, we measure the ping RTT to 20 Internet servers (landmark servers) located across the U.S. to study the end-to-end latency. The latency to the landmark servers is an approximation on the latency to the content placed at different network locations on the Internet. The 20 servers that we choose are very popular servers geographically distributed across 20 states. To estimate the benefit of placing content close to GGSN, we compare the latency to landmark servers with the latency to the first cellular IP hop, i.e., the first IP hop along the outbound path where GGSN is located.

Each time MobiPerf's application runs, it only probes these landmark servers twice to save the resource consumption on devices. In order to eliminate the variability from air interface so that we can isolate the impact from the wireline hops, we follow the splitting method in §3.2.1 dividing the U.S. continent into `N` tiles. Within each tile, we compare the minimum RTT to the first cellular IP hop against these 20 landmark servers. In Figure 3.9(a), we show the absolute difference between the latency to the first cellular IP hop and the minimum latency the landmark servers. Because these 20 landmark servers are widely distributed across the U.S., the minimum latency to landmark servers should be a good estimation of the latency to the current content providers. We can observe that placing content close to the GGSN can reduce the end-to-end latency by 6ms. Note that the 6ms saving may be minor to 3G networks, but can be very critical to 4G such as LTE networks, where the median end-to-end latency is around 60ms [61].

3.3.2 Server Selection

Besides the challenge of mobile content placement, server selection is another important issue for CDN service providers. Some existing CDN services, e.g., *Akamai* and *Limelight*, choose the content server based on the incoming DNS requests from the local DNS server assuming the address of the local DNS can accurately represent the location of those end hosts behind the local DNS server. However, this assumption rarely holds for cellular networks. In §3.2.2.2, we know that AT&T, Verizon, and Sprint have different local DNS servers for different GGSN clusters, while T-Mobile's clusters share the same set of local DNS servers.

Although AT&T, Verizon, and Sprint have different local DNS server for different GGSN clusters, the IP addresses are very similar. Without the information of the correlation between the local DNS server and the GGSN cluster, it is difficult to choose content servers for different GGSN clusters according to their local DNS server IP address. As T-Mobile's GGSN clusters share the same set of local DNS servers, it is impossible to choose content servers for different GGSN clusters based on the DNS request alone.

Interestingly even if content providers can obtain the accurate physical location based on some application-level knowledge, e.g., Google Gears [7], directing the traffic to the content server physically closest to the mobile device can be grossly suboptimal due to the placement of the GGSN and the cellular network routing restrictions. Traffic still needs traverse through the GGSN, despite the close proximity between the mobile device and the content server. To estimate the difference in performance between choosing a server physically closest to the mobile device and one closest to the GGSN node, we do the following analysis. Using the GPS location information reported by MobiPerf's application, in all the experiments from AT&T's Cluster 2, we compare the latency to the landmark server closest to the mobile device with the latency to the landmark server closet to the corresponding GGSN. Figure 3.9(b) shows that the latency to the closet landmark server has high probability to be larger than the latency to the Georgia landmark server and on average by about 10ms, indicating that choosing the server according to the physical location of the mobile device is suboptimal due to the routing restriction imposed by GGSNs.

Overall, if mobile content providers want to adopt the short-term solution to reduce the end-to-end latency, they have to solve two issues: (i) placing content servers as close as to GGSNs; and (ii) effectively directing traffic to the content server closest to the GGSN that originates the traffic based on information such as the correlation between local DNS servers and GGSNs.

3.4 Summary of Cellular Infrastructure Charateristics

In this chapter, we comprehensively characterized the infrastructure of cellular data network of four major wireless carriers within the U.S. including both UMTS and EV-DO technology. We unveiled several fundamental differences between cellular data networks and the wireline networks in terms of placement of GGSNs, local DNS server behavior, and routing properties. One of the most surprising findings is that cellular data networks have severe restriction on routing by traversing only a few limited GGSNs to interface with external Internet networks. We observed that all 4 carriers we studied divide the U.S. among only 4–6 GGSNs, each serving a large geographic area. Since the GGSN is the first IP hop, it implies that CDN servers cannot consistently serve content close to end users.

Our study also showed that in the best case local DNS servers for some carriers can be close to GGSNs. Since traffic from and to local DNS servers and cellular users must traverse one of those few GGSNs, using local DNS servers and the knowledge of the mapping to the GGSN to identify the best server to deliver mobile content currently can be sufficient despite the routing restrictions.

Regarding content placement, we investigated and compared two choices: (i) placing content at the boundary between the cellular backbone and the Internet; and (ii) placing content at the GGSN in the cellular backbone. We observed that pushing content close to GGSNs could potentially reduce the end-to-end latency by more than 6ms. If pushing content into the proprietary cellular backbone is not permitted, placing content at the boundary still gives considerable benefit.

We believe our findings in characterizing the infrastructure for cellular data networks directly motivate future work in this area. Our observations on the cellular infrastructure guide CDNs to provide better service to mobile users, and our methodology for discovering cellular data network properties will continue to reveal new behavior as cellular networks evolve.

CHAPTER IV

APPLICATION USAGE IDENTIFICATION

In §III, we identified the routing restriction issue due to the limited number of cellular network gateways, and we further investigated the impact of such issue on latency sensitive applications starting with CDN services. Besides YellowPage, we have other projects showing certain previously little known impact due to cellular network infrastructure. For example, in NetPiculet [110], we observed that cellular middleboxes, such as NAT boxes and firewalls apply policies that can seriously interrupt application communications and lead to additional energy waste. A common impression from these observations is that application designs should adapt to those fundamentally unique cellular network characteristics in order to in maximum improve application performance. However, before we introduce our hand-on experience in application optimizing in §V, we in general characterize mobile application behaviors.

The rapid adoption of mobile devices is dramatically changing the access to various networking services: instead of using web browsers, mobile users increasingly choose mobile apps[1] as the preferred "gateways" connecting them to the Internet [11]. Android has 150K apps and 350K daily activations [55]. Pre-installed with marketplace portals such as the AppStore on iOS, Google Play on Android, and MarketPlace on Windows Phone, popular smartphone platforms

[1]We use "apps" to emphasize more on individual application packages throughout this section.

have made it easy for users to discover and start using many network-enabled apps quickly. By January 22, 2011, more than 350K apps are available on the AppStore with downloads of more than 10 billion [27]. Furthermore, the appearance of tablets and mobile devices with other form factors, which also use these marketplaces, has increased the diversity in apps and their user population. The existence of marketplaces and platform APIs have also made it more attractive for some developers to implement apps rather than complete web-based services.

Despite the increasing importance of apps as gateways to network services, we have a much sparser understanding of how, where, and when they are used compared to traditional web services, particularly at scale. To achieve this goal, we divide the problem into two: (i) we investigate how to identify apps at cellular network gateways, e.g., GGSNs, and (ii) we characterize the usage patterns of identified apps.

4.1 Traffic Classification at Network Gateways

Understanding the presence and communication of apps can be quite helpful. Equivalent use exists for Internet based apps, but we argue that for mobile platforms the need for app classification is stronger due to constrained radio and battery resources. The ability to determine the app identities of traffic flows, which we define as app identifiers such as `com.rovio.angrybirds` used by app markets, opens an opportunity for mobile network operators to make use of this unique insight in mobile network traffic and users.

Traditional approaches for identifying applications/protocols (e.g., email, news, and VoIP) on the Internet [36, 49, 68, 45, 116, 65, 35] and for discerning P2P traffic [99], is too coarse-grained for identifying mobile apps, which cannot tell apart individual apps that may run the same protocols or contact same content servers.

Signature generation for a small number of apps is achievable with manageable cost through either user studies or app emulation [111, 89, 42, 12]. However, such approaches do not scale to classifying individual traffic flows generated by hundreds of thousands of mobile apps in real time due to the following challenges.

- **Similarity.** Smartphone apps employ HTTP predominantly [122] and the number of contacted hostnames is disproportionally small compared against the number of apps due to the prevalence of CDNs and cloud services. Protocol features based on hostnames and ports utilized by previous approaches are not distinctive enough.
- **Scalability.** The significant number of apps in networks prevents us from creating app signatures solely through supervised learning. Signature generation and matching both need to be efficient to allow real-time flow identification. Stateful signatures that require dependency information across flows do not scale well.
- **Ground truth.** The apps that originate the real-time flows are unknown for the majority of network traffic. Though some apps may employ distinctive features in their traffic, e.g., the app developer tags, the email addresses, the hostnames, such features are generally not known a priori and cannot be employed as ground truth.
- **Coverage.** Compared with flow coverage, app coverage is more challenging. As observed in previous research [122], the top 5K apps contribute 98% of traffic volume. Sophisticated signature generation (e.g., [46] requiring supervised learning) that relies on observing sufficient traffic fails for unpopular apps without explicit offline training. High app coverage is important for security related management and for dealing with highly dynamic nature of mobile app popularity.

We develop FLOWR (i.e., Flow Recognition System) that identifies the apps originating the real-time network flows in mobile networks. We define the *app identity* to be the app identifier of the app on mainstream app markets e.g., `com.rovio.angrybirds` on Google Play. Although the content access patterns across apps can be similar, the metadata which commonly appears in communication can be very specific to individual apps, e.g., the queries in HTTP requests often carry certain identifiers to allow the respective servers to account their access. Thus, FLOWR is designed around a technique of *KV tokenization* that extracts the key-value pairs into flow signatures to best reveal app identities, and identifies apps via signature matching. As FLOWR only examines HTTP requests without assembling packets into flows, efficient flow identification is feasible in real time with negligible information loss.

To construct the knowledge base for signature matching with little supervised learning, we take advantage of the huge traffic volume in mobile networks to enable FLOWR to build the knowledge automatically. It is expected that flows with distinct signatures belonging to the same app will co-occur, which FLOWR validates repeatedly from the monitored traffic. Thus, FLOWR performs the technique we call *flow regression*, which incrementally infers the app identities of unknown flow signatures through monitoring their co-occurrences with already identified flow signatures.

The remaining challenge of initializing the knowledge base using known flow signatures is addressed by leveraging common ad and analytics services (we denote as *a* services*) in mobile networks, e.g., `doubleclick.net` and `gstatic.com`. The flows of such services are a part of app traffic and contain app identifiers, allowing the respective servers to account their access. Although paid apps may not use ad services for revenue, most still use analytics service, e.g., `gstatics.com` and `flurry.com`, because developers are motivated to track paid app usage.

The applicability of these three techniques, i.e., KV tokenization, a* service based initialization, and flow regression, is summarized in Table 4.1. The bottleneck of FLOWR in performance is the use a* services to initialize the knowledge base. However, note that without any initialization, we can still differentiate apps though

technique	applicability	app coverage
KV tokenization	HTTP apps	$>$97%
self learning w/o supervised effort	a* apps	80-84%
flow regression	all apps	100%

Table 4.1: Applicability and coverage of FLOWR's three techniques (AppSet in §4.1.3.2).

cannot identify them. We can also feed the knowledge base with additional app signatures from supervised learning as well.

To the best of our knowledge, FLOWR is the first system to identify apps on a flow basis in real time at the scale of nationwide mobile networks without employing exhaustive supervised learning. By designing, developing, and evaluating FLOWR, we make these contributions.

- We propose the technique of KV tokenization to extract the signatures from key-value pairs that can best identify mobile apps. FLOWR operates efficiently with throughput up to 5Gbps on an off-the-shelf desktop machine.
- To infer app identities without requiring exhaustive supervised learning, we propose the technique of flow regression to determine the app identities for the flow signatures produced by KV tokenization. The run-time memory consumption is $<$1GB over five days at a commercial cellular network gateway.
- We evaluate FLOWR's false positive in flow identification without supervised learning on the condition of no ground truth. In a traffic trace of 10 billion flows collected from a commercial cellular network over 6 days, FLOWR can identify 86–95% flows, i.e., uniquely identifying 26–30% of flows and narrowing down another 60–65% to 2–5 candidate apps, all with $<$1% false positive using real cellular data traffic. However, without FLOWR, only 3% of flows are identifiable under no supervised training.

The rest of this section is organized as follows. §4.1.1 describes how KV tokenization, leveraging a* services, and flow regression work and their limitations.

§4.1.2 presents the system details of FLOWR. We describe the dataset for evaluation in §4.1.3 and evaluate FLOWR in §4.1.4.

4.1.1 Techniques

The goal of FLOWR is to identify flows, defined to be a bi-directional TCP/UDP connection, generated by mobile apps with minimal supervised training. The approach is to infer the app identities of flow signatures from their co-occurrences with already identified flow signatures, and construct a knowledge base accordingly. Using this knowledge base, FLOWR can perform signature matching to identify flows efficiently in real time.

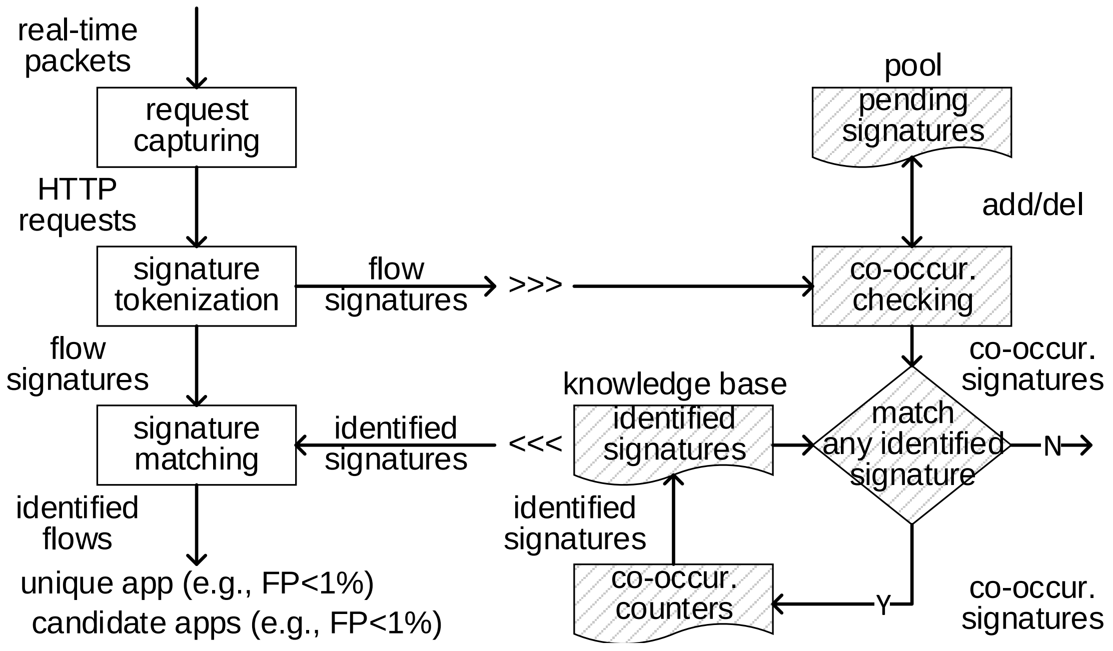

Figure 4.1: FLOWR's workflow, i.e., KV tokenization and flow regression.

To implement the strategy, FLOWR adopts two major techniques as illustrated by Figure 4.1: KV tokenization and flow regression. KV tokenization extracts signatures from real-time network packets and identifies apps via signature matching against FLOWR's current knowledge base of known flow signatures. Depending on the quality of the matched signatures, FLOWR either identifies the flow as a unique app or narrows it down to a few (e.g., 2–5) candidate apps. To minimize supervised learning, FLOWR takes advantage of the huge traffic volume available in mobile networks and applies flow regression accordingly. In flow regression, FLOWR infers the app identities for most signatures by monitoring their co-occurrences with identified flow signatures, which only requires some initial ground truth as the “seeds” to initialize its knowledge base[2].

In summary, FLOWR addresses three issues: (i) in KV tokenization, how to extract signatures from flows, i.e., discovering the potential features best representing app identities (e.g., the app ID, the package name, or the hostname); (ii) in flow regression, how to feed the initial knowledge base of identified flow signatures; and (iii) in flow regression, how to examine co-occurrence events in inferring app identifies.

4.1.1.1 Extracting flow signatures

FLOWR is designed as a general approach to be applicable to a broad class of flow signatures based on information such as user-agents, contacted hostnames, web objects, etc. However, flow signatures can have very different accuracy in identifying apps, e.g., user-agents are shared across apps, hostnames in URIs and DNS queries are not unique across apps due to cloud and CDN services (evaluated in §4.1.4.2). Among the potential flow signatures, the query fields in HTTP URIs can be a better candidate, which facilitate the exchange of additional information between apps and content servers (evaluated in §4.1.4.2). A commonly observable set of URIs is between apps and a* services [70, 59]. These URIs often embed app identifiers to enable the respective servers to account their visits, e.g., ad engines may want to perform ad delivery customization on app basis, and analytics servers may want to know the visit patterns of apps. Accordingly, we

[2]Imitating “flower/seed” is another reason for FLOWR’s name.

develop the technique of KV tokenization to extract signatures from URIs.

```
GET /getAd.php5?sdkapid=67526&...&country=US
&age=45&zip=90210&income=50000&... HTTP/1.1
Connection: Keep-Alive
Host: androidsdk.ads.mp.mydas.mobi
User-Agent: Apache-HttpClient/UNAVAILABLE (java 1.4)

GET /pagead/images/go_arrow.png HTTP/1.1
Host: pagead2.googlesyndication.com
referer:
http://googleads.g.doubleclick.net:80/&...
&app_name=4.android.zz.rings.rww2&...
User-Agent: Mozilla/5.0 (Linux; U; Android 2.3.3; ...

POST /v2/api.php HTTP/1.1
Connection: Keep-Alive
Accept-Encoding: gzip
Host: api.airpush.com
Content-Length: 598
Content-Type: application/x-www-form-urlencoded
apikey=airpush&...&packageName=zz.rings.rww2&...
```

Figure 4.2: Types of URIs used in FLOWR, i.e., `GET`/`POST`, in `referer`, and in `POST`'s payload. The green ones are potential KV signatures.

A URI's syntax is standardized as follows `scheme://authority/path?query#fragment` [31], where the `scheme` is HTTP and the `authority` refers to the contacted hostname. The `query` consists of a sequence of key-value (KV) pairs in the format of `k1=v1&k2=v2&...&kN=vN`, which enables a developer to deliver additional information to content servers, e.g., `adkapid=67526`, `age=45`, and `zipcode=90210`.

KV tokenization extracts the KVs into features that would potentially uniquely identify apps. FLOWR first locates the URIs in HTTP requests. As shown in Figure 4.2, URIs can appear at three locations in HTTP requests: after the request methods of `GET` or `POST`, in the `referer`, and in the payload of `POST` method. FLOWR does not consider the URIs in HTTP responses since the measured additional benefit is marginal ($<$0.1% additional KVs), while the cost of HTTP assembling and decompressing most plain-text web objects is expensive for the significant traffic volume in mobile networks (discussed in §4.1.2).

Once FLOWR has located the URIs in a flow, it extracts the KVs and produces a signature for each KV as `authority:key=value`[3]. To ensure the compatibility with a flow that does not contain any KV, FLOWR creates an empty signature `authority:no_key=no_value` for it. Eventually, FLOWR compares the extracted flow signatures against the app signatures in the knowledge base to identify the incoming flow.

4.1.1.2 Seeding knowledge base

There are three general types of KVs based on the amount of app identity information they contain: the irrelevant KVs (e.g., `age=45`), the KVs that explicitly refers to obvious app identifiers (e.g., `packageName=zz.rings.rww2`), and the remaining KVs, whose app identities are initially ambiguous (e.g., `sdkapid=67526`), but we need to verify how specific they are to their apps through flow regression.

The simplest task for FLOWR is to determine the KVs that explicitly refer to app identifiers, which should have the following characteristics.

- Uniqueness. An explicit identifier should be unique to the app. Otherwise, we can only use the identifier to constrain app identification to a set of candidate apps.
- Persistence. An explicit identifier should appear often in the app's traffic. Such persistence property depends on the app's implementation and usage patterns.
- Expressiveness. An explicit identifier should contain features that are indicative of the app's ID on mainstream app markets, e.g., Android's Google Play. Otherwise, the identifier only allows the differentiation between apps, without establishing an app's identity.

Apparently, the published names of apps as well as app package names (e.g., `com.instagram.android`) that appear in mainstream app markets are good candidates for explicit app identifiers. These two features are commonly present in

[3]"KV", "KV signature", and "flow signature" are used inter-changeably. An "app signature" refers to an identified "flow signature".

HTTP requests of ad and analytics services. Moreover, the app identifiers appearing in such services have a hidden advantage of augmented identification coverage, given that most apps employ a* services. According to our evaluation in §4.1.4.2, $>$80% of either free apps or paid apps utilize one or more a* services. Though paid apps may not use ad services, most of them still use analytics services to track their app usage.

Some major a* services use the app IDs (e.g., `com.instagram.android`) that are embedded in the app descriptions on Google Play or AppStore, i.e., `doubleclick.net`, `admob.com`, `airpush.com`, and `smaato.com`. FLOWR can identify these flows and the other flows originated by the same apps (using flow regression) pointed to by such a* services without any supervised learning effort. Other a* services do not employ any app market content, but instead may contain proprietary registration identifiers of apps or developers, such as their own app IDs, developer IDs, billing IDs. Such identifiers, although not expressive, are very distinct and can be related to some of the previous expressive identifiers with additional but offline supervised training. FLOWR leverages offline supervised training via techniques such as emulation described in §4.1.3.2. For apps that do not employ any a* services, it is difficult to identify them without comprehensive training due to the lack of initial ground truth.

4.1.1.3 Inferring KV identities

Although we can leverage the app identifiers on mainstream app markets to detect the majority of apps, in terms of flow identification, the coverage is negligible ($<$1% of network flows according to Figure 4.13(a)). FLOWR's flow regression is the approach to eliminate irrelevant KVs (defined in §4.1.1.2) and infer the app identities of the undetermined KVs.

Intuitively, if two flows repeatedly co-occur, i.e., they regularly share the source

IP addresses and often appear in close time proximity, then the flows are likely to be originated from the same app. Otherwise, it is impossible for them to co-occur repeatedly over various users, days, locations, devices, etc., even if the mobile devices are behind NAT boxes. As a result, to infer the app identity of an undetermined flow, FLOWR detects the co-occurrence likelihoods (described in §4.1.2) of the flow's KVs with the KVs of known apps.

FLOWR digests co-occurrence likelihoods as follows. In the background, if almost every time a $\mathtt{KV}$ appears closely to some flow related to an app $\mathtt{X}$, i.e., $\mathtt{P[A=X|KV]\approx 1}$, FLOWR adds $\mathtt{KV}$ to its signature set (i.e., UR) that uniquely identifies the app in the knowledge base of app identities. Instead of $\mathtt{P[A=X|KV]\approx 1}$, a more common case is that $\mathtt{KV}$ co-occurs with $\mathtt{X}$ with a certain likelihood less than 1, i.e., $\mathtt{0\ll P[KV|A=X]<1}$, which indicates that $\mathtt{KV}$ may be generated by apps other than $\mathtt{X}$ as well. Then, as a best effort, FLOWR puts $\mathtt{KV}$ into a signature set (i.e., CR) that narrows down the set of the flow's candidate apps.

In the foreground, FLOWR may produce more than one KV for a network flow in KV tokenization. FLOWR determines the app identity according to the best identifiable KV. The *identifiability* of a KV is defined as the co-occurrence likelihood with the most frequently co-occurred app. The identifiabilities of KVs in UR are close to 1, while for KVs in CR, the identifiabilities are far less than 1. A flow's different KVs could have very different quality in identifying the app, but as long as there is at least one KV with a high identifiability (evaluated in §4.1.4.4), the flow identification is granted.

4.1.2 System Design

As depicted in Figure 4.1, we describe the proposed techniques introduced in §4.1.1 and develop several optimizations to keep FLOWR efficient and scalable.

Request Capturing & Signature Tokenization. Expecting that most app identity information is contained within the metadata rather than the content, FLOWR only examines the packets corresponding to HTTP requests to eliminate the overhead in HTTP flow assembly. According to our investigation, the benefit of adding HTTP responses is marginal ($<$0.1%), but the HTTP assembly overhead is nontrivial as most plain-text objects are compressed. To capture an HTTP request, FLOWR only needs to examine a few packets immediately after the TCP handshake of a flow.

As discussed in §4.1.1.1, FLOWR examines URIs from three locations in HTTP requests, i.e., after `GET`, in `referer`, and in `POST`'s payload. Further, FLOWR extracts key-value (KV) pairs from the queries of URIs into signatures. Excluding the time spent on I/O, FLOWR's compute-bound throughput with in-memory reads in HTTP request capturing, signature tokenization, and signature matching is up to 5Gbps on a machine with a 2.67GHz 6-core Xeon processor and 100GB RAM, which is efficient to handle the traffic load in mobile networks (discussed in §4.1.3.2). Though FLOWR uses linear matching, it can be further optimized using complex indexing.

Once a flow is tokenized, to determine its app identity, FLOWR only needs to perform signature matching to either uniquely identify its origin app or narrow down it to a few candidates. On average, FLOWR collects 300K app signatures in the knowledge base of app signatures over 24 hours in a commercial cellular network, i.e., FlowSet (discussed in §4.1.3.1). The knowledge base for signature matching is initialized using the KVs explicitly referring to app identifiers in a* service flows (e.g., `doubleclick:app_name=com.instagram.android` and `airpush:packageName=zz.rings.rww2` in §4.1.1.2). Also, it can be enhanced using external supervised learning effort, such as done in prior approach [46].

Knowledge Base & flow regression. To keep growing the knowledge base of app signatures, FLOWR runs flow regression in the background. To implement flow regression, we need to make three design decisions in interpreting co-occurrence events: (i) how to filter the majority of KVs that are irrelevant for app identification, (ii) how to decide if two KVs co-occur; and (iii) how to compute co-occurrence likelihoods, i.e., $\mathtt{P[A{=}X|KV]}$ where $\mathtt{KV}$ is the undetermined KV and $\mathtt{A{=}X}$ is the app corresponding to the identified KV.

In examining co-occurrence events, FLOWR has to maintain a pool for pending signatures (as shown in Figure 4.1) that contains the recently appeared KVs. In order to be efficient, FLOWR has to eliminate most of the irrelevant KVs to keep the pool compact. To achieve that, FLOWR detects and eliminates conflicted KVs: two KVs are considered to be conflicted if they share the same key but have different values. If two KVs indicate the same app, they must not conflict with each other. We observe that many KVs refer to the information other than app identity such as the information of HTTP sessions, ads, devices, and user details. Such KVs will be conflicted because apps are used in variable scenarios. The conflict property exhibits transitivity. A pair of co-occurring KVs, i.e., an undetermined KV and an identified KV, will be conflicted if there is another undetermined KV that co-occurs with the identified KV but conflicts with the undetermined KV. FLOWR eliminates such flow triplets, i.e., the identified KV and two undetermined KVs.

To illustrate the co-occurrence verification algorithm, we consider two KVs, $\mathtt{KV_1}$ and $\mathtt{KV_2}$, and check whether $\mathtt{KV_1}$ and $\mathtt{KV_2}$ overlap within $\mathtt{T}$ sec, i.e., whether $\mathtt{S(KV_1)-T<E(KV_2)}$ and $\mathtt{E(KV_1)+T>S(KV_2)}$. $\mathtt{S(\cdot)}$ and $\mathtt{E(\cdot)}$ are the flow start time function and flow end time function respectively, and $\mathtt{T}$ is a time gap parameter. The impact of $\mathtt{T}$ is evaluated in §4.1.4.3.

To compute co-occurrence likelihoods, a naïve approach would be to count the number of co-occurrence events. However, we observe that some KVs in flows are generated tens of times within few seconds, which biases the computation of $\mathtt{P[A{=}X|KV]}$. This often happens on a* service flows, which are produced programmatically by ad libraries. An improvement is to count by the number of time windows, i.e., all co-occurrences within a certain time window are counted only once to avoid the over-estimation. However, the method remains biased towards the apps that keep running in the background, e.g., `com.accuweather.android`. Counted by the number of time windows, background apps may appear in many time windows, which results in that they co-occur many times with many KVs. To address these issues, FLOWR computes $\mathtt{P[A=X|KV]}$ based on the number of unique network addresses, which is an estimation on the number of users, i.e., all co-occurrence events from the same address is counted once only. We estimate $\mathtt{P[A=X|KV]}$ by dividing the number of unique addresses where `KV` co-occurs with app `X` by the number of unique addresses originating `KV`.

4.1.3 Datasets

We utilize two data sources of network traffic to evaluate FLOWR, as shown in Table 4.2. Here we describe these data sources. In practice, FLOWR does not require any specific proprietary data source.

Dataset	Source	Scalability	Availability	Duration	Description
FlowSet	network	>22K apps	real-time	07/04/12-07/09/12	Collected from a gateway in a nationwide cellular network
AppSet	Android emulator	5K apps 10K apps	4+4 runs	N/A	Top 5K free apps in Google Play, and another 10K random apps

Table 4.2: Datasets used in evaluating FLOWR. FlowSet consists of 10 billion flows from 300K re-used IP addresses behind NAT. In AppSet, one run produces 30 bidirectional HTTP flows for an app on average.

4.1.3.1 FlowSet: a cellular network trace

We use a packet trace provided by an anonymized U.S. nationwide cellular network provider, which is named as FlowSet. FlowSet is dominated by Android devices and has a fraction of Windows Phone, Blackberry, and iOS traffic as well.

FlowSet captures the traffic traversing through a gateway of the network provider of six days (from July 4th to July 9th, 2012) with more than 10 billion traffic flows. We observe 22K apps in FlowSet just by counting the KVs of `app_name` in the HTTP requests to `doubleclick.net`. However, it does not have the ground truth of the app identity for every network flow. One use of FlowSet is the input to FLOWR's flow regression, the source information of which flow signatures co-occur. The other use of FlowSet is for evaluating FLOWR's performance in §4.1.4.

4.1.3.2 AppSet: an emulation trace

As FlowSet does not provide us the ground truth of the origins of network flows, we produce AppSet by emulating apps in Android emulators. We do not and cannot simulate comprehensive app behavior in AppSet. As long as the emulated traffic covers some traffic that can be potentially observed in FlowSet, it is qualified enough. We do not emulate on other systems such as iOS and Windows Phone because the emulation on Android already meets our purpose. In §4.1.1.3, §4.1.4.2, and §4.1.4.4, we discuss how we utilize AppSet.

In order to emulate apps, we have to (i) determine the target apps as it is impossible to emulate all the apps on Google Play, (ii) crawl the installation packages of the target apps, and (iii) emulate the target apps in Android emulators configured with different Android OS versions.

- Determining target apps. Given it is prohibitive to dump the entire set of apps on Google Play, we decide to download the most popular apps first. On Google Play, only the top 5K apps are directly open to the public. As indicated by previous studies [122], no matter how apps are ordered, i.e., by the traffic volume, by the access time, or by the number of users, the total contribution of the top 5K apps should consistently cover 98% of traffic volume. Thus, the top 5K apps on Google Play should represent the dominant apps in FlowSet. In addition to the top 5K apps, we automate random searching on Google Play and discover another 10K apps.

- Crawling installation packages. In order to download installation packages through app identifiers, we modify a Chrome Browser extension named APK Downloader [2] to download the target installation packages in parallel, i.e., 6 packages per “Chrome New Page” action. On average, we can download 12 installation packages from Google Play every minute.
- Emulating apps. We run the crawled app packages on two different Android OS emulators, i.e., Gingerbread and Ice Cream Sandwich. In emulation, the emulator interacts with apps through automated random clicks and random inputs. One run of an app generates 600 random events including clicks and inputs. On average, we can emulate 10K apps once every 24 hours via 10 Ubuntu 12.04 virtual machines on an off-the-shelf machine.

4.1.4 Classification Performance

As described, to address the challenge of flow identification, FLOWR performs two-phase operations: KV tokenization and flow regression. We first evaluate KV tokenization by characterizing the flow signatures produced by KV tokenization, and then we evaluate flow regression from the aspects of false positive, flow coverage, and app coverage, along with how we develop the approach to quantify the false positive without the ground truth of app identities.

4.1.4.1 Terminology

We use the following terminology to discuss evaluation results.

- **Uniqueness.** As a KV can be related with multiple apps, such as a KV corresponds to a developer ID that holds several apps. Thus, the uniqueness of KV is to evaluate how specific it is to an app. `uniq(KV)` returns whether KV is unique to an app.

- **Identifiability.** As defined in §4.1.1.3, the identifiability of a KV is the co-occurrence likelihood with the most frequently co-occurred app, i.e., $\mathtt{id(KV)}$.
- **Probabilistic false positive.** Given a random KV whose identifiability is above a threshold $\mathtt{P_0}$, the probability that it is not unique to an app, i.e., $\mathtt{P[!uniq(KV)|id(KV)>P_0]}$.

4.1.4.2 Signature quality

We first investigate the uniqueness of user-agents and contacted hostnames, which is a baseline for the quality of the flow signatures produced from KV tokenization. Figure 4.3 shows the uniqueness of user-agents and hostnames among the traffic flows generated by apps in AppSet. As shown in Figure 4.3, among the traffic produced in emulating the 5K apps, we observe only 200 unique user-agents. Even worse in the 10K apps, we observe around 400 unique user-agents in 10K. Aggregating the 5K and 10K apps together, we observe <500 unique user-agents in total. In AppSet, a single app can have 3 unique user-agents on average. Apparently, the information revealed from the distinctness among user-agents is insufficient, particularly for a larger number of apps. Similarly, the uniqueness of the domains access by the apps in AppSet is not sufficient either although it is slightly better.

To justify if the flow signatures produced in KV tokenization are of good quality, we rely on two criteria: persistence and uniqueness. There are nontrivial KVs that are for one-time usage, e.g., the KVs of session IDs and request IDs. There are also considerable KVs that are specific to the device, the user, the time, etc. These KVs can be very unique, but not persistent over multiple runs. In flow regression, such non-persistent KVs will be eliminated by screening conflicted KV as described in §4.1.1.3. In evaluation, we eliminate these non-persistent KVs before we evaluate the uniqueness.

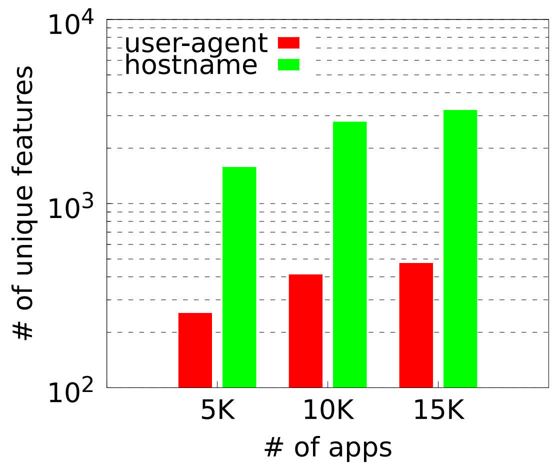

Figure 4.3: Uniqueness of user-agents and contacted hostnames.

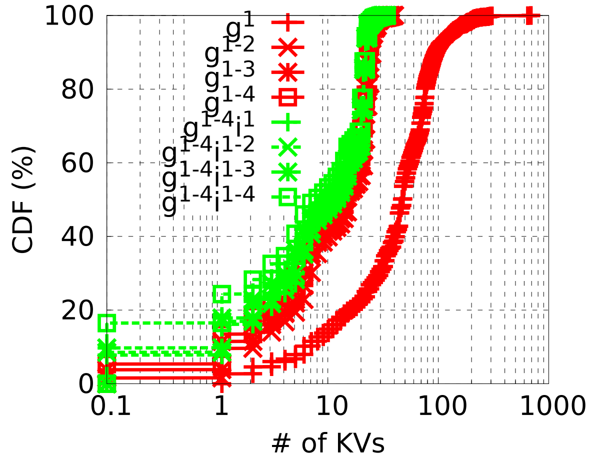

Figure 4.4: Persistence of KVs. "g^1" is especially for one run of Gingerbread. "[ig]$^{1-k}$" refers to which runs are aggregated.

Persistence. We rely on the flows in AppSet to quantify the quality of KVs because it provides us the ground truth on the origin of each flow. As shown in Table 4.2, we have 8 independent runs for each app in AppSet, among them 4 runs are on Gingerbread and the other 4 are on Ice Cream Sandwich. We consider a KV as a persistent one if it appears on both Gingerbread and Ice Cream Sandwich and it does not conflict with any KV else. We aggregate multiple runs together, eliminate conflicted KVs, and leave the remaining ones as persistent KVs. We show the distribution of the number of persistent KVs for the apps in AppSet in Figure 4.4. On average, an app has around 50 KVs in one emulation run. Aggregating two Gingerbread runs, the number of consistent KVs per app immediately drops to around 10. Apps vary a lot depending on how many content servers and a* service providers they contact. With further aggregations, the number of consistent KVs becomes stable even after we aggregate the total 4 Gingerbread and 4 Ice Cream Sandwich runs. We have two observations from Figure 4.4: (i) there are nontrivial consistent KVs although the majority of KVs are non-persistent; and (ii) the consistent KVs repeat over runs as reflected by the stabilized number of persistent KVs after aggregating two or more runs.

Uniqueness. To prevent the quantification on the uniqueness of consistent KVs being limited by the apps in AppSet or the emulation setup, we attempt to discover certain trend that is applicable to universal apps. We measure the entropy of the dissimilarity across flows signatures from the apps that visit the same domain in AppSet.

Given a domain $\mathtt{D}$ that appears in AppSet, we know all the apps in AppSet visit the domain and the consistent KVs for each of these apps. Across apps visiting $\mathtt{D}$, they may or may not have the same set of consistent KVs. Assuming these consistent KV sets are $\{\mathtt{KV}\}_1, \{\mathtt{KV}\}_2, \ldots, \{\mathtt{KV}\}_\mathtt{K}$, where $\mathtt{K}$ is the number of unique consistent KV sets. The entropy of $\mathtt{D}$ is $-\sum_{i=0}^{K} \mathtt{P}[\{\mathtt{KV}\}_\mathtt{i}] \log_2 \mathtt{P}[\{\mathtt{KV}\}_\mathtt{i}]$.

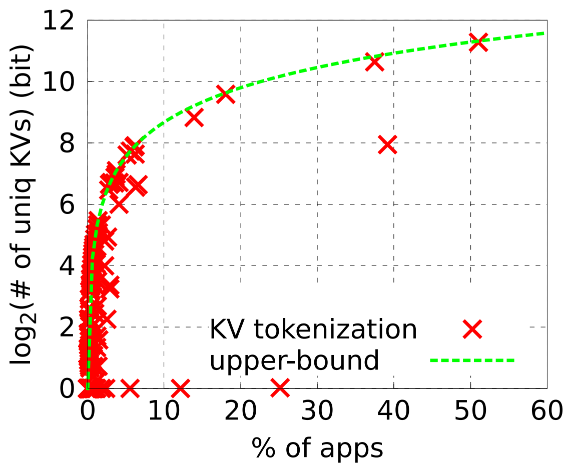

Figure 4.5: Uniqueness of KVs. A k-bit difference means classifying a flow to 2^k candidates.

Figure 4.5 shows the scatter distribution of the entropy of all domains observed in AppSet as the function of the percentage of apps that visit the domain. According to Figure 4.5, most domains are visited by very few apps, while a few domains (e.g., a* services) are very popular in apps. Given a domain visited by N apps, the upper-bound of its entropy is $\log_2(N)$, which happens only if each of the N apps has a unique set of consistent KVs. A k-bit difference from the upper-bound indicates that the N apps visiting this domain originate $\frac{N}{2^k}$ unique consistent KV sets, which means that we can only account the flows to a set of 2^k candidate apps. The entropy for most domains cannot be far away from the upper-bound because these domains are visited by limited numbers of apps. For the remaining few domains that are visited by a large number of apps, the entropy is extremely close to either the upper-bound or zero. If a popular domain attempts to keep track of apps, it often allocates unique identifiers which can ease app management. Otherwise, the entropy will be close to zero because it is very difficult to differentiate a large number of apps without identifiers allocated. Overall, the entropy revealed from the KVs produced by KV tokenization is close to the one allowing us to identify flows to apps uniquely. As the distribution of the number of apps accessing the same

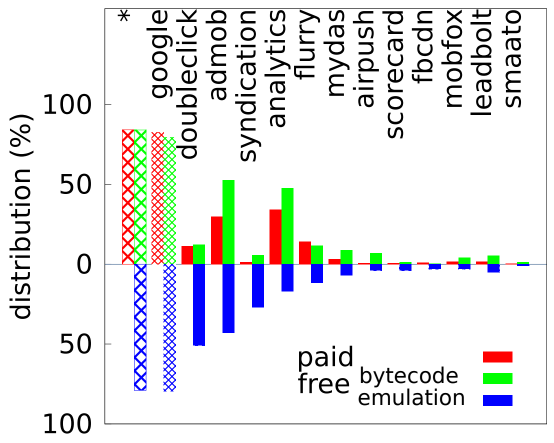

Figure 4.6: Web analytics and ad services in paid and free apps.

domain should be consistent for universal apps, we expect that the quality of flow signatures should be the same good.

Applicability. The popularity of a* services among apps is another important factor affecting the quality of the KV signatures. If a* services are not widely used, FLOWR can only distinguish but cannot identify apps without further supervised learning. There are two ways to determine the popularity: (i) in AppSet, we can detect whether an app contacts any a*service; and (ii) we can perform well-established bytecode analysis [48] on the installation packages to determine the included a* service libraries. In comparison, AppSet may under-estimate the presence of a* services due to incomplete emulation, while bytecode analysis may over-estimate it since a compiled ad library may not be invoked in run-time. According to Figure 4.6, in both estimations, 80% of the apps in AppSet use one or more a* services. Due to some inconsistency among google services, e.g., `admob` library may produce `doubleclick.net` traffic, we aggregate google services into "google" in Figure 4.6. To confirm that analytics services are still widely used by paid apps, we perform the same bytecode analysis on the top 500 paid apps as well. According to Figure 4.6, around 83% of paid apps use a* services.

4.1.4.3 Resource utilization

As described in §4.1.1.3, given two KVs, $\mathtt{KV}_1$ and $\mathtt{KV}_2$, FLOWR considers them co-occurred if $\mathtt{KV}_1$ and $\mathtt{KV}_2$ overlap within `T` sec. If the chosen `T` is under-estimated, i.e., $\mathtt{KV}_1$ and $\mathtt{KV}_2$ are from the same app but their time difference is greater than `T`, FLOWR will be more likely to miss some valid co-occurrence events. On the opposite, if `T` is over-estimated, FLOWR will be more likely to consider two flow signatures from two different apps co-occurred. As FLOWR can repeatedly validate if $\mathtt{KV}_1$ and $\mathtt{KV}_2$ are from the same app, FLOWR can tolerate an over-estimated `T` a bit to prevent under-estimation.

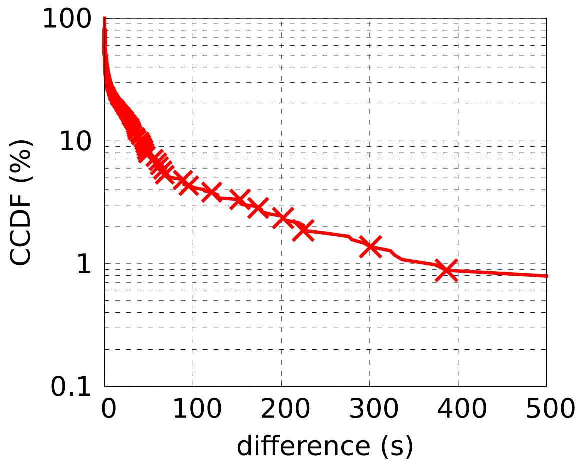

Figure 4.7: Time difference between two flows (likely) from the same app.

Co-occurrence timeout. In order to identify an appropriate `T`, we leverage the doubleclick flows in FlowSet because the app identities of doubleclick flows are explicitly expressed in the KVs of `app_name=XYZ`. For every KV in FlowSet, we search for the timely closest doubleclick flow. For these KVs that always stick to only one app identifier expressed in doubleclick flows, we can confidently expect that they are from the corresponding apps, and then we can calculate the time difference between them and the corresponding doubleclick flows. Figure 4.7 shows the complementary cumulative distribution function (CCDF) of the time differences. According to Figure 4.7, 99% of flows co-occur with their closest doubleclick flows within 300 sec. Accordingly, FLOWR sets `T` to 300 sec as the threshold to cover most co-occurrence events. According to our further evaluation, the additional benefit from increasing `T` to 600 and 1200 sec is negligible.

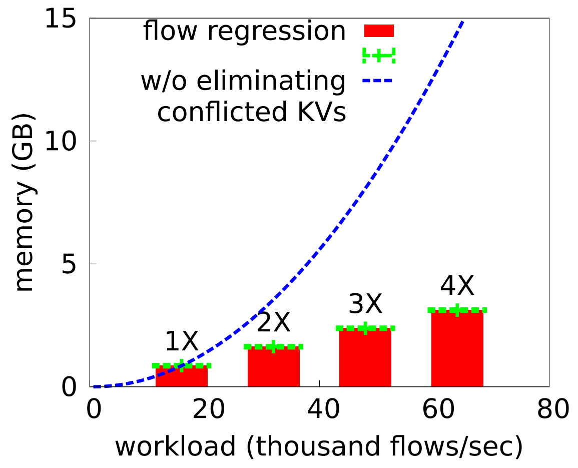

Figure 4.8: System memory consumption under (1X, 2X, 3X, and 4X) workload growth.

Memory. Given the parameter setup, understanding FLOWR's resource utilization is important, e.g., allowing us to evaluate its scalability particularly for exponentially growing mobile data traffic. The memory consumption for examining co-occurred flow signatures is `N`-square over traffic volume growth, but FLOWR can save significant memory consumption in eliminating conflicted KVs. To estimate the memory consumption when traffic volume increases `N` times, we merge the traffic of `N` days into one by offsetting timestamps. Figure 4.8 shows the run-time memory consumption over FlowSet (e.g., 1X), and the cost when traffic volume is increased 2X, 3X, and 4X. Under the current workload, i.e., 16K flows per second, the memory consumption is $<$1GB. Also, it is roughly linear to the traffic volume growth, which is far less the expected `N`-squared growth without eliminating conflicted KVs.

4.1.4.4 Identification accuracy

According to Figure 4.6, the apps utilizing a* services such as `doubleclick.net` and `airpush.com` generate traffic with app identifiers embedded somewhere so that FLOWR can identify them through flow regression without any supervised learning effort. For the apps utilizing other a* services without app identifiers but with some unique identifiers such as `google-analytics.com` and `fbcdn.com`, FLOWR can identify them with negligible training effort in mapping the unique identifiers to the app identifiers on app market. It can be done via various approaches such as the emulation in §4.1.3.2. In evaluating flow regression, we consider only doubleclick apps[4]. The evaluation results should be extendable to apps using other a* services. In previous §4.1.1.3 and §4.1.4.3, we show the detection of co-occurrences. In the following, we evaluate the performance of the identified flow signatures from the aspects of the false positive (§4.1.4.4), the flow coverage (§4.1.4.5), and the number of identified apps (§4.1.4.5).

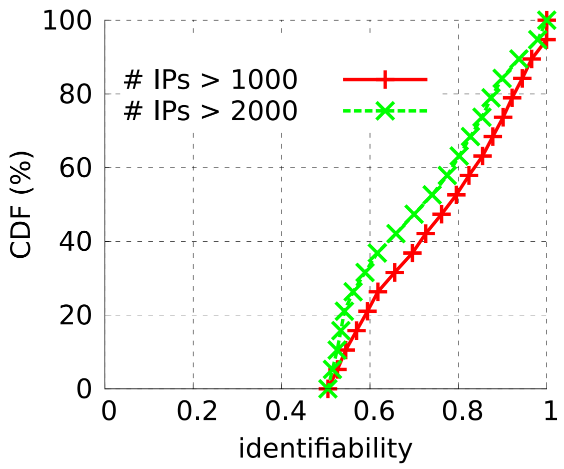

Figure 4.9: Identifiability of the KVs whose $\mathtt{id(KV)}>0.5$.

Identifiability. Once we have identified the appropriate timeout `T` sec for co-occurrence examination, a remaining decision is how we decide if the

[4]We name the apps with doubleclick flows as doubleclick apps.

co-occurrence likelihood is great enough to indicate the KV belonging to an app uniquely, i.e., the co-occurrence likelihood that meets $\mathtt{P[A=X|KV]\approx 1}$. Before we decide the threshold on the co-occurrence likelihood, we first investigate the identifiability distribution of KVs (defined in §4.1.1.3) in Figure 4.9, we only consider those KVs with the identifiabilities greater than 0.5, which is an aggressive threshold to filter out the non-persistent KVs and the KVs in CR but keep the KVs in UR according to Figure 4.10 (discussed in §4.1.4.4). Figure 4.9 shows the distribution of the identifiabilities for the KVs observed from more than 1000 unique IPs and 2000 unique IPs. Although the majority of the remaining KVs are in UR, the identifiabilities are not 1.

There can be two conditions for a KV to have the identifiability far from 1: (i) the KV can be originated by more than one app; and (ii) the KV is uniquely originated by a certain app, but due to some app specific reasons such as the app implementation and the user interaction behavior, the KV may not always co-occur with any flow identified as the app. As we cannot easily differentiate these conditions for all KVs, an alternative solution is to determine the false positive if we account a KV to an app when the identifiability is above any given threshold, i.e., $\mathtt{P[!uniq(KV)|id(KV)>P_0]}$, where $\mathtt{P_0}$ is a given identifiability threshold.

In order to determine the mapping from the identifiability to the false positive, we combine FlowSet and AppSet, utilizing FlowSet to determine the identifiabilities of KVs and adopting AppSet to estimate the uniqueness of KVs. As mentioned, AppSet includes the top 5K apps on Google Play, which can representatively generate most traffic in FlowSet no matter how Google Play ranks the top 5K apps [122]. In AppSet, if a KV is observed to be unique to an app in the top 5K apps, this KV is likely to be originated by the same app in FlowSet as well. Even though the KV may be originated by some other app outside the top 5K apps, the traffic contributed by the other app should be negligible, which means that in practice, the false positive should be small if FLOWR accounts the flows matching the KV to the app in top 5K. Similarly, we can also estimate the non-unique KVs from AppSet, i.e., the KVs that appear from more than one app in AppSet. We name the KVs estimated to be unique from AppSet as estimated-unique KVs and the KVs estimated to be non-unique from AppSet as estimated-non-unique KVs, respectively.

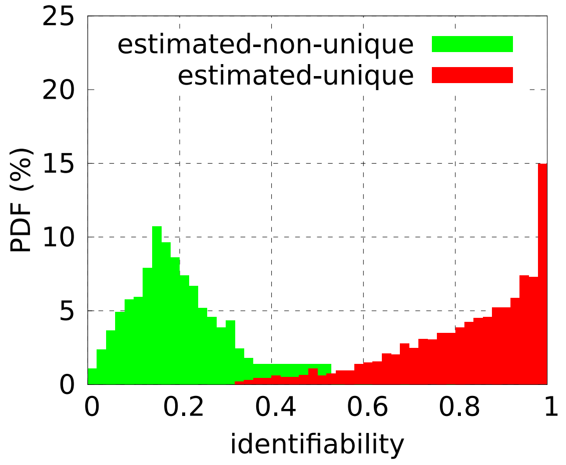

Figure 4.10: Identifiability of unique/non-unique KVs.

False positive. According to FlowSet, we can determine the identifiabilities of both the estimated-unique KVs and the estimated-non-unique KVs. Figure 4.10 shows the probability distribution function (PDF) of the identifiabilities of the two types of KVs. As shown in Figure 4.10, the identifiabilities for the estimated-unique KVs are much greater than the estimated-non-unique KVs. The majority of the estimated-unique KVs have the identifiabilities greater than 0.5, while most estimated-non-unique KVs have the identifiabilities less than 0.5. Thus, in general, if a KV's identifiability is high, it is likely that the KV is unique to an app, i.e., the false positive to account the flows matching the KV to the app is low. As the estimated-unique KVs include some non-unique KVs due to the limited coverage of AppSet, the identifiabilities of unique KVs should be further higher.

Given an identifiability threshold P_0, Figure 4.10 is still a step away from

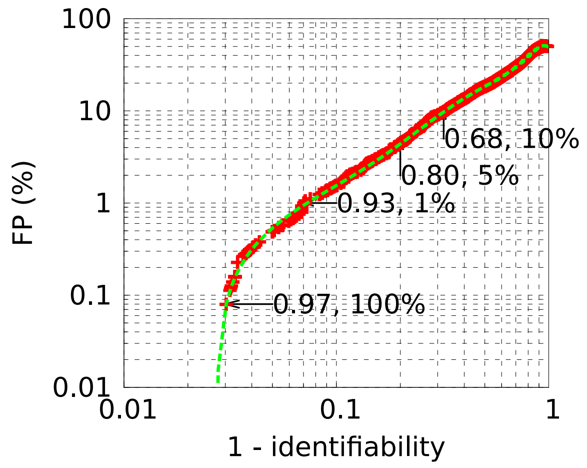

Figure 4.11: Mapping from identifiability to false positive.

determining the probabilistic false positive, i.e., $\mathtt{P}[!\mathtt{uniq}(\mathtt{KV})|\mathtt{id}(\mathtt{KV})>\mathtt{P}_0]$. Figure 4.10 tells us two functions: $\mathtt{P}[\mathtt{id}(\mathtt{KV})>\mathtt{P}_0|\mathtt{uniq}(\mathtt{KV})]$ and $\mathtt{P}[\mathtt{id}(\mathtt{KV})>\mathtt{P}_0|!\mathtt{uniq}(\mathtt{KV})]$, denoted as $\mathtt{PU}$ and $\mathtt{PN}$ respectively. Applying Bayes' theorem, we have $\mathtt{P}[\mathtt{uniq}(\mathtt{KV})|\mathtt{id}(\mathtt{KV})>\mathtt{P}_0]=\frac{\mathtt{PU}\cdot\mathtt{P}[\mathtt{uniq}(\mathtt{KV})]}{\mathtt{PU}\cdot\mathtt{P}[\mathtt{uniq}(\mathtt{KV})]+\mathtt{PN}\cdot\mathtt{P}[!\mathtt{uniq}(\mathtt{KV})]}$. $\mathtt{P}[\mathtt{uniq}(\mathtt{KV})]$ and $\mathtt{P}[!\mathtt{uniq}(\mathtt{KV})]$ can be estimated from AppSet. Based on the above transformation, Figure 4.11 shows the mapping from the identifiability to the false positive, which is weighted based on the number of flows that each KV matches in FlowSet. According to Figure 4.11, it is common that a flow signature is unique to an app but its identifiability is far less than 1. To guarantee the false positive less than 5%, FLOWR can label all flows whose flow signatures have the identifiabilities greater than 0.8. If FLOWR wants to further relax the false positive lower-bound to 10%, all flows whose flow signatures have the identifiabilities greater than 0.68 can be uniquely identified, but the benefit in terms of flow coverage is marginal (to discuss in Figure 4.13(a)). After the threshold on the identifiability is increased to 0.93, the false positive drops to less than 1%. In our dataset, we never see that any flow signature with the identifiability higher than 0.97 is originated by more than one app.

4.1.4.5 App and flow coverage

The number of flows that can be identified by FLOWR depends on the knowledge base of app signatures, while the knowledge base keeps growing as FLOWR determines the identities of new KVs via backend flow regression. In order to determine the flow coverage of FLOWR, we iterate FlowSet round by round as the input to flow regression. In each round, FLOWR captures the co-occurrence events between the undetermined KVs and the identified KVs with zero false positive (i.e., the identifiabilities greater than 0.97 according to Figure 4.11) and updates the knowledge base. In the next round, FLOWR can detect the co-occurrence events between the remaining undetermined KVs and the updated the knowledge base. In practice, without supervised learning, the flow coverage of FLOWR should be close to the converged flow coverage over iterations.

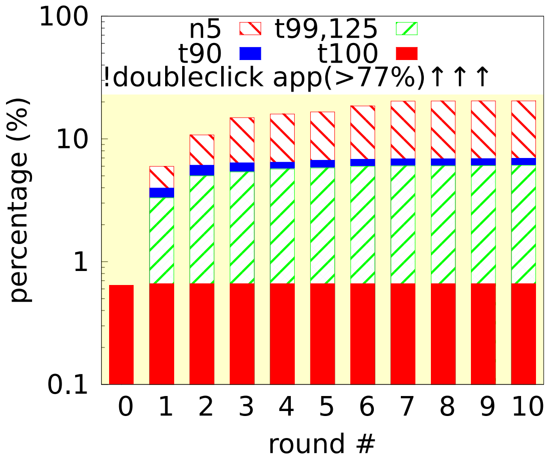

Figure 4.12: Flow coverage starting with doubleclick apps. We use the baseline of $<$23% of flows (flow fraction of doubleclick apps), because the knowledge base is initialized using only doubleclick flows.

Flow coverage. As the quality of KVs in the knowledge base of app signatures differs, in identifying flows to apps, FLOWR classifies flows based on their identifiabilities into the 5 categories listed in Table 4.3. Four categories correspond to flows that can be uniquely identified: 100% true positive ("t100"), 99% ("t99"), 95% (“t95”), and 90% (“t90”). To determine if a flow belongs to these four categories, we can refer to Figure 4.11 to decide the threshold on the identifiability. Besides the four categories of uniquely identified flows, there is another one category: the flows narrowed down to 2–5 apps with the false positive less than 1% (“n5”). The true positive for FLOWR to narrow down a flow signature to no more than 5 apps is the co-occurrence likelihood between the flow signature with any one of the 5 apps.

Tag	Condition	Accuracy	Description
t100	$\exists \mathtt{KV}, \mathtt{id}(\mathtt{KV}) \geq 0.97$	$\mathtt{FP}=0$	The maximum identifiability is at least 0.97. This leads to FLOWR’s true positive in labeling the flow with 100%.
t99, t95,t90	$\exists \mathtt{KV}, \mathtt{id}(\mathtt{KV}) \geq 0.93, 0.80, 0.68$	$\mathtt{FP} \leq 1,5,10\%$	Similar to “t100”, the maximum identifiability is at least 0.93, 0.80, or 0.68. This leads to true false positive of 99%, 95%, or 90%.
n5	$\exists \mathtt{KV}_\mathtt{i}, \mathtt{i}=1...5, \sum_{\mathtt{i}=1}^{5} \mathtt{id}(\mathtt{KV}_\mathtt{i}) \geq 0.99$	$\mathtt{FP} \leq 1\%$	FLOWR cannot classify the flow to a single app“t100”, but can narrow down it to 2–5 apps with true positive $>$ 99%.

Table 4.3: Categories of flow signatures. The “t100”, “t99”, “t95”, and “n5” KVs are considered as identified.

Figure 4.13(a) shows the fraction of flows in each category listed in Table 4.3 over iterations of flow regression. Without flow regression, FLOWR can only identify the app identities of doubleclick flows, which account ≈0.7% of flows in FlowSet. Although the fraction of identifiable flows with zero false positive (i.e., “t100”) is consistently small over iterations, as a probabilistic approach, FLOWR can uniquely identify 6–7% of flows with no more than 5% false positive. According to Figure 4.13(a), further relaxing the false positive requirement does not obviously improve FLOWR’s flow coverage since “t90” only contributes 1% of flows in addition to “t95”. “n5” contributes another 14% of flows. Combining the 6–7% of flows uniquely identified from “t100”, “t99”, and “t95”, and the 14% of flows narrowed down to no more than 5 apps, FLOWR can identify 21% of flows in FlowSet.

Although we can determine the flow coverage of FLOWR, and the corresponding false positive in each category in Table 4.13(a), so far, we do not know how good the 21% flow coverage is, which is an important indicator on the benefit from other a* services with either app identifiers (e.g., `admob.com`, `bugsense.com`, and `umeng.com`) or other unique identifiers (e.g., `google-analytics.com`, `mobclix.com`). Hypothetically, if the 21% is close to the percentage of flows generated by doubleclick apps, FLOWR's flow coverage is good, and we can expect that FLOWR can have similar flow coverage for the apps with other a* services.

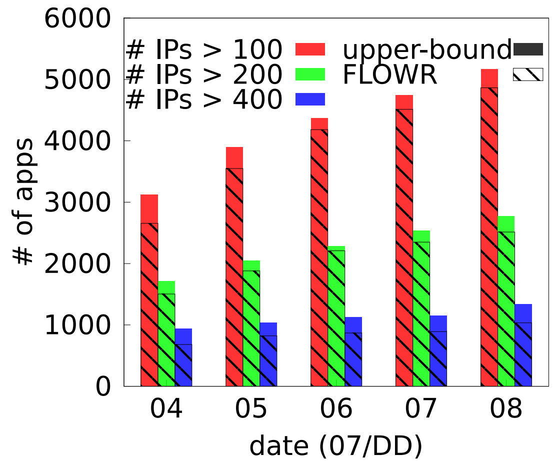

Figure 4.13: Number of identified doubleclick apps.

To estimate the fraction of the flows generated by doubleclick apps, for each flow in FlowSet, if there is no doubleclick flow from the same IP address within 30 min, we assume that the flow is unlikely produced by any doubleclick app. 30 min is longer than the app session length of 99% of apps and 99% of users [122, 50]. Through the over-estimation on the number of flows not generated by doubleclick apps, we determine that 77% of flows do not co-occur with any doubleclick flows on the same device in 30 min. In other words, there should be no more than 23% of flows that originated by doubleclick apps. Translated into flow coverage, FLOWR can uniquely identify 26–30% (i.e., 6–7% in 23%) flows and narrow down 60–65% (i.e., 14–15% in 23%) to 2–5 candidate apps. Without FLOWR, only 3% (i.e., 0.7%

in 23%) can be identified.

App coverage. Above we evaluate the performance of FLOWR based on the flow coverage. As flow contribution is uneven across apps due to their diverse usage, we are interested in the number of identified apps by FLOWR in addition. FLOWR has a threshold on the number of occurrences of flow signatures to prevent that the flow signatures with the high identifiabilities but insufficient samples from polluting FLOWR's the knowledge base. Given the threshold on the number of occurrences of flow signatures, we compare (i) the baseline, i.e., the number of apps producing doubleclick flows against (ii) the number of apps whose flows are identified by FLOWR in Figure 4.13(b). On July 4th 2012, the total number of appeared doubleclick apps from more than 100 IPs is around 3000. Among the flows generated by these 3000 apps excluding doubleclick flows, FLOWR identifies around 2700 apps, which means that FLOWR's flow regression technique works for 90% of apps. If we further increase the threshold on the number of flow occurrences to 200 and 400, FLOWR can identify 1500 from 1700 apps, and 700 from 900 apps respectively. Another aspect is that the number of identified apps by FLOWR should grow over time rather than converge after sometime. To evaluate the number of additional identified apps over time, we aggregate the flows from July 4th to different end dates, i.e., 5th–8th. According to Figure 4.13(b), the number of identified apps grows linearly over time, consistently identifying more than 90% of doubleclick apps.

4.1.5 Limitation

FLOWR has the weakness in identifying encrypted or hashed network traffic or the traffic originated by the apps not using any a* services.

4.1.5.1 Encrypted or Hashed Flows

In KV tokenization, FLOWR performs traffic inspection on HTTP requests. Thus, for non-plain-text flows such as HTTPS or hashed flows, KV tokenization does not work although the fraction of such traffic is limited [122].

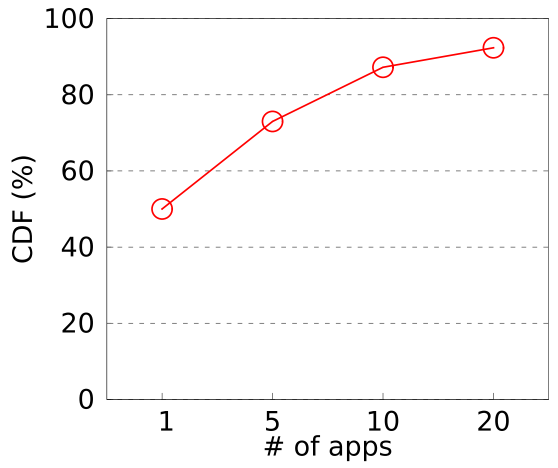

Figure 4.14: The uniqueness of HTTP certificates.

HTTPS traffic. For HTTPS traffic, one compromise solution is extending KV tokenization to extract app identity features from HTTPS certificates. We investigate the uniqueness of HTTPS certificates across the 342 apps that produce any HTTPS flows in AppSet. Figure 4.14 shows the cumulative distribution function (CDF) of the apps with respect to the uniqueness of their HTTPS certificates. According to Figure 4.14, 50% of apps have unique HTTPS certificates and 75% of apps have HTTPS certificates shared by no more than 5 apps.

Hashed traffic. Compared with HTTPS traffic, hashed traffic is much easier to identify using existing binary tokenization techniques [45]. Figure 4.15 shows the Android app `Blogger-droid` using `dataflurry.com` service. By comparing the traffic generated from different runs on Gingerbread and Ice Cream Sandwich, we can tell the string consistent over all runs (i.e. `9Q6GVJQ7BEN9PZDXUF9S`) and the string consistent over the same platform (i.e. `23AND9224b2b6a7bd7410`). Such

```
\0\10\0\0\0\3\0\36\0\0\x017\xA1>\21~\0\x149Q6GVJQ7BEN9PZDXUF9S\0\x052.0.4\0\
23AND9224b2b6a7bd7410\0\0\x017\xA1>\21i\0\0\x017\xA1>\21i\0\4\0\14device.mod
el\0\3sdk\0\1build.brand\0\7generic\0\10build.id\0\5GRI34\0\17version.releas
e\0\x052.3.3\0\0
```

(a) Gingerbread #1.

```
\0\10\0\0\0\3\0\36\0\0\x017\xA1>\21j\0\x149Q6GVJQ7BEN9PZDXUF9S\0\x052.0.4\0\
23AND9224b2b6a7bd7410\0\0\x017\xA1>\21W\0\0\x017\xA1>\21W\0\4\0\14device.mod
el\0\3sdk\0\1build.brand\0\7generic\0\10build.id\0\5GRI34\0\17version.releas
e\0\x052.3.3\0\0
```

(b) Gingerbread #2.

```
\0\10\0\0\0\3\0\36\0\0\x017\xB9\xC3k2\0\x149Q6GVJQ7BEN9PZDXUF9S\0\x052.0.4\0\
23AND29cec3acc3ae100a\0\0\x017\xB9\xC3k"\0\0\x017\xB9\xC3k"\0\4\0\14device.mod
el\0\3sdk\0\13build.brand\0\7generic\0\10build.id\0\3MR1\0\17version.releas
e\0\x054.0.4\0\0
```

(c) Ice Cream Sandwich #1.

Figure 4.15: Tokenization over compressed or hashed traffic flows (`dataflurry.com`). The red strings are unique to the app, and the green ones are unique to the platform.

hashed IDs allow us to differentiate the app, but it requires training effort to construct the knowledge base that associates such hashed IDs with the corresponding apps.

4.1.5.2 Developer Intentions to Avoid FLOWR

The developers of malicious apps may want to bypass the identification from FLOWR. We are insterested to explore the performance of FLOWR if a developer wants to intentionally hide from FLOWR. The developer anyway needs to decide where to place the server, either a personal owned one or certain public service, such as Amazon EC2. If he chooses a personal owned server, then the IP address or hostname of the server can be a very unique feature to identify his app. Otherwise, if the app mainly communicates with a public service, since most public services perform authentication on their customers using developer/app IDs/keys, such IDs/keys embedded in network flows can be leveraged as flow signatures.

4.1.5.3 Remaining Apps Not Using A*

Without training effort, the optimal flow coverage that FLOWR can pursue is the flows originated by the a* services embedded with either app identifiers on app market or other unique identifiers as shown in Table 4.1. However, some apps do not use a* services. To save supervised learning effort for the remaining 20% of apps, we need to explore further intelligence such as CAPTCHA [5].

4.2 Application Usage Characterization

Given the prerequisite for understanding mobile app usage is fulfilled by FLOWR, we start to investigate the usage patterns of smartphone apps in this section. A previous study found evidence that there is substantial diversity in the way that different people use smartphone apps [50]. However, because the study relied on volunteers using instrumented phones, it was limited to two platforms and less than three hundred users in a few geographic areas. Other studies of mobile application/app usage [53, 77, 108] have been similarly limited in scope. Thus, it is difficult to extrapolate these results to make representative conclusions about spatial locality, temporal variation, and correlation of apps at scale. For example, “where are apps more popular?”, “How is their usage distributed across a country?”, “How does their usage vary throughout the day?”. While there have been studies of smartphone performance at larger scales [62, 29, 52], which use volunteer measurements or network data to obtain measurements at scale, measuring the usage of different apps from these data sources is more challenging. Volunteer measurements are typically obtained by deploying a measurement tool via an app marketplace, but many popular platform APIs do not permit the measurement of other apps in the background, so it is difficult to write an app that captures this information. Network data may contain information that can identify app behaviors, but this information is not typically part of standard traces. To make representative conclusions about apps, we require a network data set that identifies apps in network traffic and contains a significant number of measurements covering a representative number of devices, users, locations, and times.

We address the limitations by collecting anonymized IP-level networking traces in a large tier-1 cellular network in the U.S. for one week in August 2010. In contrast to previous work, we use signatures based on HTTP headers (included in the IP-level trace) to distinguish the traffic from different apps. Due to the format of `User-Agent` in HTTP headers when mobile apps use standard platform APIs, this technique gives us the ability to gather statistics about each individual app in a marketplace, not just categories of network traffic characterized by port number. Moreover, our work examines the spatial and temporal prevalence, locality, and correlation of apps at a national scale, not just in one area or over a small population of users.

To our best knowledge, this is the first to investigate the diverse usage behaviors of individual mobile apps at scale, and we make the following five contributions:

- The data set that we use to study mobile apps is significantly more diverse geographically and in user base than previous studies. It covers hundreds of thousands of smartphones throughout the U.S. in a tier-1 cellular network. This allows us to make more generalizable conclusions about smartphone usage patterns.
- We find that a considerable number of popular apps (20%) are *local*, in particular, radio and news apps. In terms of traffic volume, these apps are accountable for 2% of the traffic in the **smartphone apps** category (i.e., all the marketplace apps that can be identified by `User-Agent`) – that is, their user base is limited to a few U.S. states. This suggests significant potential for content optimization in such access networks as LTE and WiFi where content can be placed on servers closer to clients.

Furthermore, it suggests that network operators need to understand the impact of different app mixes in different geographical areas to best optimize their network for user experience.

- Despite this diversity in locality, we also find that there are similarities across apps in terms of geographic coverage, diurnal usage patterns, etc. For example, we find that some apps have a high likelihood of *co-occurrence* on smartphones – that is, when a user uses one app, he or she is also likely to use another one. Users also use several alternatives for the same type of app (e.g., multiple news apps). These findings suggest that some apps can be treated as a “bundle” when trying to optimize for their user experience and that there may be opportunities for integration.
- We also find that the diurnal patterns of different genres of apps can be remarkably different. For example, news apps are much more frequently used in the early morning, sports apps are more frequently used in the evening, while other apps have diurnal patterns less visible and their usage is more flat during a day. These findings suggest that cloud platforms that host mobile application servers can leverage distinct usage patterns in classes of apps to maximize the utilization of their resources. Furthermore, network operators may be able to leverage these results by optimizing their network for different apps during different times of the day.
- Mobility patterns can be inferred from network access patterns. Some apps are more frequently used when users are moving around; some of them are used more often when users are stationary. Mobility affects connectivity and performance, so bandwidth sensitive apps that are mobile may need to consider techniques to compensate for bandwidth variability. We find that there is a significant degree of diversity in the mobility of apps.

The rest of this section is organized as follows: §4.2.1 describes our data set,

§4.2.2 presents our measurement results, §4.2.3 outlines some implications.

4.2.1 Datasets

We use an anonymized data set from a tier-1 cellular network provider in the U.S. It is collected during the week of August 24th, 2010 – August 30th, 2010. The data set contains flow-level information about IP flows carried in PDP Context tunnels (i.e., all data traffic sent to and from cellular devices). This data set is collected from all links between SGSNs and GGSNs in tier-1 network's UMTS core network. Hence, we have a nationwide view of cellular data traffic. Due to volume constraints, only traffic from a uniform random sample of devices is collected. For a random sample of devices, the data contains the following information for each IP flow per minute: the start and the end timestamps, per-flow traffic volume in terms of both the bytes and the number of packets, the device identifier, and the app identifier. All device and subscriber identifiers (e.g., IMSI, IMEI) are anonymized to protect privacy without affecting the usefulness of our analysis. Furthermore, the data sets do not permit reversing the anonymization or re-identification of subscribers.

We are concerned about four main features per app: **traffic volume**, **access time**, **unique subscribers**, and **locations**. We estimate traffic volume as the sum of the flow byte counts, access time as the sum of the flow durations (with a precision of seconds), and the number of unique subscribers as the number of distinct anonymous device identifiers. There is only one anonymized identifier per distinct device. To determine the location of each device at the time a flow is in progress, we use the cell sector identified in the PDP context used to tunnel the flow. This cell sector is typically recorded when the PDP context begins, when a device moves far enough that the SGSN its traffic routes through changes, switches from 2G to 3G (or vice versa), or switches from 3G to WiFi. While this sector may be slightly stale, previous work [119] showed that they are still almost always accurate to within 40 kilometers. Thus, they suffice for most of our results that only look at U.S. states as distinct regions. For other results we present on sector changes, we may underestimate the number of changes due to this limitation.

In total, the sample data set includes approximately 600K distinct subscribers and approximately 22K distinct smartphone apps.

4.2.2 Smartphone Application Usage Patterns

In this section, we investigate how, where, and when smartphone apps are used from spatial, temporal, and user perspectives. We first choose appropriate metrics to evaluate smartphone apps, and then attempt to understand the impact of location, time, user, and app interest accordingly.

4.2.2.1 Overall app usage

We begin our analysis by presenting some broad characteristics of smartphone app usage. For our analysis, we choose a number of different natural metrics that profile network activity. We use the following three metrics for each app through most of our analysis: (i)**traffic volume**, defined as the number of bytes consumed by all subscribers using the app; (ii)**number of subscribers**, defined as the number of unique subscribers using this app throughout our week-long data set; (iii)**network access time**, defined as the total duration summed across all the IP flows generated by the app over our week-long data set.

Figure 4.16 shows CDFs of these metrics for the apps. For each metric, we aggregate together all the users of a particular app. The long tail of these CDFs directly shows the huge diversity in smartphone apps and their network characteristics. The top app in Figure 4.16(a) is a "personalized Internet radio app", and is responsible for more than 3TB data in one week, while the majority of

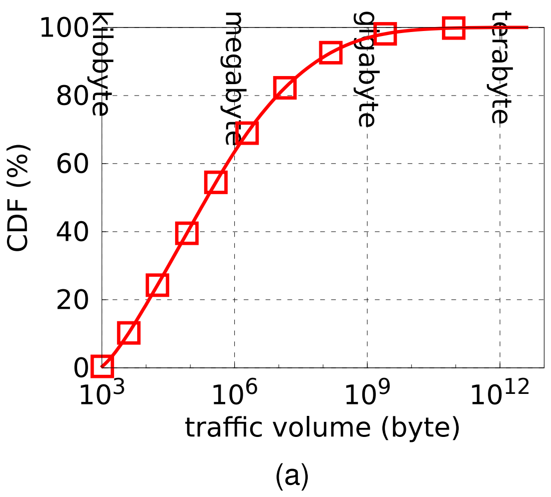

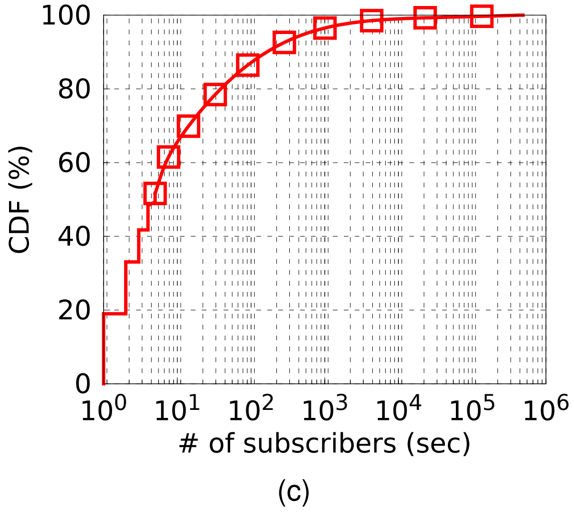

Figure 4.16: Traffic volume/access time/number of users for individual apps (aggregating users together in one week): (a) traffic volume, (b) access time, and (c) number of unique subscribers.

smartphone apps generate only 1 – 10 MB over the same time period. Note that this top app is by itself responsible for generating over 50% of the total traffic volume in the smartphone apps category. This dramatic variation in the traffic volume is due to many factors, e.g., app genres, popularity of apps, device types, preferences of the user base, content of apps, etc. For example, both news apps and radio apps may provide users with the latest news, but news apps typically deliver most of their content via text while radio apps deliver content via streaming audio; thus, users of these two apps would receive news on their smartphones with a substantial difference in the volume of traffic generated.

We observe a similar variation in Figure 4.16(b). The top app here is a “social utility connecting people", with a total network access time exceeding 100 years (aggregated across all its users). This app alone contributes to 86% of the total network access time of the smartphone apps category, but the majority of the smartphone apps are seen accessing the network for only about 1 minute – 1 hour. This "social utility" app also has the largest number of unique subscribers, 540,230 according to Figure 4.16(c). The total number of unique subscribers in our data set is 633,892 by examining the number of unique subscribers with DNS requests. Thus, we may estimate that 6 in every 7 subscribers use this "social utility" app on their smartphones. Recall that this data set contains only a random sample of subscribers, so the numbers here do not reflect the total number of subscribers in the cellular network. Around 60% smartphone apps have no more than 10 unique users in our data set, thus illustrating the long tail of smartphone apps on the market. Because of this long tail, we filter out the smaller apps for some of our analysis as they do not have enough measurements. We discuss this further in §4.2.2.2.

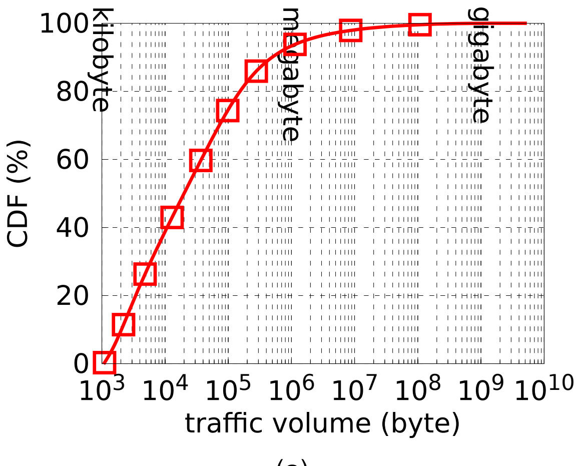

(a)

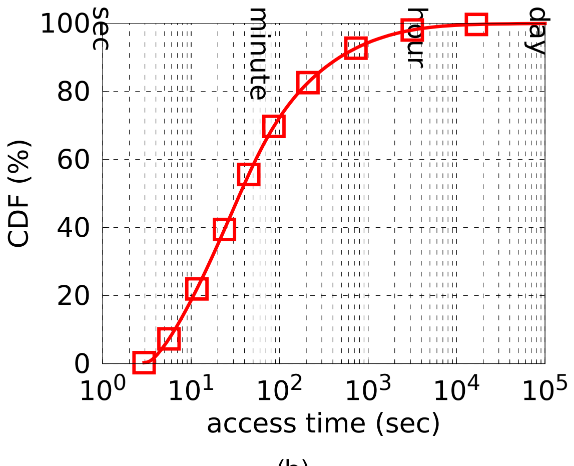

(b)

Figure 4.17: Single-user traffic volume/access time for individual apps.

Figure 4.17 shows the CDFs of the apps' traffic volume and access time, now normalized by the number of subscribers that use the app. We see a similar variation across apps in these CDFs as well. For example, in Figure 4.17(a), the app with the largest traffic volume per subscriber consumes 5GB in one week, but the majority of apps consume less than 1MB data per subscriber in the week. Likewise, in Figure 4.17(b), the app with the longest access time per subscriber lasts for 2 days in one week, while the majority of apps access the network for only 10 seconds – 1 hour per subscriber in the week. From Figure 4.16 and Figure 4.17, we also observe apps with very marginal usage in the long tail, e.g., the app consuming only less than 1KB, the app accessing the network less than 10 sec, and the app with only one user. These numbers indicate why we need to filter out these tiny apps for our analysis.

4.2.2.2 Popular apps

Figure 4.16 shows that there are a substantial number of smartphone apps with only 1 subscriber and that 60% of the smartphone apps have no more than 10 unique subscribers. Thus, these apps do not provide enough data for analysis, and, in this section, we explore how to decide systematically which apps can be considered popular and how we can eliminate the effect of apps with marginal usage on our analysis.

In effect, we want to identify the popular smartphone apps based on the numbers of their unique subscribers, but at the same time, we do not want to discriminate against apps with few subscribers that have a significant impact on the network, i.e., generate a lot of traffic or access the network for long time periods. So, we have two questions to answer: (i) is the number of unique subscribers a good metric for filtering? (ii) if so, what is a reasonable threshold on the number of unique subscribers?

Intuitively, if the number of unique subscribers is a good metric for filtering, the top `X` apps based on the number of unique subscribers should contribute similar amounts of traffic volume and access times as the top X apps based on the traffic volume or access time. We first compare the contribution of the top X apps based on different metrics. Figure 4.18 compares the contribution of the top X apps based on the number of unique subscribers against the top X apps based on the traffic volume and based on the network access time. We can observe that the cumulative contributions of the top X apps based on access time and the top X apps based on number of unique subscribers are quite close, by comparing the “access time” and the “access time by top subs”. Likewise, the contributions of the top X apps based on traffic volume and number of unique subscribers are also close, although a little difference does exist. We note that over 90% of the total volume and access time is accounted for by the top 1000 apps based on the number of unique subscribers.

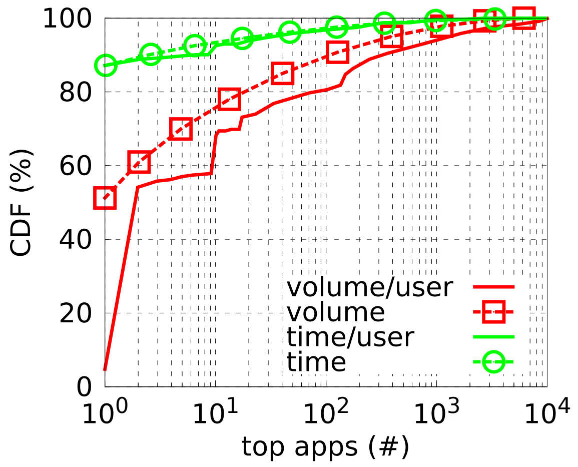

Figure 4.18: Contributions of the top X apps to traffic volume or access time. Is the number of unique subscribers a good metric for filtering?

Thus, Figure 4.18 indicates that somewhere above 1000 would be a reasonable boundary to distinguish popular apps from apps in the tail given the 90% coverage. We further explore the marginal nature of the apps ranking above 1000. The network access time and the traffic volume per user for apps ranking in 1000 – 4000. For both traffic volume and access time. The app accessing network the most consumes in the range of top 1000–4000 is only 250 seconds per user in a week, and the app transferring the most data generates only 500 KB per user in a week. Because of these small traffic volumes and short access times, we do not consider these apps to be sufficiently active for our analysis.

genre	books	business	education	entertainment	finance	games	healthcare	lifestyle	medical	music	navigation	news	photography	productivity	reference	social net.	sports	travel	utilities	weather	unknown
total	351	418	643	1827	283	3108	368	1298	205	1296	450	1126	475	527	515	721	787	590	1079	236	5865
popular	7	8	13	95	13	199	23	71	4	34	23	89	17	23	26	58	33	29	49	16	170

Table 4.4: Genres of apps.

Our discussion suggests that a natural threshold would be the top 1000 apps ranked by the number of unique subscribers. Table 4.4 shows the number of apps in each genre, both for the top 1000 apps as well as all the 22K apps. In the remainder, we will refer to these top 1000 apps as **popular apps**.

4.2.2.3 Spatial patterns: geographic usage distribution

Next, we investigate the diversity of smartphone apps being used by subscribers in different geographic locations. Understanding the spatial usage patterns of smartphone apps suggests ways to improve user experience and performance from many aspects, such as content placement, context-aware applications, and mobile advertisement system. Taking content placement as an example, if content providers know that some of their apps are most used at certain locations, they may choose to place content close to those locations so that users experience better performance.

We first examine whether any apps are **local apps**, i.e., whether the majority of an app's traffic comes from a region. We perform the following analysis: for each app, we divide its traffic by (U.S.) state of the user, and compute the top 1, 3 and 5 state(s) that contribute the most traffic volume or the longest network access times.

We expect that if an app's usage is truly localized, most of its traffic or access time (e.g., 90%) will originate from a small number of states.

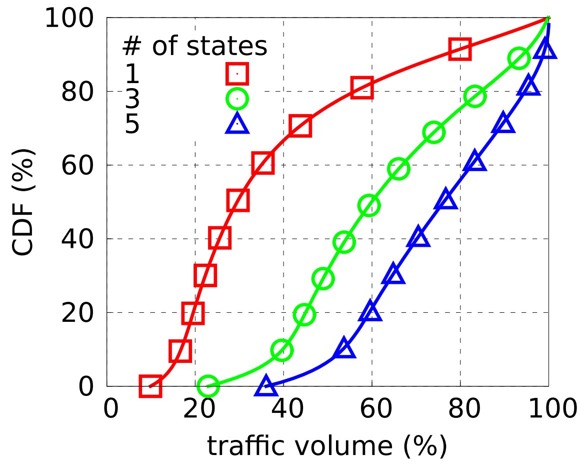

Figure 4.19: Traffic volume contribution from the top `X` states.

Figure 4.19 shows the CDF of the fraction of the traffic volume from top 1, 3, and 5 states for top 1000 apps that we have chosen in §4.2.2.2. According to Figure 4.19, 20% of the popular apps have more than 90% of their traffic volume originating from 3 states, 5.8% of the popular apps have 90% of the traffic originating from only 1 state, and 1.7% of the popular apps have all their traffic from 1 state. These 20% apps, which have more than 90% of their traffic volume originating from 3 states, account for 2% traffic in the smartphone apps category. The distribution of the contribution of access time of popular apps are very close to the one of traffic volume. Thus, we see that a significant number of the popular apps are local.

To explore what these local apps are and where they are localized, we examine in more detail the 100 most local apps based on the contribution of the top 3 states; for each of these apps, the top 3 states contribute at least 97% of their total traffic volume. Figure 4.20 shows the distribution of the top 3 states of the 100 most local apps; we differentiate the rank of the top 3 states for these 100 local apps as well so that we know, for example, California is the state that originated the most traffic

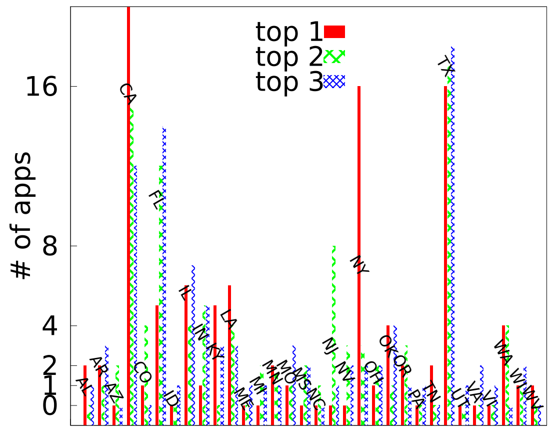

Figure 4.20: Breakdown of the top X states of the local apps.

app	description on Google
WWLTV	New Orleans News, Breaking News, Weather ...
KATC	News Coverage at Acadiana-Lafayette, Louisiana ...
KSLANews12	News, Weather and Sports at Shreveport, Louisiana ...
KPLC 7 News	Lake Charles, Louisiana – kplctv.com ...
WBRZ	TV Channel 2 Baton Rouge, LA ...
GoWAFB	Local news, weather ... at Baton Rouge, LA ...

Table 4.5: Local apps from Louisiana.

for 19 apps, the state originated the second most traffic for 15 apps, and the state originated the third most traffic for 12 apps. As expected, California, Texas, and New York are the states with most local apps – these are the states with large populations of smartphone users. However, there are many states with much smaller populations such as Louisiana, Wyoming, and Kentucky that also have some local apps; upon further analysis, this turn out to be because content from some apps is tailored specifically for users from some regions, e.g., local TV programs, news, radio, weather apps, etc. As an example for validation, we show the local apps for Louisiana in Table 4.5; we see that the six apps that have most of their traffic originating from Louisiana provide TV, news, radio and weather specifically for Louisiana residents.

Next, we examine the spatial patterns of smartphone app usage nation-wide.

For this analysis, we remove the 100 apps identified as local in the previous analysis (Section 4.2.2.3), and examine the nation-wide usage of the remaining apps' traffic. We term these remaining apps as **national apps**. Our analysis explores whether certain genres are more popular (or have heavier usage) in some areas than in other areas; in general, we do not expect users to prefer using apps of a specific genre as a function of their geographic location, but our results show that this does happen under certain conditions.

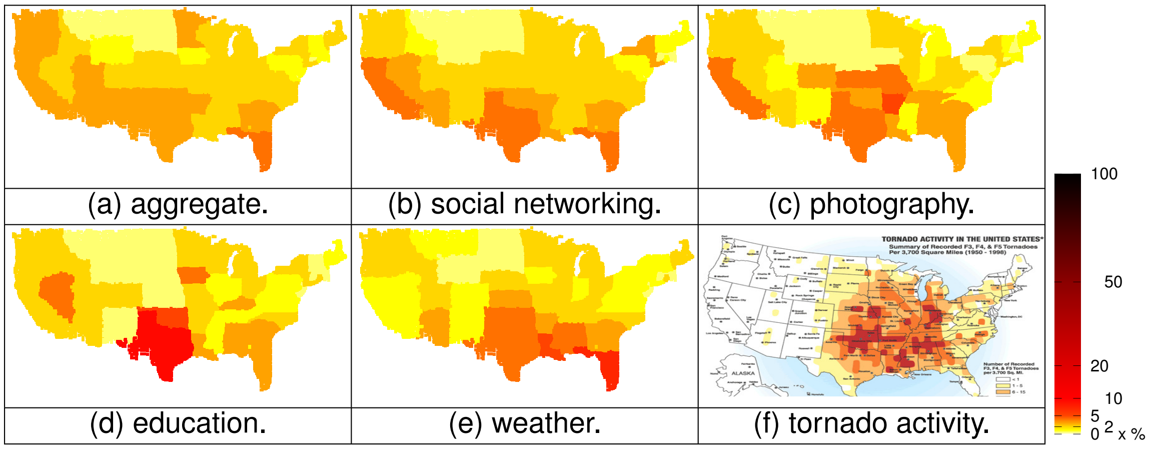

Figure 4.21: Geographic usage distribution of app genres.

For ease of reference, we term **geographic usage distribution** of a quantity X to be the the empirical probability distribution function (PDF) of X by U.S. state. First, we compute the geographic usage distribution of the unique subscribers and of the aggregate traffic volume generated by all national smartphone apps. We then use them to compute the geographic usage of traffic volume normalized by the number of unique subscribers in the state. Figure 4.21(a) is the PDF of the geographic usage of the aggregate traffic of all national apps together, while Figure 4.21(b) is the PDF of the geographic usage of the normalized traffic of all national apps. As expected, California, Texas, New York, Florida, and Illinois are the states that have the highest aggregate traffic from the national apps in Figure 4.21(a). However, after normalizing the volume to account for the number of subscribers, the distribution looks flatter in Figure 4.21(b). We perform the rest of our analysis (Figure 4.21(c-f)) on the normalized traffic, since it makes differences across states be easier identified.

Figure 4.21(c-f) illustrates the geographic usage of some representative genres (all genres are listed in Table 4.4). Figure 4.21(a) demonstrates the PDF of traffic volume from each state of all nation-wide apps. Lifestyle, music, news, and social networking genres have very similar patterns of geographic usage as the aggregate traffic. As an example, we show the social networking apps in Figure 4.21(c), which is is most similar to the aggregate traffic in Figure 4.21(b). Education apps in Figure 4.21(d) appear to be extremely popular in Texas; further analysis revealed that this is because some apps produced by universities (e.g., TAMU) generate a significant fraction of traffic among the education apps. Likewise, Figure 4.21(f) shows that weather apps seem to be highly used in the south-eastern U.S. This may perhaps have happened because the time periods of our data coincide with the peak hurricane season in those areas [51, 84] – such variable and dangerous weather conditions may cause users to check weather forecasts more frequently.

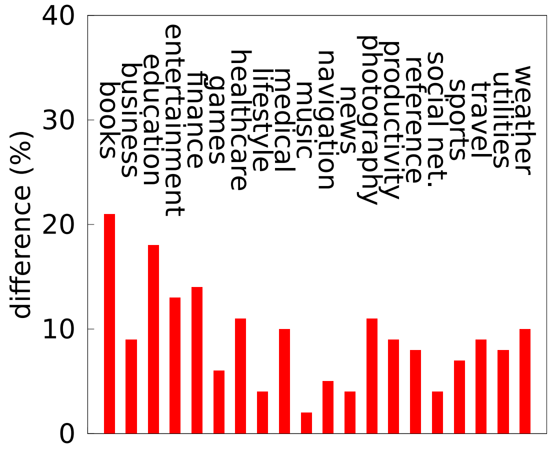

Figure 4.22: Geographic usage difference across app genres.

Next, we measure how far the geographic usage of different genres are from the aggregate geographic usage of the apps. We use the Euclidean distance to measure the distance between a pair of geographic usage distributions. The Euclidean distance between a pair of distributions $[x_1,x_2,\cdots,x_n]$ and $[y_1,y_2,\cdots,y_n]$ is defined as $\sqrt{\sum_{i=1}^{n}(x_i-y_i)^2}$. Figure 4.22 shows the distance between each genre's geographic usage distribution and the distribution of aggregate national apps. We note that some genres, such as books and education, are disproportionately used in some states, while others, such as social networking apps generate traffic more proportionate to the total traffic generated by that state.

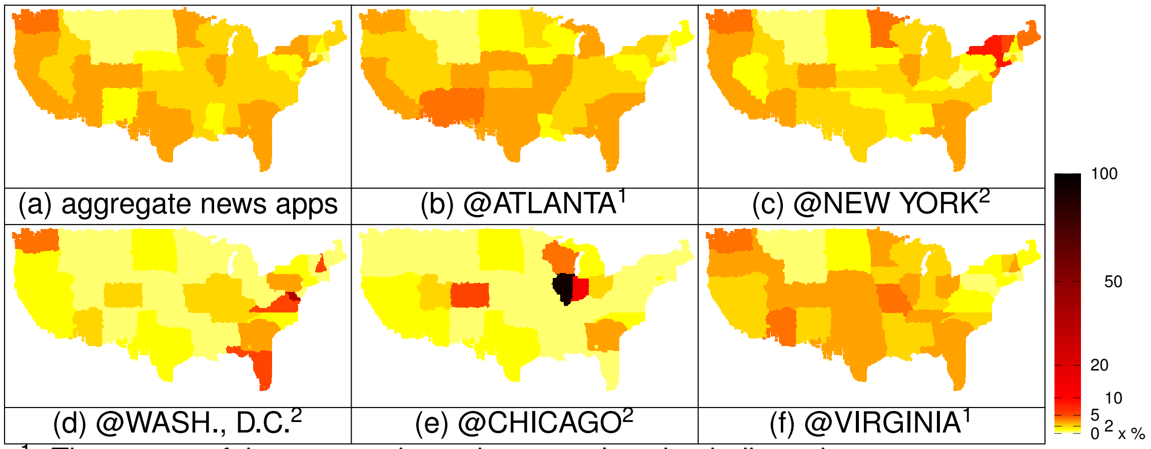

1: The names of these apps do not have any location indicated.
2: The names of these apps include locations.

Figure 4.23: Geographic usage distribution in the same genre (news).

The distribution of geographic usage of different apps *within* the same genre may also differ. Figure 4.23 shows the geographic usage distribution of a number of smartphone apps in the news genre. For this analysis, we select the apps of a few newspapers that are well-known across the entire U.S., and cover news relating to any part of the world. The location of each news app in Figure 4.23 only reflects where the newspaper headquarter is located. However, some of them have a location indicated in their names (marked with ^{2} in Figure 4.23). Although all these apps are used nation-wide, we note that apps whose names have a location indicated seem to be disproportionally preferred at those respective locations. In addition, the Washington D.C. news app seems to be highly preferred in

Washington state as well, thus suggesting users look for apps that appear to be local to their region.

Our final analysis of the spatial patterns of app usage examines whether individual users use some apps across larger geographic areas than others, e.g., whether Internet radio apps, which users may listen to during their commute, are used across a larger area than books. Such an analysis can help understand what kinds of apps need to be more robust to variations in network quality.

For this analysis, we define the **travel area** as a smartphone's geographic coverage per individual subscriber over short time, e.g., 6 hours. We use the number of sectors to estimate the geographic coverage, since we do not have access to the device's exact locations. As noted in Section 4.2.1, the number of sectors observed in our data set is an underestimate of the actual number of sectors that the device passes through, but our results still give an idea of the relative travel area of different apps. Specifically, for each app, we compute the average number of unique sectors used by active subscribers in each 6 hour time interval.

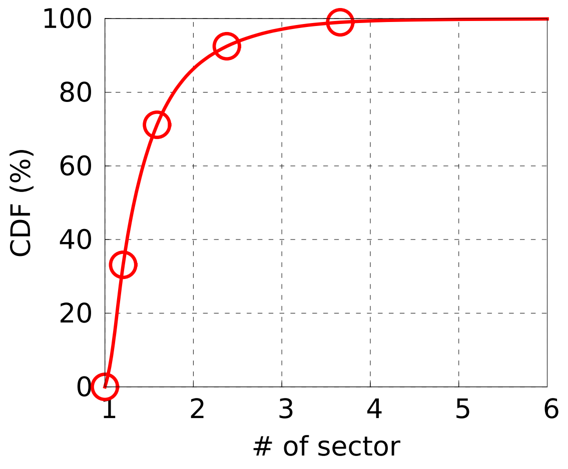

Figure 4.24: Travel area of apps.

Figure 4.24 shows the distribution of the average travel area of the top 1000 popular apps. It shows that 10% apps access the network from more than two

genre	books	business	finance	games	healthcare	lifestyle	music	news	productivity	reference	social net.	sports	travel	unknown
# apps	2	1	4	19	3	5	6	1	3	1	31	2	1	18

Table 4.6: Genres of the apps with large travel areas.

sectors. Thus, our results indicate that a significant fraction of the apps are used when users move around, creating another issue for content caching and delivery techniques. Base stations in future cellular network designs (e.g., LTE) have been considered potential locations for content caching and optimization (since they would be the first IP hop), so significant amount user movement could make it more difficult to cache content appropriately. Table 4.6 shows that the majority of these apps are games or social networking apps, but there are also a few music and news apps.

4.2.2.4 User patterns: effect of user interests

The needs and interests of individual users are the primary factors that inform their usage of apps. Because of user interests, the usage of different apps tends to be correlated. In this section, we analyze the extent to which user apps are correlated. Our analysis has many motivations: knowing what sets of apps are correlated would be helpful for both app developers as well as OS vendors, as they can factor this correlation into their designs and help the apps work better with each other. From a network perspective, such knowledge could help optimize performance or user experience for a set of apps as a bundle, and may also enhance troubleshooting. In addition, app markets can leverage this information for recommending new apps to users.

We use the **Jaccard Similarity Coefficient** to quantify the overlap between a pair of apps `a` and `b`: we count the number of unique subscribers who have used both a and b, i.e., joint(a,b), and the number of unique subscribers who have used either a or b, i.e., union(a,b). We can obtain $\frac{\text{joint(a,b)}}{\text{union(a,b)}}$ for all pairs of apps in the popular 1000 apps.

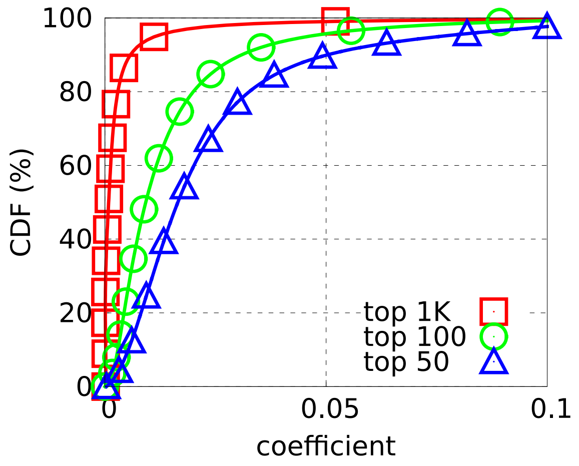

Figure 4.25: Coefficient between the apps sharing users.

Figure 4.25 shows the distribution of the Jaccard Similarity Coefficient between the top 1000, 500, 100, and 50 apps. We observe that there is a small fraction of app pairs that have a very high Jaccard Similarity Coefficient. For example, consider a pair of apps a,b whose $\frac{\text{joint(a,b)}}{\text{union(a,b)}}=0.05$, and assume that a and b have 2000 unique subscribers together (each of the top 50 most popular apps has over 2000 unique subscribers). Then at this value of the Jaccard Similarity Coefficient, a and b share 100 unique subscribers. Given that there are more than 600,000 unique subscribers in our data set, the overlap of 100 subscribers is unlikely to be due to random chance, indicating that users of app a have a tendency to also use app b. We also note that as we increase the number of popular apps from 50-1000, there is a smaller fraction of app pairs that have a significant overlap in subscribers. This is expected, since an app is more likely to have subscribers overlap with other apps when gets used by more and more subscribers.

Next, we analyze how likely it is for a pair of apps to have a substantial overlap in their users. Our analysis compares the empirical probabilities of a subscriber

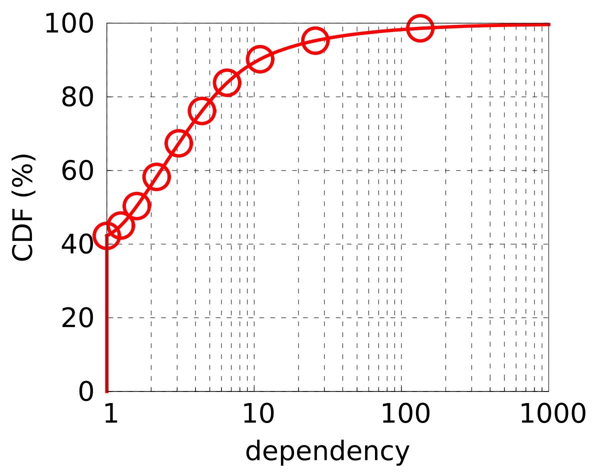

Figure 4.26: Dependency between popular apps.

.

using each app individually to the empirical probability of a subscriber using both apps together. More precisely, let a,b denote apps, and Pr[a],Pr[b] denote the empirical probabilities of a subscriber using app a,b respectively. Let Pr[ab] denote the empirical probability of a subscriber using both apps a and b. If the subscribers for each app are selected at random from the total population, then we would expect that Pr[ab] to be somewhat close to the product Pr[a]Pr[b]. Figure 4.26 shows the distribution of the ratio $\frac{\mathrm{Pr[ab]}}{\mathrm{Pr[a][b]}}$ (we term this quantity the **dependency ratio** for ease of reference). It shows that nearly 10% of the app pairs have a dependency ratio that exceeds 10, and 254 pairs have a ratio exceeding 100.

Table 4.7 shows the frequency distribution of the genres of these 254 pairs (i.e., pairs with dependency-ratio exceeding 100). We can make two immediate observations from this table. First, apps in the same genre are much more likely have correlated usage. For example, 110 pairs of two games apps that have high dependency-ratio, but games apps are part of a only 230 pairs in total. Second, apps in similar genres are more likely to have high dependence-ratio, e.g., entertainment and games, news and entertainment, entertainment and social networking, travel and navigation, weather and news, social networking and news,

	books	business	education	entertainment	finance	games	healthcare	lifestyle	medical	music	navigation	news	photography	productivity	reference	social net.	sports	travel	utilities	weather
books	0	0	0	2	0	3	0	1	0	0	0	1	0	0	0	0	0	1	0	0
business	0	0	0	0	0	0	0	4	0	0	0	2	0	0	0	0	0	0	1	0
education	0	0	5	2	0	2	0	0	0	0	2	3	0	0	0	1	0	0	0	0
entertainment	2	0	2	26	0	26	1	16	0	5	1	16	4	3	3	8	4	4	7	0
finance	0	0	0	0	2	0	1	0	0	0	0	4	0	0	0	0	0	1	1	0
games	3	0	2	26	0	110	2	19	1	5	1	3	2	1	13	5	8	12	1	1
healthcare	0	0	0	1	1	2	1	2	1	0	1	8	1	0	0	1	0	0	0	0
lifestyle	1	4	0	16	0	19	2	30	0	5	0	12	0	1	7	6	4	10	6	0
medical	0	0	0	0	0	1	1	0	0	0	0	1	0	0	0	0	0	0	0	0
music	0	0	0	5	0	5	0	5	0	6	0	5	0	1	1	11	3	0	3	0
navigation	0	0	2	1	0	1	1	0	0	0	2	1	0	1	0	1	0	4	0	1
news	1	2	3	16	4	3	8	12	1	5	1	77	1	3	2	12	8	7	4	4
photography	0	0	0	4	0	2	1	0	0	0	0	1	1	1	0	0	0	0	1	0
productivity	0	0	0	3	0	1	0	1	0	1	1	3	1	0	0	9	1	0	0	0
reference	0	0	0	3	0	13	0	7	0	1	0	2	0	0	1	0	1	2	0	1
social net.	0	0	1	8	0	5	1	6	0	11	1	12	0	9	0	32	4	0	3	0
sports	0	0	0	4	0	8	0	4	0	3	0	8	0	1	1	4	13	1	0	1
travel	1	0	0	4	1	12	0	10	0	0	4	7	0	0	2	0	1	9	2	0
utilities	0	1	0	7	1	1	0	6	0	3	0	4	1	0	0	3	0	2	2	0
weather	0	0	0	0	0	1	0	0	0	0	1	4	0	0	1	0	1	0	0	1

Table 4.7: Dependency between genres (only showing the apps with high dependency ratio).

etc.

There are many reasons that pairs of apps have highly correlated usage. First, many different apps often provide the same type of content in different forms e.g., there may be multiple local news or Internet radio stations targeting the same location, and users often are interested in trying them all out. Or, there may multiple apps that allow users to access the same social networking sites with different user interfaces. A second reason may be that a pair of apps serve similar purpose, but neither may provide complete service on its own e.g., users may have accounts with multiple banks, and need to use each bank's specific app in order to keep track of all their accounts. Yet another reason may be that different apps target similar user interests, and users may try them all out to identify their favorites, e.g., crossword puzzle apps or sudoku apps.

4.2.2.5 Temporal patterns: usage over time

Understanding the diurnal patterns of apps is important for several reasons. For example, differences in when certain apps are used can help inform cloud providers on how to best multiplex resources and operators on what to optimize the network for at different times. In this analysis, we compare the traffic volumes and access times consumed by smartphone apps at different hours of the day, both in aggregate as well as for different genres. Our results show that there are diurnal patterns of app usage both in aggregate, as well as by genre, but that the patterns of different genres are noticeably different.

We first investigate the diurnal patterns by aggregating all the popular apps together. For this analysis, we map each flow to the local time of the device's geolocation (based on the sector where the device is connected to the cellular network). Figure 4.28(a) shows clear diurnal patterns of traffic volume and network access time. Around 1AM – 2AM, the total traffic volume and access time are at

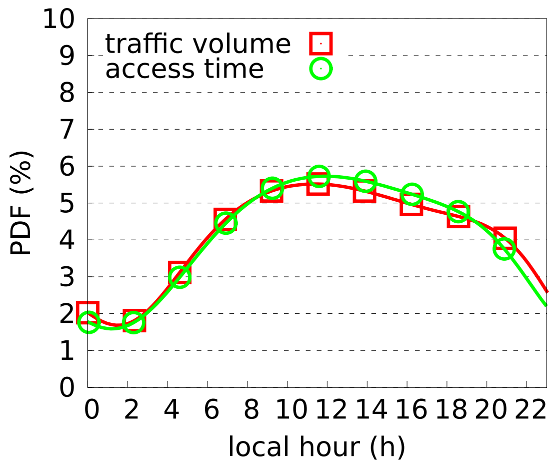

Figure 4.27: Diurnal patterns of app usage.

their minimum; they start increasing around 4AM, reach the peak usage around noon, start decreasing after 3PM and drop dramatically after 8PM.

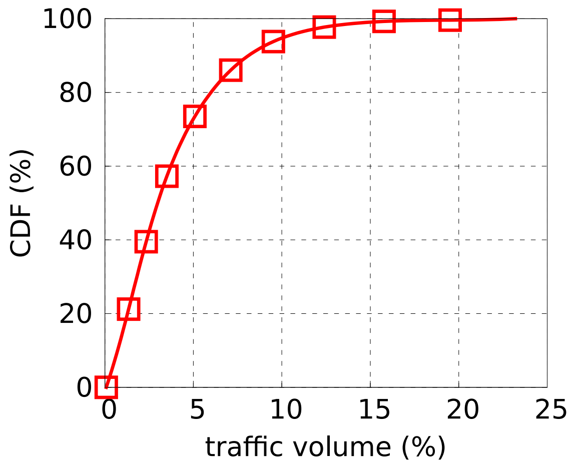

Figure 4.28: Significance of late night apps (1:00–3:59 AM).

In general, apps have more activity during the daytime than at night. However, this may not apply to every popular app. Figure 4.28(b) shows the distribution of the traffic contribution during late night for popular apps. According to Figure 4.28(a), in terms of both traffic volume or access time, the time period 1:00 AM – 3:59 AM contributes 4.2% traffic. Even if an app generates uniform traffic every hour of the day, it should generate 12.5% traffic from 1:00 AM to 3:59AM. So, Figure 4.28(b)

category	# apps	description
entertainment	20	small games, video channels, etc.
radio	28	music radio channels, news radio channels, etc.
healthcare	12	sleep aid utilities, etc.
books	6	bible, references, etc.

Table 4.8: Overview description of late night apps.

indicates that there are some apps that are quite active late at night. We manually investigate these top 66 *late night* apps according to Figure 4.28(b) that contribute more than 12.5% traffic late at night. Table 4.8 summarizes the results. It appears that several entertainment and radio apps are used more frequently than expected at night.

Finally, we analyze diurnal patterns across different genres; we expect that different genres of apps to have different usage patterns, since they appeal to different interests. As we did in earlier analysis, we aggregate together the popular apps in the same genre, and compute the distribution of traffic volumes by genre at hourly intervals (again, using the local time of the flow). Figure 4.29 shows the normalized traffic volume across the day; it clearly shows how different genres do have very different diurnal patterns. In particular, we see that social network apps have almost exactly the same pattern as the aggregate, but weather and news apps are most frequently used at early morning. Sports apps, on the other hand, peak in the early evening, perhaps because users may watch matches or check scores frequently during those hours. Games apps also peak after standard work hours as we would expect, since that is probably the typical recreation time for most subscribers.

4.2.2.6 Device patterns: differences across platforms

Finally, we compare smartphone app usage across different kinds of devices. We expect that faster devices allow for longer sessions, faster downloads, and

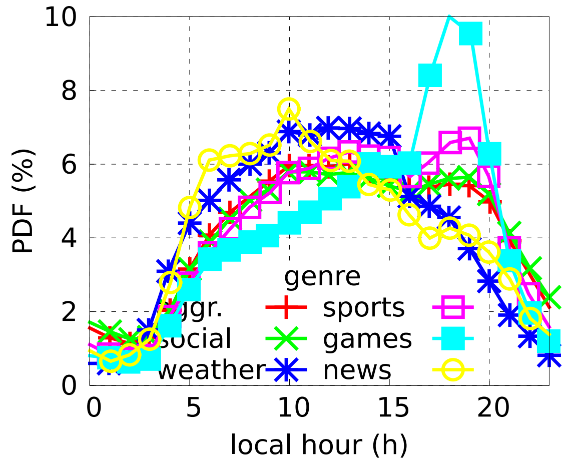

Figure 4.29: Diurnal patterns across app genres.

more interactivity, thus enhancing the end-user experience. Power users, who use their devices more, may also gravitate to newer and faster devices. We focus on three different devices from the same device family, as we expect device operating system to also affect overall usage patterns. We compare three devices in the same device family but of different generations – we term these iPhone 3, iPhone 3GS, and iPhone 4G in Figure 4.30. iPhone 3 is a HSDPA category 6 device (capable of 3.6Mbps downlink rate), and iPhone 3GS and iPhone 4G are in HSDPA category 8 (capable of 7.2Mbps downlink) [112]. iPhone 3 and iPhone 3GS are not HSUPA enabled while iPhone 4G is HSUPA category 6 (capable of 5.76Mbps uplink) [113].

For this analysis, we use slightly different metrics than we have used in the following, since our goal is to measure how long a user interacts with the device, and compare these measurements across different devices. For this, we define **individual access time** and the **individual traffic volume** to be the network access time and the traffic volume per flow respectively. We use these metrics for our analysis as we expect the individual access time to provide a measure of how long a user spends with an app, and the individual traffic volume to reflect how much data is transferred each time a user interacts with an app. Obviously not every flow will be larger or longer, but we expect that a device that allows for better interaction will have on average more large flows and longer flows.

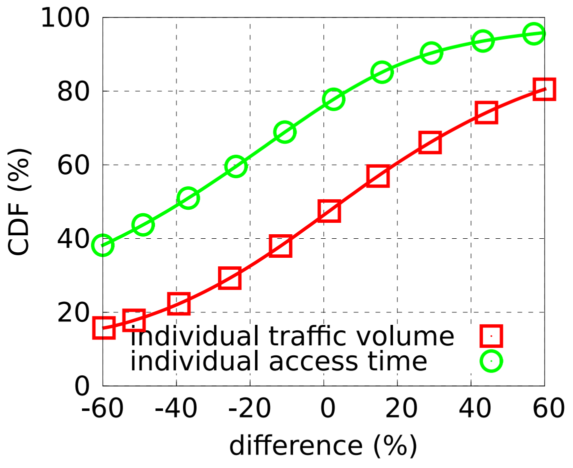

(a) iPhone 3 vs. iPhone 4G.

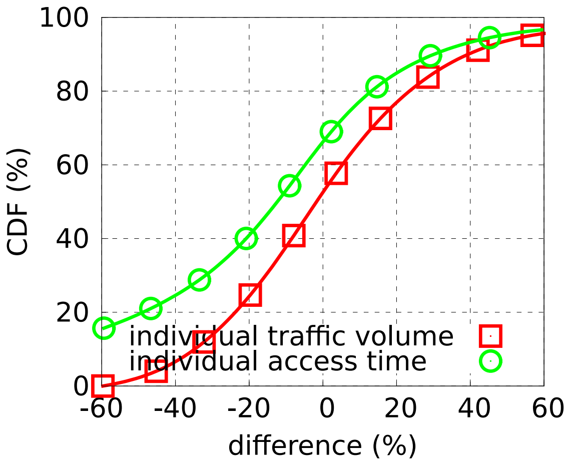

(b) iPhone 3GS vs. iPhone 4G.

Figure 4.30: Impact of the device type on app usage.

In Figure 4.30, we compare the individual traffic volume and individual access time between iPhone 3 and iPhone 4G, and between iPhone 3GS and iPhone 4G. For our analysis, we aggregate all the popular apps to first compute directly the individual access time and individual traffic volume for these three platforms, and then compute the relative differences by comparing iPhone 3 against iPhone 4G, and iPhone 3GS against iPhone 4G. According to Figure 4.30(a), the individual access time for iPhone 3 and iPhone 4G are very close, i.e., the median relative difference is 0. However, individual traffic volume for iPhone 3 is much smaller. The median difference of the individual traffic volume is -30%. Such a big difference indicates that the user experience is substantially different between these two device categories; users of iPhone 4G consume much more data, typically through video. Figure 4.30(b) shows the comparison between iPhone 3GS and iPhone 4G; these two device categories are much closer than iPhone 3 and iPhone 4G. There may be two explanations. First, a faster device tends to give users better overload experience and encourages them to download more content from the network. Second, power user are more likely upgrade to the latest smartphone, while users not as active may be more likely to keep using their older devices.

4.2.3 Implications of Application Usage Patterns

In previous sections, we investigate the usage patterns of smartphone apps from spatial, temporal, user, and device perspectives. We believe that our previous observations have important implications for the smartphone community. In this section, we discuss these implications following our previous observations.

4.2.3.1 Content providers

In the analysis of spatial patterns of smartphone usages, we observe a considerable number of local apps (20%) which contribute 2% of the traffic volume in the smartphone apps category. The content provided by these local apps are very deterministic, e.g., news apps, regional radio online services, weather forecast apps, etc. Given both the customers and locations for these apps are very closely clustered, content placement and delivery can be further optimized accordingly. It is therefore beneficial to place the content close to GGSNs in the cellular networks [120] for cellular users and place the content close to the geographic location of WiFi users. Besides local apps, for national apps, the distribution of geographic coverage is still very dependent on the genre (e.g., weather apps are highly used in the south-eastern U.S.), even the app's name (e.g., the news app headquartered in CHICAGO), etc. Therefore, content placement according to the geographic coverage is advisable for both national and local apps.

4.2.3.2 Context-aware applications

Despite very diverse usage usage patterns across different smartphone apps, they still have some common traits. According to our observations, first, apps in the same genre share similar geographic coverage. Second, some apps share a large set of common users due to the similarity of content and interests, e.g., social networking apps strongly correlate with entertainment apps, music apps, news apps, etc. Third, some apps share similar diurnal patterns due to content characteristics, e.g., the peak hours of news apps and weather apps come at early morning.

Context-aware applications can take advantage of the existing similarity/correlation across smartphone apps. Take smartphone apps recommendation systems as an example. Unlike normal PC users, smartphone users depend on apps far more than browsers. Since a smartphone apps recommendation system is the first approach for users to explore various smartphone apps that meet their interests, these systems can be quite important. As the bridge between app marketplace and app customers, if apps recommendation systems can learn user interests and dependency across apps, they can identify more appropriate apps for users, e.g., suggesting gaming fans more entertainment apps and social networking apps.

Another example of context-aware application is advertisement systems, which upon learning user's interests in apps, can deliver more relevant ads to users. Camera or camcorder advertisements may target more smartphone users that use more entertainment and game apps because photography apps are more correlated with entertainment and game apps.

4.2.3.3 Network providers

Besides content providers, cellular network providers also play an important role in content delivery and customization. By understanding the access patterns of smartphone apps, network providers can benefit in allocating radio resource, setting caching policy, compression policy, etc.

If a large number of smartphone apps are targeted, their traffic volume and access time roughly have linear correlation with their number of unique subscribers. Accordingly, cellular providers can estimate and allocate radio resources.

We observe that the several few top apps contribute the majority traffic. For example, the app with the largest traffic volume is accountable for 50% of the total traffic volume of the smartphone apps category, and the app with the longest network access time takes 86% of the total network access time of the smartphone apps category. Understanding the usage patterns of these apps, network providers may do certain optimizations case by case.

The temporal patterns of smartphone apps help network providers allocate radio resource. For example, the access time per IP flow helps network providers decide the timers in state promotion [90].

We observe that some smartphone apps have large usage radius, i.e., users of certain social networking apps and games apps are more likely to move around across several base stations. In future, LTE networks will push the first IP hop forward to base stations, which increases the flexibility of content placement and optimization. However, if users frequently move around, the corresponding mobility may increase the complexity to decide where to cache content and what content to cache.

4.2.3.4 OS vendors and apps designers

Since smartphones have limited resources, the OS is accountable for resource management, e.g., the push notification on iOS, Android, Windows Phone. Understanding the access patterns of apps on device, OS can add some flexibility to apps and optimize the resource usage. For example, if a user frequently resorts to a certain sleep aid app, then OS may allocate less resource to those apps that may interrupt the user's sleep.

Certain genres of smartphone apps have different characteristics, which may be taken advantage by apps designers. We observe that news and weather apps have distinctive diurnal patterns. Since the content of these apps usually are very time dependent and content fetching time is very predictable, apps designer can implement some prefetching mechanism to reduce the latency perceived by users. Similarly, the content of social networking apps can be prefetched before dinner time.

4.3 Summary of Identifying Application Usage

In §4.1, we developed FLOWR, a system determining the app identities of network flows in mobile networks in real time with minimal supervised learning through three creative techniques: KV tokenization, a* service based training, and flow regression. The entropy inside signatures produced by KV tokenization corresponds to the amount of information sufficient to uniquely differentiate the apps or to narrow down to a few (e.g., 2–5) candidate apps. leveraging a* services allows FLOWR to minimize supervised learning for identifying both free and paid apps. Without consuming exhaustive training effort, flow regression can determine the app identities for the flow signatures produced by KV tokenization through monitoring the co-occurrence events between flow signatures. FLOWR's throughput is up to 5Gbps an off-the-shelf machine.

Although we do not have the ground truth of the app identities of network flows, we successfully estimated the upper-bound false positive of FLOWR in evaluation. Evaluated using the apps with doubleclick, FLOWR can uniquely identify 26–30% of flows and narrow down *another* 60–65% to 2–5 candidate apps, with $<$1% false positive. In contrast, only 3% of flows can be identified without FLOWR. We believe that FLOWR enables mobile network operators to extract valuable insight from mobile network traffic.

Under the support of FLOWR, in §4.2, we comprehensively investigated the diverse usage patterns of smartphone apps via network measurements from a national level tier-1 cellular network provider in the U.S. This is the first attempt in addressing the lack of how, where and when smartphone apps are used at the scale of the entire U.S.

We observed that a considerable fraction of popular apps (20%) are local because their content are expected to serve local users such as news and radio apps. This suggests that there is significant possibility for content optimization in LTE and WiFi access networks where the flexibility of placing content is high.

We also found out that there are similarities across apps in terms of geographic coverage, diurnal usage patterns, etc. Certain apps have a high likelihood of co-occurrence – that is, (i) when a user uses one app, he is also likely to use another one; or (ii) users use alternatives for the same type of interests, e.g., multiple news apps, bank apps. These observations suggest that some apps should be treated as a "bundle" when trying to optimize for their user experience. There may be opportunities for integrating these apps together.

Diurnal patterns of smartphone apps can be remarkably different. For instance, news apps are much more frequently used in the early morning while sports apps are more frequently used in the evening. These findings suggest that content providers (e.g., hosted on cloud) can leverage distinct usage patterns in classes of apps to maximize the utilization of their resources.

Many social networking and games apps are more frequently used when users are moving around. Mobility affects connectivity and performance, so bandwidth sensitive content that are mobile may need to consider techniques to compensate for bandwidth variability.

We believe that our findings on the diverse usage patterns of smartphone apps in spatial, temporal, user, device dimensions will motivate future work in the mobile community.

CHAPTER V

APPLICATION PERFORMANCE OPTIMIZATION

One lesson we learned from YellowPage in §III is that latency sensitive application can be very challenging in cellular networks. In §IV, we also had many observations and findings showing the distinctive behaviors of mobile applications. In this section, we adapt application behaviors to cellular networks starting with real-time, interactive mobile applications in particular.

One of the biggest trends today is the accelerated adoption of mobile devices, whose power is approaching that of PCs. The rapid adoption of mobile devices is resulting in the migration of real-time communication (RTC) applications from PCs to mobile devices. RTC applications include (i) online streaming including VoIP/video conferencing applications such as Skype, FaceTime, and Google+ Hangout; (ii) interactive multi-player gaming applications such as Draw Something, Modern Combat 3, and Call of Duty; and (iii) application sharing, desktop sharing, and virtual desktop interface (VDI). RTCWeb (Real-Time Collaboration over Web) is an ongoing effort to enable RTC applications to run inside browsers without plug-ins [15].

Running RTC applications in mobile networks presents a major challenge since they require accurate short-term estimates of network metrics, e.g., loss rate, one-way delay (OWD), and throughput, whereas cellular network performance varies rapidly and widely [62, 107, 40]. Although performance adaptation solutions have been proposed [126, 96, 81, 9, 4, 1, 13], they are ineffective for RTC applications, where the end-to-end delay between content generation and content consumption is on the order of network latencies. Thus, techniques such as packet retransmissions or use of large client-side de-jitter buffers to absorb jitter variations, effective for web browsing and video playback, will lead to intolerable delays in RTC applications.

Instead, RTC applications need to rely on an appropriate amount of forward error correction (FEC) to correct for packet loss and a small yet appropriately sized de-jitter buffer to absorb varying packet delay. Over-protection using FEC wastes precious bandwidth, while under-protection negates the effectiveness of FEC, as any unrecoverable packet loss will lead to severe quality degradation in voice calling and video conferencing. Similarly, if the de-jitter buffer size is too large, it adds to the application latency. If it is too small, late arriving packets will be considered lost, which also leads to significant quality degradation. Accurate throughput prediction is also necessary to allow bandwidth intensive applications to maximize throughput without incurring additional queuing delay. Thus, short-term, fine-grained network performance prediction on mobile networks is of great importance.

Existing work on mobile network performance measurement and prediction is of limited importance to RTC applications for several reasons: (i) the measurement or prediction approaches are carried out on coarse-grained time granularity or offline, which are not suitable for RTC applications; (ii) the performance adaptation techniques react to performance only after observing any degradation, when the user experience has already been negatively impacted; and (iii) the existing techniques used by RTC applications for network prediction are usually naïve such as using the previous performance or the average of previous performance, which work well only for relatively stable wired networks.

We propose a system interface named PROTEUS designed to accurately predict fine-grained detailed network performance in real time over short time scales allowing applications to adjust their behavior to best optimize their performance. The fine-grained and accurate performance prediction in real time is necessary yet challenging from three aspects: (i) cellular network performance may be affected by a multitude of unobservable factors, such as radio resource scheduling, other users sharing the spectrum, and signal-to-noise ratio; (ii) network performance predictions on fine-grained time granularity is inherently noisier than coarse-grained predictions; and (iii) active probing is prohibitive for RTC applications due to significant resource consumption, while passive monitoring has limited visibility only based on traffic generated by applications.

To address the above challenges, PROTEUS utilizes a machine learning framework based on regression trees to learn the trend of network performance over short, fine-grained time windows using previous available observations. Even though past work has provided the evidence that cellular networks have a potential to have predictability for network performance, to our best knowledge, PROTEUS is the first system to forecast short-term network performance in real time, and the first to demonstrate the benefit of proactively adjusting the operating parameters in real time for use by mobile RTC applications. The key contributions are as follows.

- We characterize short-term network behavior and investigate the performance predictability in three major cellular networks of AT&T, T-Mobile, and Sprint based on more than 400 hours of traces across 3 locations. We identify the existence of strong predictability over short time scales for these cellular networks.
- We discover that loss rate, one-way delay, and throughput in cellular networks can be accurately predicted in real time from past measurements by feeding past network performance metrics into regression trees. For a following 0.5s time window, we can predict loss occurrence with 98% accuracy, late packet arrival with

97% accuracy, and throughput with a median error of 10kbps.

- We prototype PROTEUS, an efficient framework that forecasts achievable network performance in real time and evaluate its usage by a video conferencing system and an online game, i.e., Draw Something. By adapting its behavior through prediction from PROTEUS, the video conferencing system can improve its peak signal-to-noise ratio by up to 15dB over the state-of-the-art adaptation techniques. Utilizing PROTEUS, Draw Something can reduce the perceptual delay in viewing the stroke-by-stroke animation by up to 4s.

The rest of this section is organized as follows. §5.1 overviews the infrastructure of PROTEUS, followed by §5.2 where we characterize short-term predictability of cellular networks. §5.3 applies PROTEUS into a video conferencing system and a multi-player gaming system and evaluates the benefits from PROTEUS. We summerize the section in §5.4.

5.1 PROTEUS Overview

type	description	example	inquiry API
1	non-real-time, low rate traffic, or insensitive to prediction	Weather, Calender, Reminder, Dropbox	N/A
2	sensitive to throughput	YouTube, NetFlix. Hulu	throughput
3	sensitive to loss and one-way delay (OWD)	Skype Call, Google Voice	loss, OWD
4	sensitive to loss, OWD, and throughput	Skype Video, Google+ Hangouts, Draw Something, online games	loss, OWD, throughput

Table 5.1: Types of applications based on the sensitivity to network loss, OWD, and throughput.

PROTEUS is designed to complement the underlying transport protocol and any performance optimization techniques (e.g., FEC, de-jitter buffer, congestion control) that are widely used by RTC applications. For example, video conferencing applications using UDP have their own congestion control based on delay and loss.

Applications using TCP rely on TCP's congestion control algorithm. The goal of PROTEUS is to provide applications with prediction of delay, loss, and throughput, so that they can perform application-specific optimization such as tuning source bit-rate, amount of FEC inserted, and de-jitter buffer size.

To avoid measurement overhead, PROTEUS does not actively probe the network. Instead, PROTEUS is designed as a library that relies on application traffic to collect network measurements. This is done by appending and recording the time and sequence numbers for outgoing and incoming packets. PROTEUS can be either in the user space or inside the kernel. Inside the kernel, PROTEUS has the lower overhead. As shown in Figure 5.1, applications (e.g., `app #1`) can call `send'()` and `recv'()`, which are PROTEUS's wrapped version of standard socket API's `send()` and `recv()`. The socket wrapper allows PROTEUS to collect packet sequencing and timing information transparently. In fact, as many applications already store sequencing and timing information in their traffic, e.g., RTP packets used by many VoIP and video conferencing applications already contain such information which can be directly utilized by PROTEUS. Thus, applications (e.g., `app #2`) can alternatively stick to standard socket API, and just inform PROTEUS of the information.

PROTEUS provides applications and the socket wrapper another two sets of API: the inform API and the inquiry API. The inform API enables the socket wrapper (e.g., `app #1`) and applications (e.g., `app #2`) to inform PROTEUS packet sequencing and timing information, whereas the application issues the inquiry API to obtain from PROTEUS the predicted future network performance, as depicted in Figure 5.1. Based on this fine-grained information of packet sequencing and timing provided by either the wrapped socket (e.g., `app #1`) or the application (e.g., `app #2`) through the inform API, PROTEUS can compute current packet loss rate, one-way delay, and throughput from which it can predict future network performance. PROTEUS uses a clock drift compensation technique [82] to adjust the remote timestamp to local clock to compute one-way delay.

The overhead of adding timestamps and sequence numbers into packet headers is acceptable, which has been evaluated in previous research [97, 6]. The statistics of loss, delay, and throughput are collected over small non-overlapping time slices (i.e., time windows). This is the granularity over which statistics collection as well prediction are performed. Using the observed statistics from a certain number of previous time windows (i.e., information windows), PROTEUS trains regression trees to identify the dependencies across various network metrics and to forecast the network performance in future time windows. There could be more than one way to learn traffic histories. We resort to regression trees simply as it is one of the state-of-the-art approaches that have relatively low memory and computation overhead [34]. Another advantage of regression trees over other techniques is that it can provide a real-value prediction of a metric as opposed to simply a binary decision.

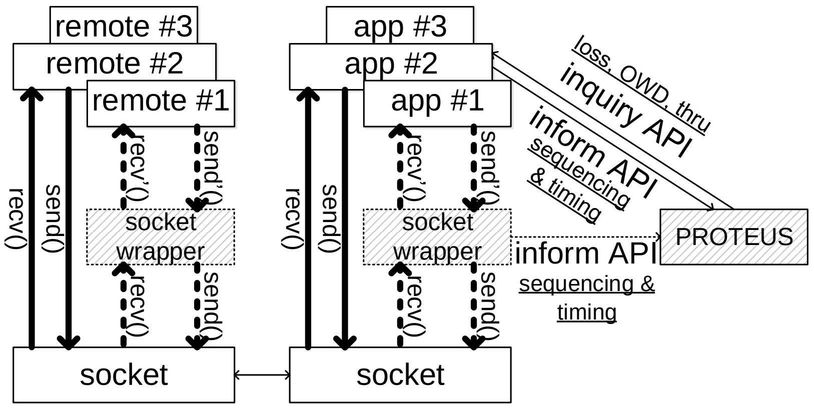

Figure 5.1: Design of PROTEUS. The details of its interaction with an application are shown in Figure 5.12.

The accuracy of PROTEUS's prediction is determined by two factors: (i) the inherent predictability of cellular network performance (described in §5.2.1), and (ii) the effectiveness of PROTEUS's forecasting technique (examined in §5.2.2).

The information exchanged through the inform API between applications and PROTEUS is common across applications. However, the information from the inquiry API and the resulting action taken by each application may be very different. In Table 5.1, we classify applications into four broad categories depending on how sensitive their performance is to the three network parameters of packet loss, one-way delay, and throughput and show how PROTEUS can be useful.

- Type 1 consists of the applications whose performance is not sensitive to loss, one-way delay, or throughput. These are either non-real-time, low bandwidth applications insensitive to network performance, or applications that do not benefit much from prediction. For example, the performance of Dropbox and other file transfer applications depend on throughput, but there is little adaptation in response to throughput prediction.
- Type 2 consists of the applications whose performance is not sensitive to packet loss or one-way delay but is sensitive to throughput. These are non-real-time, high bandwidth applications such as video on demand (VOD). Such applications can take steps to improve performance such as adapting the rate of the stream served to the client [9] in response to throughput prediction.
- Type 3 consists of the applications whose performance is sensitive to packet loss and/or one-way delay but is not sensitive to throughput. These are real-time, interactive, low bandwidth applications such as VoIP. For these applications, throughput prediction is of little benefit. However, loss prediction can be used to control the amount of FEC used [32]. The one-way delay prediction can be used to adjust the de-jitter buffer size for adaptive playout to reduce both late arrival induced loss [32] and de-jitter buffer induced delay.
- Type 4 consists of the applications whose performance is sensitive to packet loss, one-way delay, and throughput prediction. These are real-time, interactive, high bandwidth applications such as video conferencing, and real-time software

applications such as desktop sharing. PROTEUS can be used for throughput prediction to control the source rate produced by the source. The amount of FEC packets to insert can be inferred from loss prediction, and the de-jitter buffer size can be determined from one-way delay prediction.

Type 3 and Type 4 are real-time, interactive applications which can benefit from PROTEUS. Type 2 consists of *non-real-time* applications which can still benefit from throughput prediction.Although a coarse-grained predictor may work for Type 2 applications, it may not work for RTC applications. A coarse-grained predictor can be built upon a fine-grained predictor such as PROTEUS by simply averaging the prediction over multiple time windows.

Types 2, 3, and 4 applications are becoming increasingly popular and contribute to a majority of the traffic on the Internet [122]. This trend is readily visible by the increasing popularity of Skype, FaceTime, and Google+ Hangouts. The increasing push towards the cloud also makes other RTC applications such as online gaming and VDI scenarios even more important. The broad industry interest in the performance of such applications is apparent from recent efforts around RTCWeb [15] and DASH (Dynamic Adaptive Streaming over HTTP) [10].

5.2 Prediction Using PROTEUS

In this section, we investigate the predictability of cellular network performance and evaluate the accuracy of PROTEUS's forecasting.

5.2.1 Characterizing Cellular Networks

Although the understanding of the channel estimation scheme on mobile devices and the radio resource scheduling algorithm at base stations, along with the performance predictability observations from previous studies [75] give us confidence that cellular network performance is predictable, it is still uncertain (i) how much predictability there is in cellular networks, particularly in the short term as is needed by RTC applications; (ii) what network features can be the best predictors; and (iii) how much overhead is required to achieve accurate prediction. These challenges have not been fully addressed by any previous research but need to be studied to improve the performance of Type 3, and Type 4 applications in Table 5.1.

Autocorrelation for the same network metric. To quantify the predictability of cellular network performance, we first study the correlation across network metrics over time. A high correlation of a particular network characteristic would indicate that the feature should be predictable whereas a low correlation would imply difficulty in prediction. We take network measurements across non-overlapping time intervals, i.e., aforementioned time windows, and then compute the correlation coefficient between current time window with a time window t in the past, i.e., the time lag, using $R_t = \frac{E[P_0 \cdot P_t] - E[P_0] \cdot E[P_t]}{\sigma[P_0] \cdot \sigma[P_t]}$, where $E[\cdot]$ is the expectation operation, $\sigma[\cdot]$ is the standard deviation operation, and P is the stochastic process of any network performance metric[1]. A high autocorrelation coefficient would indicate that the metric is predictable using a linear predictor.

device	carrier	network	downlink[1]	uplink[1]
iPhone 4	AT&T	UMTS	77(4)	42(4)
Captivate	AT&T	UMTS	159(N/A)	72(N/A)
Atrix	AT&T	HSPA	42(N/A)	20(N/A)
Nexus	T-Mobile	HSPA+	109(N/A)	108(N/A)
dongle	Sprint	EV-DO	44(N/A)	115(N/A)

[1] The number of UDP(TCP) flows, each lasting at least 1 hour.

Table 5.2: Devices and cellular networks covered by the experiments. Traffic-Set refers to the AT&T flows.

To study if cellular network performance can be predicted using fine-grained

[1]The value of the autocorrelation function lies in the range $[-1,1]$, with 1 indicating perfect correlation, -1 indicating perfect anti-correlation, and 0 indicating no correlation.

time windows, e.g., 0.5s, we collect a large number of traces from various cellular networks in Table 5.2 and compute the autocorrelation of throughput using each trace choosing a time window of 0.5s, i.e., `tw=0.5`. We plot the distribution of the autocorrelation coefficient as a function of the time lag in Figure 5.2(a) for the flows in TrafficSet, as defined in Table 5.2. Given a time lag, we show the distribution across flows via the 5th, 25th, 50th, 75th, and 95th percentiles.

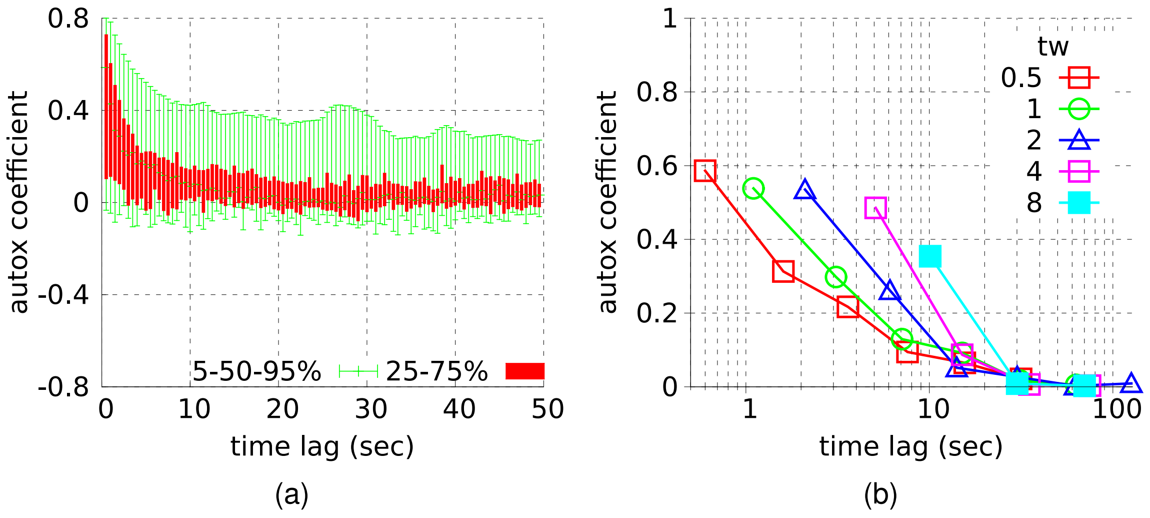

Figure 5.2: Autocorrelation coefficient of throughput under the impact of (a) the time lag and (b) the time window size ("tw").

In Figure 5.2(a), more than half of the time, the autocorrelation coefficient at a time lag of 0.5s is more than 0.6, indicating that the network performance using a time window of size 0.5s is indeed inferrible to some degrees using previous time windows. From Figure 5.2(a), we also see that once the time lag is above 20s, the median autocorrelation coefficient is close to 0, and the 25-75th percentiles are in the range of [-0.05, 0.05]. Therefore, we expect that using the time windows that are within the last 20s is sufficient to predict network performance. The results presented here show the autocorrelation function for throughput, we see similar behavior for packet loss and one-way delay.

Time granularity of performance prediction. One parameter affecting the autocorrelation coefficient is the size of the time window. If the time window chosen is small, the measurements may show high variability which may be more difficult to predict. However, if the time window chosen is large, the measurements may be affected by long term drift and cannot accurately reflect the fine-grained performance needed by RTC applications. To appropriately select a time window size, we study the effect of time window size on the autocorrelation function. Figure 5.2(b) shows the median autocorrelation coefficient for UDP throughput as a function of the time lag for various time window sizes, i.e., 0.5s, 1s, 2s, 4s, and 8s. We expect that as the time window size increases, the autocorrelation coefficient for a given time lag should also increase until it eventually converges. In Figure 5.2(b), "`tw=4`" being close to "`tw=8`" indicates that using time windows greater than 4s provides no additional benefit. However, we see that even with a window size of "tw = 0.5", the average autocorrelation coefficient at a time lag of 0.5s is above 0.6 and is similar to that using a larger time window. Thus, we conclude that we can indeed predict network performance from previous time windows using fine-grained windows, e.g., 0.5s, as needed by RTC applications.

In total, we have three observations from studying the autocorrelation function: (i) the current network performance is correlated with the network performance in the previous time windows; (ii) to predict the network performance, the time window size can be as short as 0.5s as required by RTC applications; and (iii) using information within the previous 20s should be sufficient for accurate prediction.

Cross correlation between network metrics. These three observations answer the question of whether network performance is predictable on cellular networks using previous values of a particular metric to predict future values of the same metric. However, the question of whether previous values of other metrics can also be used to improve prediction remains. To study this, we study the cross-correlation coefficient across various different network metrics.

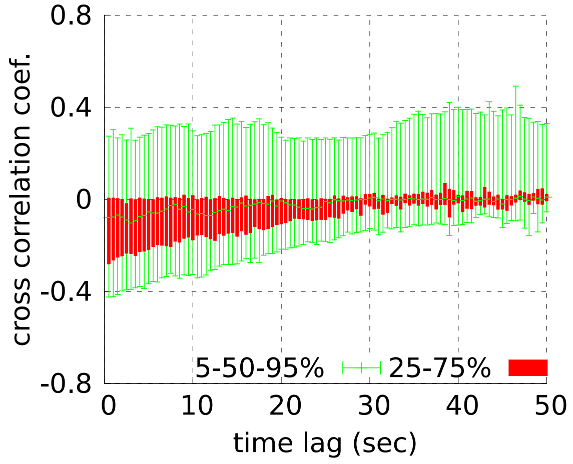

(a)

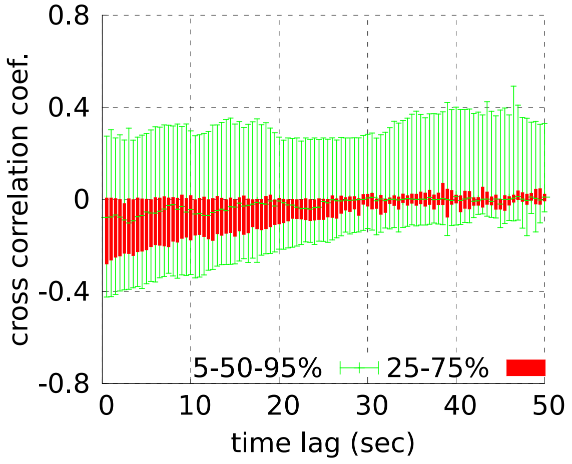

(b)

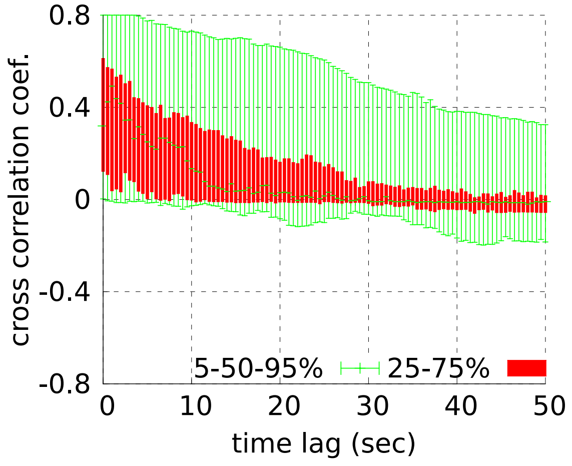

(c)

Figure 5.3: Cross correlation coefficient between performance metrics: (a) throughput and loss rate, (b) throughput and one-way delay, (c) loss rate and one-way delay. The cross correlation is computed per flow and the distribution across flows of the correlation coefficient under a given time lag is presented as 5-, 25-, 50-, 75-, and 95- percentiles. The correlation coefficient is normalized so that the maximum value is 1 for each flow.

Since packet loss and end-to-end network delay are commonly used as congestion signals by congestion control protocols as well indicates overbuffering in cellular networks [64], we expect that these metrics may be correlated. To confirm this understanding, we investigate the cross correlation between the various network performance metrics. The distribution of the cross-correlation coefficient as a function of the time lag is shown in Figure 5.3. From Figures 5.3(a) and (b), we find that throughput does not correlate well with either loss or one-way delay. The maximum absolute median cross correlation coefficient between throughput and loss is less than 0.1, and between throughput and one-way delay is less than 0.15. We believe that this is because the throughput is decided more by the DRC on the link between the device and the base station, while the loss and one-way delay are affected more by the congestion along the path. However, from Figure 5.3(c), we see that loss rate and one-way delay do have a strong correlation with each other. When the time lag is close to 0, the median cross correlation coefficient is around 0.5.

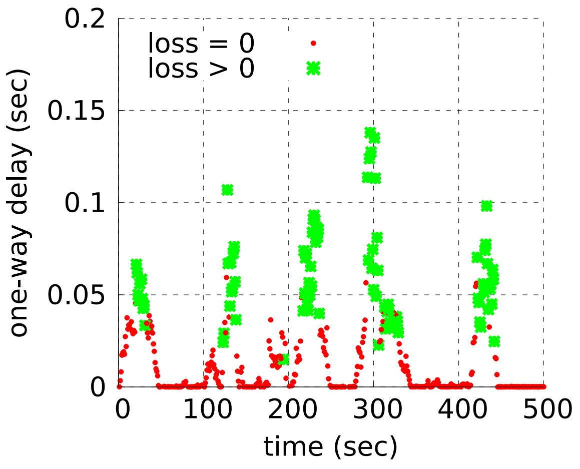

Figure 5.4: One-way delay for the time windows with and without loss.

Figure 5.4 further shows this correlation by showing the average one-way delay for each time window as a function of time for time windows with loss and those without loss. We clearly see that for those windows where loss occurs, the average one-way delay is also significantly higher than for those where there is no loss. As a result, the forecasts of loss and one-way delay use both previous loss rate and one-way delay, while throughput prediction uses just the throughput from previous time windows.

5.2.2 Constructing Regression Trees

We utilize a framework based on regression trees to automatically learn the correlation between previous network performance and current network performance [34].

5.2.2.1 Background of regression trees

Because the input can have lots of features which interference in complicated, non-linear ways, applying a single linear model can be very difficult. An alternative approach to nonlinear regression is to partition the input space into smaller regions, where the interactions are more manageable. Thus, we resort to prediction trees to mine performance patterns in cellular networks. Between the two varieties of predictions trees, i.e. regression trees and classification trees, we choose regression trees because the predicted results of regression trees can be real numbers.

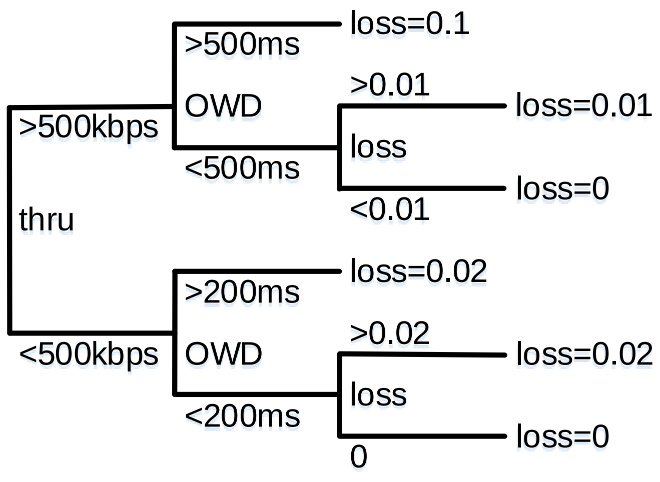

Figure 5.5: Example of a regression tree predicting loss rate.

Regression tree based learning is a commonly used method in data mining scenarios. The goal is to create a model that predicts the value of a target variable based on input variables. An example is shown on the right in Figure 5.5 – Each non-leaf node corresponds to a input variable; The leaves represent the values of the target variable. The tree is (dynamically) constructed by splitting the input date set into subsets based on the values of input variables. This construction process repeats on each subset in a recursive manner called partitioning. The partitioning is completed when the subset at a node has all the same value of the target variable, or when the splitting does not adds additional value.

5.2.2.2 Tuning regression trees

we construct a regression tree for each of the network metrics, with the target of the tree being the metric predicted and the attributes being the metrics used to perform the prediction. The loss regression tree predicts the loss rate in the next time window using the loss rate and one-way delay values from previous time windows. The delay regression tree uses the same attributes to predict the one-way delay in the next time window.

The throughput regression tree predicts the throughput in the next time window using the throughput values from previous time windows and the sending rate from the immediate previous time window. The sending rate is included to address the case in which the application is sending at a rate much below the throughput.

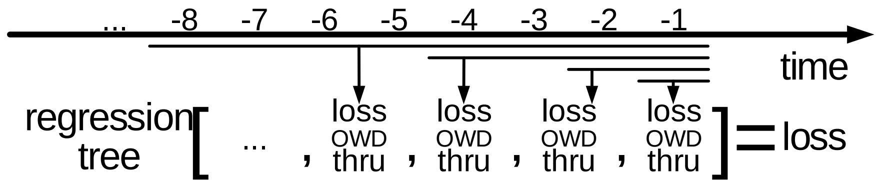

Figure 5.6: Attributes of the loss regression tree.

The number of attributes in the regression trees can be controlled by selecting an appropriate information window size from the correlation analysis (Figures 5.2 and 5.3). As illustrated by Figure 5.6, the attributes are computed using time windows in an exponential backoff fashion, i.e., the attributes are the average values of a given metric in the previous $1,2,4,8,\ldots,2^{\lceil \log_2(M) \rceil}$ time windows, where M is the information window size. Creating attributes using this approach allows us to place greater importance on the more recent time windows as the more recent time windows are represented in multiple attributes. It also controls the number of attributes since we only have $\lceil \log_2(\mathtt{M}) \rceil + 1$ attributes for a given information window of $\mathtt{M}$ time windows instead of $\mathtt{M}$ attributes. With a time window of 0.5s and an information window of 20s, we have only 7 attributes referring to the average of previous 1, 2, 4, 8, 16, 32, 64 time windows. In PROTEUS, the time window size is 0.5s and the information window size is 20s by default without particular specification.

According to Figure 5.2(a), the correlation between the current network performance and the performance tens of seconds ago is too weak to be useful. Thus, PROTEUS does not perform offline training which can be inefficient and expensive. PROTEUS keeps feeding the regression trees with the most recent performance metrics, allowing the regression trees to perform hyper-correction internally. Based on the knowledge of performance histories, the regression trees output the respective performance predictions for the next time window.

5.2.2.3 Advantages of regression trees

There could be more than one way to learn traffic histories and predict network performance, e.g., Markov chain. Aside from having relatively low memory and computation overhead, regression trees have other advantages as follows:

- **Simplicity.** We have tried to use a Markov chain to model the short-term network performance behavior, however, tuning the parameters for the model is ad hoc. Moreover, as there are so many unknown hidden factors affecting cellular network performance, utilizing a simply model is more realistic to such a blackbox scenario.
- **Nonlinearity.** Because the leaves in a regression tree are located at different levels (as shown in Figure 5.5), they differ in weights. Besides, when a attribute (e.g., a 1s ago measurement of $<$loss=0, owd=0.01ms, thru=500kbps$>$) is inserted into the tree, its location is decided by its value (e.g., $<$loss=0, owd=0.01ms, thru=500kbps$>$) rather than its time lag (e.g., 1s), which means that the model

based on regression trees is not linear.

- **Dynamic.** We need a model that can dynamically adapt to performance changes. In cellular networks, the performance can change rapidly, so does the performance model. However, utilizing regression trees, the model can dynamically grow towards the most recently observed performance measurements.

5.2.3 Evaluating Forecast Accuracy

To evaluate the performance of PROTEUS, we carry out controlled experiments to measure its forecasting accuracy. The forecasting accuracy may be variable due to several aspects. When a mobile device is in communication over cellular networks, the network, the device, and even the different cellular technology generations under the same network can influence network predictability. Thus, we conduct the experiments using diverse setups as shown in Table 5.2. Table 5.2 lists the device, the network, and the cellular technology used. As TCP has built-in congestion control and retransmission, the objective of evaluating TCP is its direct impact to RTC applications, described in §5.3. To minimize bias, we repeat our experiments at different time of day and at different locations. To directly control the sending rate and to easily observe loss, one-way delay, and throughput, we conduct most of our experiments over UDP. Even though most RTC applications operate directly over UDP, the applicability of PROTEUS is not limited by the transport protocol used by the application.

In the experiments, the mobile device communicates with a remote server in our campus in either the downlink or uplink direction and keeps the packet rate constant over the entire flow. To choose the sending rates, we saturate the end-to-end connection using UDP and estimate the bandwidth from the receiving rate. Based on the estimated bandwidth, the sending rate steps from 50% of the estimated bandwidth to 150% by 10% every time and each flow of a sending rate lasts at least one hour. On both the mobile and the remote server, we monitor packet traces using `tcpdump`. From the collected packet traces, we identify throughput, loss rate, and one-way delay. Here, we investigate one-way delay instead of round trip time because one-way delay is a more accurate measurement of network characteristics in a single direction and directly affects application performance. As mentioned in §5.1, PROTEUS performs clock drift compensation to compute one-way delay.

In the evaluation, we compare PROTEUS with two performance adaptation approaches, AD^1 and AD^2, which represent the state-of-the-art [9, 4, 1, 13, 23]. AD^1 and AD^2 are described as follows.

- AD^1 assumes the performance in the next time window is the same as the performance observed in the current time window.
- AD^2 is less aggressive than AD^1 to circumvent random variation in cellular networks. AD^2 assumes that the performance in the next time window is the average of the performance in the information window, i.e., the same as PROTEUS's information window.

Although AD^1 and AD^2 may seem simple and naïve, most existing RTC applications estimate loss rate and one-way delay using such methods since they work relatively well on wired networks.

PROTEUS's performance in loss prediction. We first investigate PROTEUS's accuracy in predicting the presence of any packet loss in the next time window by measuring the false positive and false negative rates in TrafficSet. A false positive occurs when PROTEUS predicts a packet loss in the time window but there is none. False positives can cause inefficient usage of network resources. For example, an application may introduce unnecessary FEC which would reduce the rate available for the actual coding of media. In contrast, a false negative occurs when PROTEUS predicts no packet loss but packet is lost in a time window. For many applications, the false negatives may result in degraded application

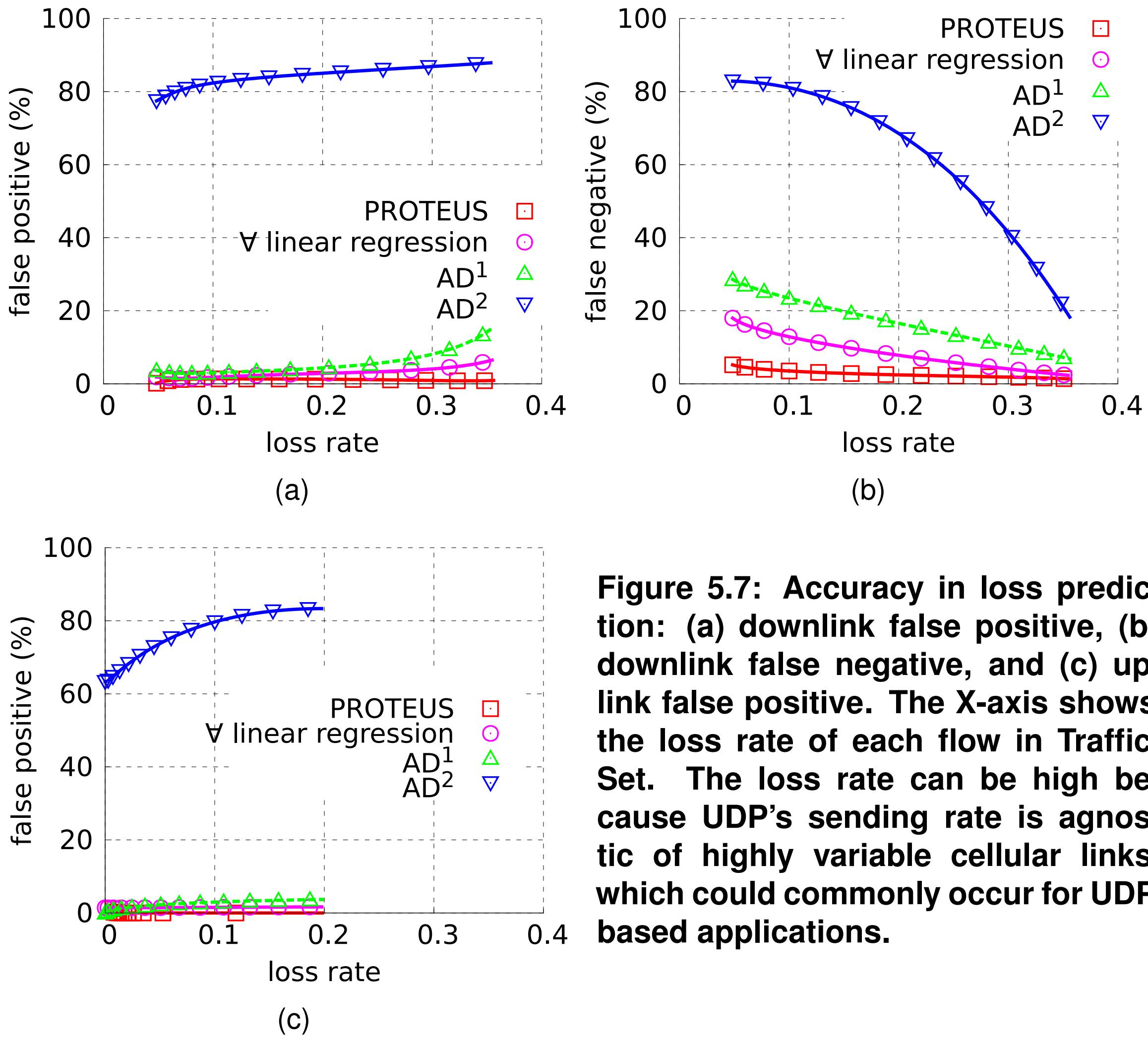

Figure 5.7: Accuracy in loss prediction: (a) downlink false positive, (b) downlink false negative, and (c) uplink false positive. The X-axis shows the loss rate of each flow in TrafficSet. The loss rate can be high because UDP's sending rate is agnostic of highly variable cellular links, which could commonly occur for UDP based applications.

performance.

In Figures 5.7(a)-(c), we show the false positive and false negative rates as a function of the actual loss rate for downlink and uplink traffic. From Figure 5.7(a), we see that PROTEUS's false positive rate is consistently around 1-2% when the loss rate is in the range from 0.05 to 0.4, while AD^1's false positive is around 2-5% when the loss rate is less than 0.3 and increases to 20% after the loss rate grows to 0.35. AD^2 performs even worse with the false positive rates higher than 80%. Note that the loss rate can be as high as 0.35, because UDP's sending rate is agnostic of highly variable cellular network performance [109, 29], which could commonly occur for UDP based applications. Without capturing the performance trend in previous time windows, AD^1 and AD^2 can only achieve the accuracy as poor as random guessing by merely estimating based on the last time window or aggregated history information.

In Figure 5.7(b), we show the false negative rate of the flows in TrafficSet. As mentioned, a false negative is more critical than a false positive, for RTC applications. From Figure 5.7(b), PROTEUS's false negative is consistently less than 1%, AD^1's false negative is 5-20% and AD^2's false negative is around 2-4%, slightly worse than PROTEUS. When the loss rate is low, the running flow may not provide sufficient information of true positives, i.e., lost packets. Thus, as the loss rate decreases, PROTEUS, AD^1, and AD^2 all have increasing false negative rates. Although AD^2's false negative is only slightly worse than PROTEUS, PROTEUS's false positive is significantly better. Compared to AD^1, AD^2 has low false positive rate, but does not retain a low false negative rate at the same time.

Besides downlink traffic, we also investigate uplink traffic as uplink traffic is significant in applications such as Skype, FaceTime, and Google+ Hangouts. Similar to Figure 5.7(a), PROTEUS is slightly better than AD^1 and much better than AD^2 in false positive according to Figure 5.7(c). PROTEUS's false positive is less than 1% over the flows in TrafficSet, AD^1's false positive ranges from 3% to 5%, and AD^2's false positive is no less than 40%. We observe similar performance for PROTEUS, AD^1, and AD^2 in their false negative for uplink flows.

The false positive and false negative results for the packet loss presented above show the prediction accuracy. Moreover, the regression tree used in PROTEUS also predicts the packet loss rate quantitatively rather than giving a simple binary decision of whether there will be packet loss. In Figure 5.8(a), we show the accuracy of this quantitative prediction of packet loss rate. We show the error in packet loss rate prediction for each of the three categories according to the error type, i.e., false negative, false positive, and true positive. Only true negative does

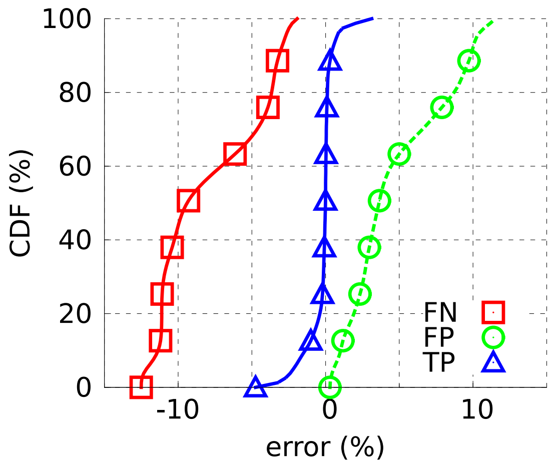

(a)

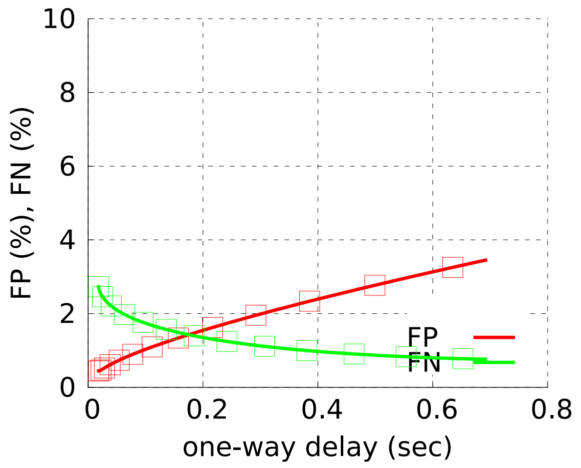

(b)

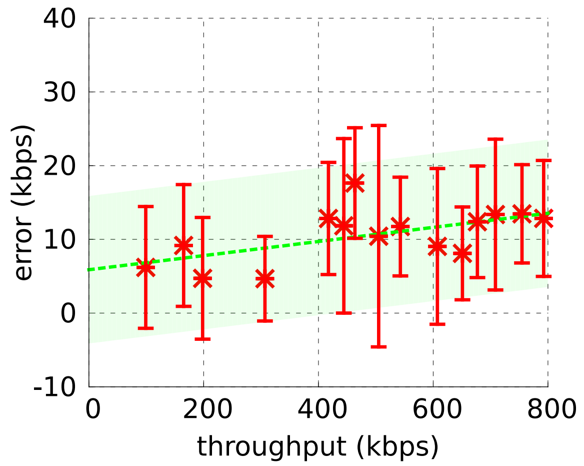

(c)

Figure 5.8: Quantitative accuracy on (a) loss rate, (b) one-way delay, and (c) throughput. In (c), only 15 randomly chosen flows are presented to avoid overlapping.

not lead to error because both the predicted and the ground truth loss rate are zero. We show the cumulative distribution function (CDF) of the error for each of these three error types in Figure 5.8(a).

Among true positive predictions, PROTEUS could either overestimate or underestimate the loss rate. If the loss rate is overestimated, similar to false positives, applications may introduce unnecessary FEC. If loss rate is underestimated, similar to false negatives, applications may experience information loss, which may be more critical. In Figure 5.8(a), 70% of true positive predictions have no error or the negligible error of less than 0.001 and 95% of them have the error within 0.05. PROTEUS's median false negative error is around 0.1 and 98%

of false negative errors are less than 0.2. With false positives, PROTEUS's median error is less than 0.02 and 99% of predictions are less than 0.2, which indicates that our design will not make applications introduce unnecessary protection traffic.

PROTEUS's performance in delay prediction. Besides loss rate prediction, RTC applications can also benefit from one-way delay prediction. One-way delay prediction allows applications such as video conferencing and VoIP to appropriately set their de-jitter buffer sizes, which determine how long the application waits for a packet before declaring it to be lost. Most VoIP and video conferencing systems do not use a fixed de-jitter buffer. The de-jitter buffer starts at something small and grows to some maximum value if packets do not arrive in time. This maximum is set to something which is tolerable for the given application. For example, a 150-200ms end-to-end delay is the maximum that video conferencing systems can tolerate [33]. Once packets start to arrive in time, the de-jitter buffer size shrinks according to some schedule (e.g., 10% every 5s) to lower the end-to-end delay seen by the application. Usually, de-jitter buffer size adaptation is accomplished by using an adaptive rate playout (either speeding up or slowing down media playback) [32]. Accurately predicting one-way delay can allow an application to more intelligently control this adaptation to improve performance.

Inappropriate de-jitter buffer size selection can result in suboptimal performance. If it is set larger than needed to absorb the inherent network delay variation, the application suffers from larger delay than needed. Otherwise, if it is set too small, a large number of packets that arrive late will be declared lost which results in poor application performance. In Figure 5.8(b), we show the accuracy of PROTEUS in predicting if the delay in the following time window will exceed the tolerable end-to-end delay (i.e., 150ms [33]) as a function of the true one-way delay. This can answer the question whether we should grow the de-jitter buffer size. Note that the one-way delay is calibrated so that the one-way delay is 0ms if there is no congestion on the network [82]. Similar to before, a false positive occurs when we predict the delay to be larger than 150ms but in reality it is not. A false negative is when we predict the delay to be smaller than 150ms, but in reality it is larger. According to Figure 5.8(b), the false positive is around 1-2% and the false negative is around 2-3%.

PROTEUS's performance in throughput prediction. Predicting the throughput in the next time window is also important for certain bandwidth intensive applications such as video conferencing and VOD. For RTC applications such as video conferencing, throughput prediction can be combined with loss rate prediction to appropriately set the encoder bitrate and the FEC rate. For non-RTC applications such as VOD using chunked video streaming, throughput prediction can be used to appropriately assign bit allocation across video chunks to improve video quality. Overestimating the achievable throughput may lead to application level information loss or increased delay, while underestimating the achievable throughput prevents applications from maximally utilizing the network.

Since PROTEUS passively monitors network traffic, it cannot predict the achievable throughput of the following time window at an arbitrary sending rate. PROTEUS makes the prediction assuming the sending rate of the next time window is the same as the previous one. We evaluate PROTEUS's accuracy in throughput prediction as a function of the actual throughput and show the results in Figure 5.8(c). To ensure Figure 5.8(c)'s readability, 15 flows in TrafficSet are randomly chosen. Each flow corresponds to an error bar showing the median and standard deviation of the predicted throughput over all the time windows. We see that throughput prediction is fairly accurate across the entire range of throughput, i.e., the median error is around 10kbps with a standard deviation of around 10kbps.

PROTEUS's performance in other networks. So far, we have investigated the accuracy of using PROTEUS to predict the loss rate, one-way delay, and

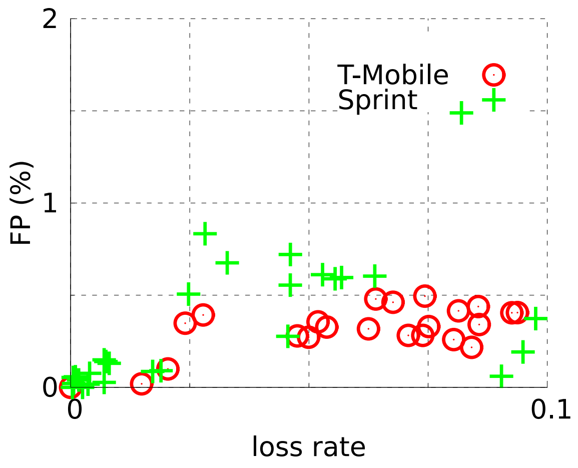

Figure 5.9: Impact of the cellular network.

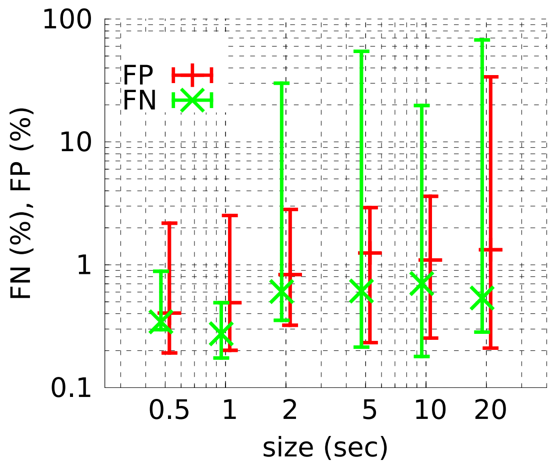

Figure 5.10: Impact of the time window size.

throughput for one particular cellular carrier. To be broadly applicable, we need to verify if PROTEUS's accuracy applies to other cellular carriers as well. Figure 5.9 shows the false positive rate of loss predictions for T-Mobile and Sprint, whose setup is described in Table 5.2. According to Figure 5.9, both T-Mobile and Sprint have even a lower false positive than AT&T. We only include the evaluation on false positive rate of T-Mobile and Sprint, but have verified that PROTEUS also has high prediction accuracy in terms of the false negative and false positive rates in one-way delay and throughput prediction.

PROTEUS's performance affected by the time and information window

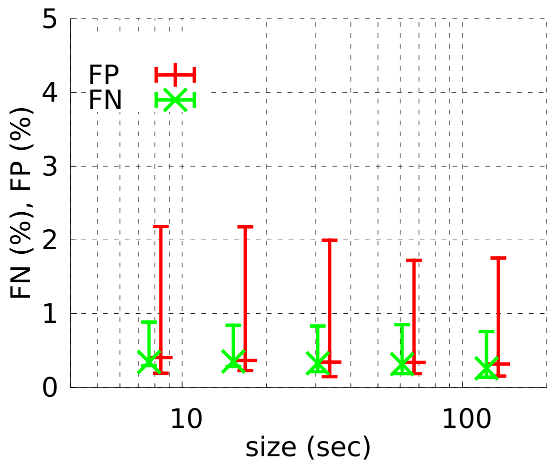

Figure 5.11: Impact of the information window size.

size. We also study the impact of the time window size and the information window size. We have investigated the impact of the time window size on autocorrelation coefficient in Figure 5.2(a). Here we investigate the impact of time window size on PROTEUS's prediction accuracy. Figure 5.10 shows the distribution of the false positive and false negative rates as functions of the time window size. Unlike Figure 5.2(a), PROTEUS's false positive rate is the minimum when the time window size is 0.5s, while PROTEUS's false negative is the minimum when the time window size is 1s. If the time window size further increases, the variation of the false positive can be extremely high (>50%). Using a large time window with a fixed information window size suffers from high performance variability due to the fact that only a few time windows are available. Using a small time window with the same amount of history allows predicting performance on a finer granularity and is preferred. We choose a time window of 0.5s as the lower bound since it is reasonable to keep the time window larger than typical network round trip time.

Another parameter is PROTEUS's information window size which in conjunction with the time window size determines the number of time windows used in the prediction. Similar to the autocorrelation results in Figure 5.2(b), we see from Figure 5.11 that prediction gains in PROTEUS are marginal once the information window size used for prediction is larger than 8s. Thus we can achieve accurate prediction using time windows within the last 8s.

5.3 Application of PROTEUS

Applications can take advantage of network metric prediction to improve their performance. The exact benefit will depend on how each application uses the information obtained from PROTEUS. Here we show the improvement PROTEUS can provide to two RTC applications: a video conferencing application and an interactive software application, i.e., Draw Something.

5.3.1 Video Conferencing System

Equivalent video conferencing emulation. We describe how we realistically evaluate the video conferencing application to make use of PROTEUS in a working system, considering all the overhead of the associated changes with the small difference of running the client software on a legacy laptop instead of a mobile device due to software constraints.

There are standard methods to evaluate video conferencing using the H.264/AVC reference software [8] on PCs. However, there is no such equivalent open-source encoding/decoding suite on mobile platforms. Thus, to best effectively evaluate video conferencing on mobile platforms, we take the following steps: (i), we modify the H.264/AVC reference software so that the H.264 encoder can adjust the video codec bitrate and FEC rate for each video frame rather than sticking to fixed codec bitrate and FEC rate for an entire video stream; (ii), we use a 2GHz dual core Thinkpad T60 with 2G RAM to run the H.264 decoder, with the computation performance as close to off-the-shelf mobile devices as possible; and (iii), we replay the packet traces collected in cellular networks (i.e., TrafficSet) to emulate mobile network performance for H.264, which ensures identical, reproducible, and representative mobile network condition.

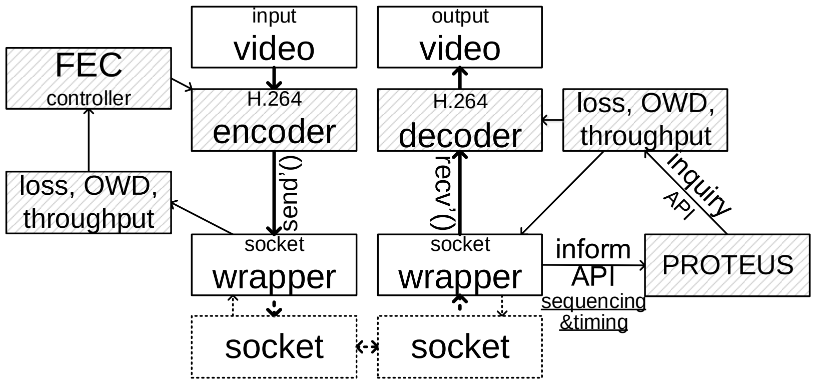

Figure 5.12: Platform setup to emulate mobile video conferencing. The dashed blocks and arrows are replayed using TrafficSet to guarantee realistic mobile network condition.

The packet sequencing and timing information seen by PROTEUS is exactly the same as it is in TrafficSet, enable PROTEUS to make the same predictions as it does in cellular networks. The emulation setup results in only two overestimations in evaluating the perceptual video quality. One is due to the Thinkpad T60 is more powerful than a mobile device, and the other is due to the elimination of the cost for traffic transmitting over its network interface. The overestimations should be acceptable given that video conferencing applications such as Skype can work perfectly well on mobile devices with excellent network connections.

As depicted in Figure 5.12, we focus on evaluating the performance in downlink video conferencing, i.e., the video stream is adaptively encoded and sent from the server to the client, where we can evaluate the perceptual quality of the received video stream. The H.264 decoder in Figure 5.12 represents the video conferencing application on the client, i.e., the mobile device emulated by the 2GHz dual core Thinkpad T60, while the H.264 encoder and FEC controller represent the counterpart on the server.

By replaying network traces collected from the cellular network in TrafficSet, we can reproduce representative mobile network condition. We measure the video quality performance using standard video sequences shown in Table 5.3 (referred as VideoSet) [19]. As illustrated in Figure 5.12, given a video sequence in VideoSet, the H.264 encoder on the server translates the video sequence to a RTP network stream. To test the video quality under various and reproducible network condition, for each flow in TrafficSet, we replace its content with the encoded network stream respectively. On the client, the H.264 decoder decodes the received network stream and constructs the video for users. According to TrafficSet, if a packet is lost or does not arrive in time at the de-jitter buffer, the corresponding frame may be corrupted so that the perceptual quality of the decoded video will be affected.

PROTEUS utilization in video conferencing. Based on past work, there are well established adaptations that applications take in response to changing network condition. The quality of video conferencing is very sensitive to three network metrics, i.e., the packet loss, the one-way delay, and the throughput. To ensure good quality, the video conferencing application can tune several parameters.

- The video codec can adjust the compression ratio, trading source video quality with codec bitrate, by adjusting the quantization parameter (QP) of macroblocks [73, 74]. A smaller QP value results in better visual quality at the expense of a higher bitrate and higher bandwidth requirement.
- The application can insert an appropriate number of forward error correction (FEC) packets. This process allocates the total transmission rate amongst source bitrate and channel (error correction) bitrate.
- The application can adjust the de-jitter buffer size which specifies how long the receiving end waits for data to arrive before it is played back. The de-jitter buffer size trades application latency with *late loss*. A larger de-jitter buffer size increases the chance that a packet will arrive in time for playback, but increases the end-to-end application latency. For video conferencing applications, the user

cannot perceive an end-to-end delay (including propagation delay, network queuing delay, and time spent in the de-jitter buffer) lower than 200ms [20]. However, when the end-to-end delay is above this threshold, there is perceived degradation.

video	# of frames	sequence	resolution	size (MB)
akiyo	300	10/IPPP	QCIF,CIF	44
bowing	300	10/IPPP	QCIF,CIF	44
bridge(close)	2001	10/IPPP	QCIF,CIF	291
bridge(far)	2101	10/IPPP	CIF	305
foreman	300	10/IPPP	QCIF,CIF	44
highway	2000	10/IPPP	CIF	291

Table 5.3: Video sequences to reproduce video conferencing streams (VideoSet). The frame rate for all these video sequences is 30fps.

We denote the predicted packet loss rate, one-way delay, and throughput by the triplet with $(\epsilon,\delta,\mathtt{T})$. This is the predicted network performance obtained from the regression tree on the mobile device and delivered to the server. Given this network prediction, we set the application parameters as follows: (i) the video codec bitrate for a given frame is set to $\mathtt{R}=(1-\alpha\epsilon)\mathtt{T}$ $(\alpha\geq 1)$; (ii) the FEC rate to $\alpha\epsilon\mathtt{T}$; and (iii) the receiver de-jitter buffer size to $\beta\delta$ seconds. α is a constant that determines the actual amount of FEC protection used. In the evaluation, $\alpha=1$. The total estimated throughput $\mathtt{T}$ is divided amongst source rate and FEC rate. As an example, suppose $\mathtt{T}$ is estimated as 500kbps, the estimated loss rate is $\epsilon=0.06$, and $\alpha=2$ is used. With this, 440kbps should be used for source coding and 60kbps for FEC protection. With a video frame rate of 15fps and a packet size of 500 bytes, this approximately translates to 7 packets per frame of source coding and 1 packet per frame of FEC.

Once the video frames are coded into packets, the evaluation platform assumes that these packets go through a network which has characteristics obtained from the collected network trace. If the actual loss on the network is less than or equal to $\alpha\epsilon\mathtt{T}$, the receiver has sufficient information to decode the frame, otherwise the frame is assumed to be lost. In addition to packet loss on the network, we also consider delay in the evaluation, assuming a de-jitter buffer size of $\beta\delta$ ($\beta \geq 1$), which is slightly larger than the estimated δ. In the above example, if two or more packets are lost or delayed later than $\beta\delta$, the respective frame is lost. In the evaluation, $\beta = 1$.

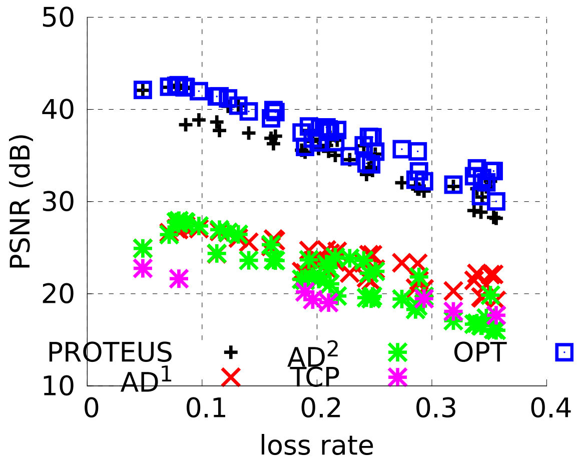

(a) 5th percentile PSNR.

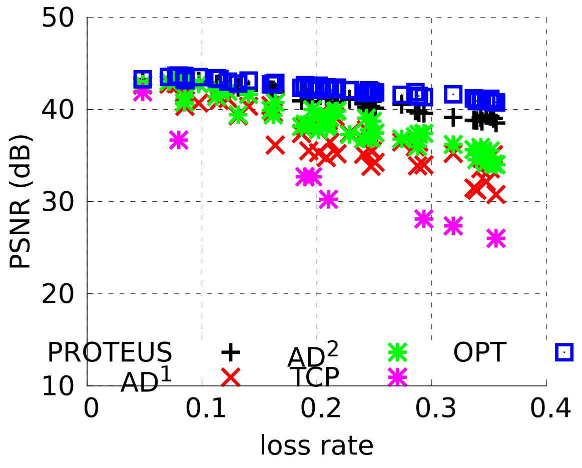

(b) 25th percentile PSNR.

Figure 5.13: PSNR for PROTEUS, AD[1], AD[2], TCP, and OPT, , which assumes that we a priori know the exact loss rate.

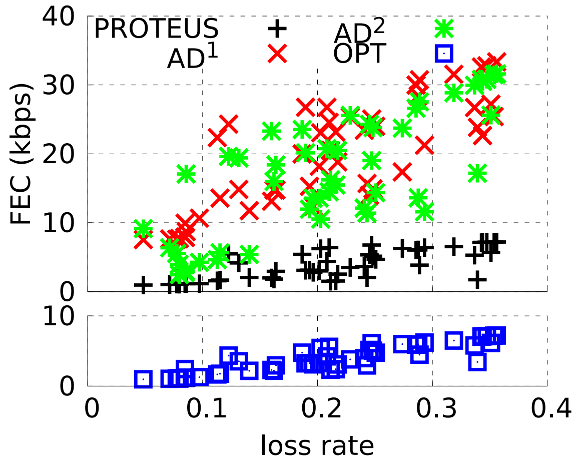

Figure 5.14: FEC overhead. "OPT" shows the total FEC overhead in the optimal scenarios.

Perceptual video quality assessment. The H.264 decoder provides the ability to conceal lost frames. Upon decoding the sequence, which may potentially have some frames lost, we compare the decoded video sequence to the original and measure the peak signal-to-noise ratio (PSNR) which is a commonly used metric to measure video quality. This setup is used to repeatedly measure the video quality using the prediction obtained from PROTEUS, AD^1, and AD^2 over the various video sequences in VideoSet and over the various network traces in TrafficSet.

If we underestimate ϵ (i.e., loss rate), then the application may add insufficient redundancy which results in unrecoverable packet loss for the application. Otherwise, if we overestimate ϵ, then the application may add too much redundancy which causes the video codec bitrate to be lower than needed, resulting in poorer video quality. Thus, both underestimation and overestimation of the future network performance can lower the perceptual video quality. We analyze the effect of network parameter mis-prediction on video quality for the three prediction techniques, PROTEUS, AD^1, and AD^2. We also analyze the performance hypothesizing that we exactly know the loss rate and insert just the right amount of FEC to counteract any packet loss. It is possible as we have the network traces. This optimal scheme is denoted as OPT.

For each video sequence in VideoSet, we run all the network traces from TrafficSet using each of the four methods (PROTEUS, AD^1, AD^2, and OPT). For each of the four methods, we compute a distribution of PSNR. In Figure 5.13, we show the 5th and 25th percentiles of the PSNR as a function of loss rate for each of the four methods. We purposefully show the low PSNR values in the distribution since this is what most affects overall user satisfaction and is a measure of how each of the three schemes performs in tough network condition. In addition to the four adaptive methods using UDP, we evaluate the adaptive bitrate streaming over TCP as well assuming that the encoded bitrate is always adapted to the throughput in the current time window. To guarantee the network condition for TCP and UDP experiments are comparable, for each TCP flow, we create UDP packets back-to-back lasting for the same duration. In Figure 5.13, the distribution of PSNR for TCP flows is represented as the function of the loss rate of the back-to-back UDP flow's loss rate.

In general, if a frame is lost, the PSNR of the other frames that reference the lost frame becomes very low, e.g., PSNR$<$25dB. Since PROTEUS can accurately predict loss rate with almost 99% accuracy, there are very few cases (i.e., $<$1%) where we see unrecoverable packet loss. Thus, as we see from Figure 5.13(a), even the 5th percentile PSNR shows no packet loss using PROTEUS. The only reason the 5th percentile PSNR is below OPT is due to over-protection which reduces the video codec bitrate. This reduction in PSNR in PROTEUS when compared to OPT (due to over-protection) is on the order of 1dB, whereas the reduction in PSNR in AD^1 and AD^2 (due to unrecoverable lost packets) is on the order of 15dB. As loss rate increases, the PSNR using PROTEUS decreases but stays close to OPT. It is obvious that increasing loss rate results in decreased capacity. Since a larger portion of the total throughput has to be allocated to FEC, we see a reduction in PSNR. To show the visual effect of unrecoverable packet loss, we show representative frames in the 5th percentile of PSNR values in Figure 5.15 using the schemes $AD^{1,2}$, TCP, and PROTEUS. It is clear that unrecoverable packet loss results in substantial video quality degradation.

As PROTEUS may overestimate the actual loss rate, there will inevitably be some cases where we over-protect. In Figure 5.14, we show the bitrate taken by FEC packets which are not used to correct any loss. The bottom plot shows the amount of needed FEC to correct for packet loss. As we see, as the loss rate increases, the amount of needed protection also increases. The top plot in Figure 5.14 shows the amount of additional FEC beyond the needed amount which is applied when using each of the three schemes to predict the loss rate. We see

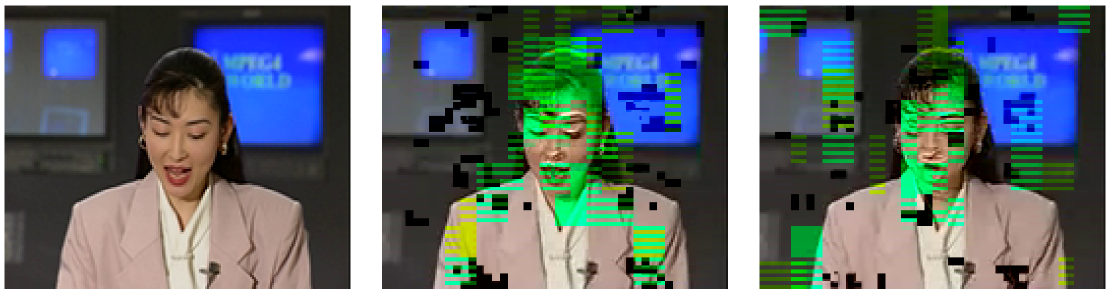

Figure 5.15: Perceptual video quality corresponding to the 5th-%ile PSNR according to Figure 5.13 for PROTEUS, AD^1, AD^2, and TCP (using "akiyo" in Table 5.3): (a) 36dB – PROTEUS, (b) 23dB – AD^{1,2}, and (c) 20dB – TCP.

that indeed PROTEUS does add a certain amount of FEC overhead. However, it is fairly small, and as we have seen from Figure 5.13, it only results in about a 1dB reduction in PSNR. Even at high loss rates, this overhead is less than 10kbps. The overhead for AD^1 and AD^2 is actually much higher as it only reacts once loss has already started occurring. Just because there was loss in the previous time window does not guarantee that there will be loss in the future time windows. So not only do AD^1 and AD^2 suffer from unrecoverable packet loss, they also actually insert more FEC than PROTEUS.

5.3.2 Interactive Software Application

Many interactive software applications have bursty traffic patterns, e.g., the burst can consist of a screen update. A good measure of the performance of such interactive software applications can be the time taken to deliver the burst of data. However, as opposed to throughput sensitive applications such as file downloading, a burst is relatively small in duration and thus the latency caused by packet loss recovery becomes significant in determining performance. Therefore, an adaptive UDP based scheme which appropriately controls the throughput allocated to source and FEC becomes important in determining application performance [80], especially for the channels with packet loss such as wireless networks.

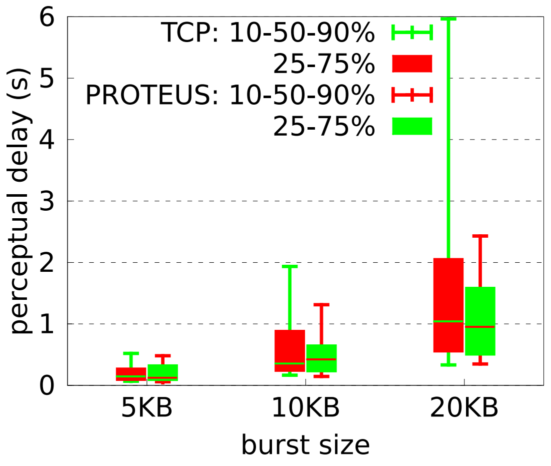

Figure 5.16: Perceptual delay in Draw Something.

Here we consider a particular application, Draw Something, to show how PROTEUS can benefit interactive software applications such as desktop sharing and multi-player gaming. In Draw Something, two players alternate turns between drawing a picture to convey a guessword for the partner to guess. In each turn, the stroke-by-stroke drawing animation playing back to the partner results in a traffic burst. We rely on trace analysis to evaluate how PROTEUS can benefit such an application. We capture the application traffic via `tcpdump` on Android and identify the traffic bursts corresponding to drawing animations. The trace consists of a duration lasting five hours and consisting of hundreds of bursts.

To measure the improvement of an adaptive UDP scheme using PROTEUS over TCP, we replay the traffic using UDP plus PROTEUS (UDP/PROTEUS) and measure the time between the first packet of a burst being sent to the last packet in the burst being received. UDP/PROTEUS adds an appropriate amount of FEC if packet loss is anticipated. A poor prediction of loss rate can result in higher burst delivery time due to either retransmission or over-protection. To verify that the traffic replaying under UDP/PROTEUS experiences roughly the same network condition as the Draw Something's original trace over TCP, we compare their median perceptual delay. Figure 5.16 shows the distribution of the perceptual delay over different burst size. As the median perceptual delay for UDP/PROTEUS is very close to TCP's, we expect that UDP/PROTEUS experiences similar network condition. According to Figure 5.16, when the burst size is very small, TCP and UDP/PROTEUS perform equally at any percentile in the distribution. However, when the burst size grows to 10KB and larger (e.g., 20KB), UDP/PROTEUS performs much better, particularly in the 75-90th percentile perceptual delay, which may easily produce user dissatisfaction. UDP/PROTEUS reduces the 90th percentile perceptual delay by roughly 1s When the burst size is around 10KB. When the burst size is around 20KB, UDP/PROTEUS's 90th percentile perceptual delay is 2s while TCP's is up to 6s.

5.4 Summary of Optimizing Real-Time, Interactive Applications

In this section, we systematically quantified the predictability of network performance metrics in three major cellular networks: AT&T, T-Mobile, and Sprint. In all three carriers, we identified the existence of strong predictability of network performance, even over a short term window e.g., 0.5s. To take advantage of this predictability, we proposed a system PROTEUS, which collects network performance information being observed by applications, employs regression trees to learn network performance patterns, and forecasts future network performance to benefit application performance. PROTEUS can predict the occurrence of packet loss within a time window for 98% of the time windows, occurrence of long one-way delay for 97% of the time windows, and the throughput within a median error of 10kbps. By using PROTEUS in a video conferencing scenario, we can improve the PSNR of the perceived video by 15dB when compared against traditional performance adaptation techniques. Compared with the hypothesized optimal scenario in which the application knows exactly which packets will be lost, PROTEUS is only 1-2dB worse.

We believe that PROTEUS is a comprehensive and effective network performance forecasting framework for use by mobile applications especially for use over cellular networks. PROTEUS can also inspire the development of challenging applications on mobile devices.

CHAPTER VI

RELATED WORK

We broadly classify previous studies into (i) cellular infrastructure, (ii) application usage, and (iii) application optimization, and position our studies accordingly as follows.

6.1 Cellular Infrastructure

YellowPage is motivated by numerous previous measurement studies [105, 125, 76], e.g., Rocketfuel [102] to characterize various properties of the Internet through passive monitoring using data such as server logs and packet traces, as well as active measurement such as probing path changes. Efforts on reverse engineering properties of the Internet [103] have been shown to be quite successful; however, very little work has been done in the space of cellular IP networks. Complementary to YellowPage, the most recent work by Keralapura et al. profiled the browsing behavior by investigating whether there exists distinct behavior pattern among mobile users [68]. Their study implemented effective co-clustering on large scale user-level web browsing traces collected from one cellular provider. As far as we know, our study is the first to comprehensively characterize cellular IP networks covering all the major cellular carriers in the U.S., focusing on key characteristics such as network topological properties and dynamic routing behavior. From the characterization of the cellular data network structure, we also draw conclusions on content placement, which is essential given the rapidly growing demand for mobile data access.

We build our work upon a recent study by Balakrishnan et al. [28] in which they highlighted unexpected dynamic behavior of cellular IP addresses. YellowPage performs a more complete and general study covering a wider set of properties, illustrating carrier-specific network differences, explaining the observed diverse geographic distribution of cellular IP addresses, also investigating associated implications of observed network designs.

Although there have been studies characterized the CDNs relative to the end users accessing from the wireline networks [79, 100, 41, 92, 60], very little attention has been paid to the cellular users. These previous studies are mainly from two perspectives, i.e., content placement and server selection. YellowPage is complementary to these studies by investigating the implication of cellular network infrastructure on mobile data placement and server selection. To our best knowledge, YellowPage is the first to investigate the content placement and content server selections for cellular users.

Previous studies on cellular networks can be classified approximately into several categories, namely from ISP's view point of managing network resources [54, 104], from end-user's perspectives of optimizing energy efficiency and network performance at the device [25, 126, 30], and finally developing infrastructure support for improving mobile application performance [38, 94]. YellowPage is complementary to them by exposing the internal design of the cellular data network structure that can be useful to guide such optimization efforts.

There have also been several measurement studies in understanding the performance and usage of cellular networks. One recent study focuses on mobile user behavior from the perspective of applications such as [108] which characterized the relationship between users' application interests and mobility. Other examples include a study of the interaction between the wireless channels and applications [75], and performance of TCP/IP over 3G wireless with rate and delay variation [40]. Note that our work fills an important void in the space of cellular data network by focusing on the network architectural design: IP address allocation, local DNS service setup, and routing dynamics.

6.2 Application Usage

There have been numerous previous effort in investigating mobile apps from different aspects. Among the previous work, mobile or smartphone app profiling has yielded insights into many ones in the mobile community including users, developers, OS vendors, network operators, and content partners. To our best knowledge, none of the prior studies have proposed any online approach to trace network traffic back to individual apps, which is essential in many practical scenarios.

There have been studies focusing on profiling apps at the granularity of app types (e.g., email, social networking, music, and
gaming) [68, 108, 122, 116, 66, 45], or groups of apps (e.g., P2P vs. non-P2P) [99]. compared with identifying individual apps, identifying app types or groups is easier by the port number, the hostname, and the application-level protocol. Identifying individual apps has different usage scenarios such as app-wise policy enforcement, anomaly detection. Thus, FLOWR is a further step along the path of profiling apps. In app-wise profiling, NetworkProfiler [46], ProfileDroid [111], PowerTutor [14], TaintDroid [47], and App Profiles [3] perform individual app profiling via instrumented devices or emulators, which limit themselves to small scales. Unlike these studies, FLOWR is an attempt to identify individual apps at a large scale

targeting the majority of apps on mainstream app markets. Without on-device information, FLOWR is aimed at identifying the network traffic originated by apps. Thus, FLOWR is complementary to previous on-device app profiling approaches.

Diverse information inside network traffic has been explored by previous studies from many aspects, e.g., user browsing pattern [68, 108], content diversity [122, 77], privacy leakage [70, 83, 71, 93]. Standing on the shoulder of previous studies, FLOWR leverages the rich information inside traffic that can reveal app identities to construct flow signatures. Rather than investigating the user-centric information, it emphasizes on app-centric information. FLOWR attempts to determine which part of the network traffic originated by apps can best identify apps.

Also related are studies that proposed measurement tools for smartphone devices characterizing either the device performance or the performance of certain apps [62, 124, 89], e.g., 3GTest [62] measures the network performance of popular smartphone platforms, PowerTutor [124] profiles energy consumption of running apps on Android, ARO [89] characterizes the radio resource usage of mobile apps, etc. Compared to these studies, we focus on usage patterns of mobile apps rather than their performance, but our work also has implications on resource consumption.

Besides app usage, app selection has been explored as well in context-aware mobile apps recommendation systems [114, 123]. A key requirement for an app recommendation system is to identify the users who share certain similar app interests so that it can predict apps of interest. Understanding patterns in user interests is fulfilled in DIVERSITY.

We believe that our study makes an important step in addressing the lack of knowledge of usage behaviors of mobile apps.

6.3 Application Optimization

A group of studies attempted to improve the performance of mobile apps via OS infrastructure support [44, 58, 52, 47], e.g., offloading resource intensive computation to cloud [44], providing clean intermediate interface for apps by the OS [58], and signaling mobile devices by network providers via notification channel to save resource [52]. PROTEUS is complementary to these, as it focuses on real-time, interactive applications in cellular networks.

There has been a significant amount of previous work proposing solutions for adapting to varying network performance [81, 126, 39, 1, 4, 9, 13, 98, 57]. However, all of these proposed solutions only adjust application behavior once degradation is observed. PROTEUS is fundamentally different from these previous adaptation approaches in that PROTEUS proactively forecasts the achievable network performance rather than passively reacting to performance degradation. This allows applications to modify their behavior in anticipation of degrading network condition which can significantly improve performance.

The key to the effectiveness of PROTEUS is network performance predictability. There have been previous measurement studies to investigate the network behavior of cellular networks [75, 62, 40, 39, 107, 78, 26]. Among these measurement studies, the existence of network predictability has been indicated from certain aspects. For example, Liu et al. observed that the time for a mobile device to stay in any particular data rate state is on the order of hundreds of time slots (with each time slot being 1.67ms) in a EV-DO network [75]. Manweiler et al. found that in AT&T and T-Mobile networks, the network latency measured in a 15 min time window has certain dependency on the latency of a previous time window [78]. Standing upon the shoulder of previous studies, PROTEUS answers the following three questions. First, how predictable are cellular networks? Second, what network features can be used for performance prediction? Third, how accurate is the prediction?

There has also been a significant amount of previous work which studies predictability in mobile (cellular) networks with the goal of improving application performance [86, 78, 115, 96, 95]. Access pattern predictability is investigated with the attempt to reduce connectivity overhead due to frequent user mobility in [86, 85] and with the attempt to switch to better access networks in [101, 24, 88]. PROTEUS distinguishes itself from these studies in two aspects. First, PROTEUS forecasts network performance in run time, rather than offline. As cellular networks are well-known to be highly variable, a one-time, offline prediction will not work well because it will be quickly out-dated. Second, PROTEUS's performance prediction is much more fine-grained. Unlike previous studies that usually attempt to improve performance for non-real-time bandwidth intensive applications which are not sensitive to packet loss and one-way delay, PROTEUS targets a broad spectrum of applications including RTC applications which are sensitive to packet loss and one-way delay.

To our best knowledge, PROTEUS is the first one proposing a fine-grained, real-time solution for predicting future network performance over cellular networks which allows applications to react before network degradation occurs.

CHAPTER VII

CONCLUDING REMARKS

The dissertation is dedicated to address four challenges: (i) revealing the internal of cellular network infrastructure, (ii) isolating the impact of a multitude of factors on cellular network performance, (iii) identifying diverse usage patterns of smartphone applications, and (iv) optimizing networking performance of real-time, interactive applications.

In YellowPage, we identified the routing restriction issue due to the limited number of cellular network gateways, which narrows down the performance bottleneck to the part from the mobile device to the GGSN, i.e., the IP gateway. The routing restriction could affect latency sensitive applications significantly. In particular, even placing content servers close to GGSNs, the saving in latency is limited, i.e., $<$6ms.

The routing restriction in cellular networks negatively affect latency sensitive applications. To improve one type of latency sensitive applications, i.e., real-time/interactive applications to cellular networks, we quantified the network performance predictability in short-term time granularity, and proposed PROTEUS to allow applications to leverage such predictability. Using PROTEUS, a video conferencing application can improve its PSNR of the perceived video by 15dB against traditional performance adaptation techniques.

Moving beyond optimizing a single type of applications to more, we proposed FLOWR to identify individual mobile applications at cellular network gateways, and then comprehensively characterized the usage patterns of mobile applications in DIVERSITY and collected many mobile application specific observations and findings that can benefit application design in practice.

Although cellular technologies have been upgraded to LTE, our research contributions remain. The routing restriction issue identified in YellowPage still applies for cellular network operators due to management overhead and flexibility concern. As high performance variation is a nature of cellular networks, we expect that PROTEUS always benefit performance sensitive applications, which are expected to enrich mobile users significantly in future. The techniques in FLOWR, the motivations for understanding application usages, and the observations and findings in DIVERSITY are independent from the technology.

BIBLIOGRAPHY

BIBLIOGRAPHY

[1] Adobe HTTP Dynamic Streaming. http://www.adobe.com/products/hds-dynamic-streaming.html.

[2] APK Downloader. http://codekiem.com/2012/02/24/apk-downloader.

[3] APP Profiles. http://appprofiles.eecs.umich.edu.

[4] Apple HTTP Live Streaming. https://developer.apple.com/resources/http-streaming.

[5] CAPTCHA: Telling Humans and Computers Apart Automatically. http://www.captcha.net/.

[6] Cisco TelePresence Secure Communications and Signaling. http://www.cisco.com/en/US/docs/solutions/Enterprise/Video/telepresence.html.

[7] Google Gears API – Google Developers. https://developers.google.com/gears.

[8] H.264/AVC JM Reference Software. http://iphome.hhi.de/suehring/tml.

[9] IIS Smooth Streaming. http://www.iis.net/download/SmoothStreaming.

[10] ISO/IEC DIS 23009-1.2 Dynamic Adaptive Streaming over HTTP (DASH). http://www.iso.org/iso/iso_catalogue/catalogue_tc/catalogue_detail.htm?csnumber=57623.

[11] Mobile Apps Put the Web in Their Rear-View Mirror. http://blog.flurry.com/bid/63907/.

[12] Netsense. http://netsense.nd.edu.

[13] Octoshape Broadcasting Flash Media Multi-Bit Rate. https://support.octoshape.com/entries/20655458-broadcasting-flash-media-multi-bit-rate.

[14] PowerTutor. http://powertutor.org.

[15] RTCWeb Status Pages. http://tools.ietf.org/wg/rtcweb/.

[16] Stoke / Home / Mobile Broadband Access Solutions.
http://www.stoke.com/.

[17] University of Oregon Route Views Archive Project. www.routeviews.org.

[18] YPMobile - Yellow Pages on your iPhone, BlackBerry or Android!
http://www.yellowpages.com/products.

[19] YUV Video Sequences. http://trace.eas.asu.edu/yuv.

[20] ITU-T recommendation G. 114, 2000.

[21] 3GPP. General Packet Radio Service (GPRS); GPRS Tunnelling Protocol GPT) across the Gn and Gp Interface.
http://www.3gpp.org/ftp/Specs/html-info/0960.htm, 2003.

[22] 3GPP. Analysis of Higher Chip Rates for UTRA TDD Evolution. http://www.3gpp.org/ftp/tsg_ran/tsg_ran/TSGR_25/Docs/PDF/RP-040361.pdf, 2004.

[23] AKHSHABI, S., BEGEN, A., AND DOVROLIS, C. An Experimental Evaluation of Rate-Adaptation Algorithms in Adaptive Streaming over HTTP. In *Proc. ACM MMSys* (2011).

[24] ALJADHAI, A., AND ZNATI, T. Predictive Mobility Support for QoS Provisioning in Mobile Wireless Environments. *IEEE J. Selected Areas in Communications* (2001).

[25] ANAND, M., NIGHTINGALE, E. B., AND FLINN, J. Self-Tuning Wireless Network Power Management. *SPRINGER Wireless Networks 11*, 4 (2005).

[26] ANTUNES, N., FRICKER, C., ROBERT, P., AND TIBI, D. Metastability of CDMA Cellular Systems. In *Proc. ACM MOBICOM* (2006).

[27] APPLE. Apple's App Store Downloads Top 10 Billion.
http://www.apple.com/pr/library/2011/01/22appstore.html.

[28] BALAKRISHNAN, M., MOHOMED, I., AND RAMASUBRAMANIAN, V. Where's That Phone?: Geolocating IP Addresses on 3G Networks. In *Proc. ACM SIGCOMM IMC* (2009).

[29] BALASUBRAMANIAN, A., MAHAJAN, R., AND VENKATARAMANI, A. Augmenting Mobile 3G Using WiFi: Measurement, System Design, and Implementation. In *Proc. ACM MobiSys* (2010).

[30] BALASUBRAMANIAN, N., BALASUBRAMANIAN, A., AND VENKATARAMANI, A. Energy Consumption in Mobile Phones: A Measurement Study and Implications for Network Applications. In *Proc. ACM SIGCOMM IMC* (2009).

[31] BERNERS-LEE, T., FIELDING, R., AND MASINTER, L. Uniform Resource Identifier (URI): Generic Syntax. RFC 3986, 2005.

[32] BOLOT, J.-C., AND VEGA-GARCÍA, A. Control Mechanisms for Packet Audio in the Internet. In *Proc. IEEE INFOCOM* (1996).

[33] BOUCH, A., SASSE, M., AND DEMEER, H. Of Packets and People: A User-Centered Approach to Quality of Service. In *Proc. IEEE/ACM IWQoS* (2000).

[34] BREIMAN, L. *Classification and Regression Trees*. Chapman & Hall/CRC, 1984.

[35] BRUMLEY, D., CABALLERO, J., LIANG, Z., NEWSOME, J., AND SONG, D. Towards Automatic Discovery of Deviations in Binary Implementations with Applications to Error Detection and Fingerprint Generation. In *Proc. USENIX Security* (2007).

[36] CABALLERO, J., YIN, H., LIANG, Z., AND SONG, D. Polyglot: Automatic Extraction of Protocol Message Format Using Dynamic Binary Analysis. In *Proc. ACM CCS* (2007).

[37] CASADO, M., AND FREEDMAN, M. J. Peering through the Shroud: The Effect of Edge Opacity on IP-Based Client Identification. In *Proc. USENIX NSDI* (2007).

[38] CHAKRAVORTY, R., BANERJEE, S., AGARWAL, S., AND PRATT, I. MoB: A Mobile Bazaar for Wide-Area Wireless Services. In *Proc. ACM MOBICOM* (2005).

[39] CHAKRAVORTY, R., BANERJEE, S., RODRIGUEZ, P., CHESTERFIELD, J., AND PRATT, I. Performance Optimizations for Wireless Wide-Area Networks: Comparative Study and Experimental Evaluation. In *Proc. ACM MOBICOM* (2004).

[40] CHAN, M., AND RAMJEE, R. TCP/IP Performance over 3G Wireless Links with Rate and Delay Variation. In *Proc. ACM MOBICOM* (2002).

[41] CHENG, S. J., JIN, C., KURC, A. R., RAZ, D., AND SHAVITT, Y. Constrained Mirror Placement on the Internet. In *Proc. IEEE INFOCOM* (2001).

[42] CHIN, E., FELT, A., GREENWOOD, K., AND WAGNER, D. Analyzing Inter-Application Communication in Android. In *Proc. ACM MobiSys* (2011).

[43] CHUAH, M., LUO, W., AND ZHANG, X. Impacts of Inactivity Timer Values on UMTS System Capacity. In *Proc. IEEE Wireless Communications and Networking Conference (WCNC)* (2002).

[44] CUERVO, E., BALASUBRAMANIAN, A., KI CHO, D., WOLMAN, A., SAROIU, S., CH, R., AND BAHL, P. MAUI: Making Smartphones Last Longer with Code Offload. In *Proc. ACM MobiSys* (2010).

[45] Cui, W., Kannan, J., and Wang, H. Discoverer: Automatic Protocol Reverse Engineering from Network Traces. In *Proc. USENIX Security* (2007).

[46] Dai, S., Tongaonkar, A., Wang, X., Nucci, A., and Song, D. Networkprofiler: Towards Automatic Fingerprinting of Android Apps. In *Proc. IEEE INFOCOM* (2013).

[47] Enck, W., Gilbert, P., Chun, B., Cox, L., Jung, J., McDaniel, P., and Sheth, A. TaintDroid: An Information-Flow Tracking System for Realtime Privacy Monitoring on Smartphones. In *Proc. USENIX OSDI* (2010).

[48] Enck, W., Octeau, D., McDaniel, P., and Chaudhuri, S. A Study of Android Application Security. In *Proc. USENIX Security* (2011).

[49] Falaki, H., Lymberopoulos, D., Mahajan, R., Kandula, S., and Estrin, D. A First Look at Traffic on Smartphones. In *Proc. ACM SIGCOMM IMC* (2010).

[50] Falaki, H., Mahajan, R., Kandula, S., Lymberopoulos, D., Govindan, R., and Estrin, D. Diversity in Smartphone Usage. In *Proc. ACM MobiSys* (2010).

[51] Federal Emergency Management Agency. Tornado Activity in the United States. `http://www.fema.gov/plan/prevent/saferoom/tsfs02_torn_activity.shtm`.

[52] Ficek, M., Pop, T., Vláčil, P., Dufková, K., Kencl, L., and Tomek, M. Performance Study of Active Tracking in a Cellular Network Using a Modular Signaling Platform. In *Proc. ACM MobiSys* (2010).

[53] Gember, A., Anand, A., and Akella, A. A Comparative Study of Handheld and Non-Handheld Traffic in Campus WiFi Networks. In *Proc. International Conference on Passive and Active Network Measurement (PAM)* (2011).

[54] Ghaderi, M., Sridharan, A., Zang, H., Towsley, D., and Cruz, R. TCP-Aware Resource Allocation in CDMA Networks. In *Proc. ACM MOBICOM* (2006).

[55] Google. Eric Schmidt at Mobile World Congress 2011. `http://www.youtube.com/watch?v=ClkQA2Lb_iE&feature=related`.

[56] Gueye, B., Ziviani, A., Crovella, M., and Fdida, S. Constraint-Based Geolocation of Internet Hosts. *IEEE/ACM Trans. Networking*.

[57] Higgins, B., Flinn, J., Giuli, T., Noble, B., Peplin, C., and Watson, D. Informed Mobile Prefetching. In *Proc. ACM MobiSys* (2012).

[58] HIGGINS, B. D., REDA, A., ALPEROVICH, T., FLINN, J., GIULI, T. J., NOBLE, B., AND WATSON, D. Intentional Networking: Opportunistic Exploitation of Mobile Network Diversity. In *Proc. ACM MOBICOM* (2010).

[59] HORNYACK, P., HAN, S., JUNG, J., SCHECHTER, S., AND WETHERALL, D. These Aren't the Droids You're Looking for: Retrofitting Android to Protect Data from Imperious Applications. In *Proc. ACM CCS* (2011).

[60] HUANG, C., WANG, A., LI, J., AND ROSS, K. W. Measuring and Evaluating Large-Scale CDNs. In *Microsoft Research Technical Report MSR-TR-2008-106* (2008).

[61] HUANG, J., QIAN, F., GERBER, A., MAO, Z. M., SEN, S., AND SPATSCHECK, O. A Close Examination of Performance and Power Characteristics of 4G LTE Networks. In *Proc. ACM MobiSys* (2012).

[62] HUANG, J., XU, Q., TIWANA, B., MAO, Z. M., ZHANG, M., AND BAHL, P. Anatomizing Application Performance Differences on Smartphones. In *Proc. ACM MobiSys* (2010).

[63] JALALI, A., PADOVANI, R., AND PANKAJ, R. Data Throughput of CDMA-HDR a High Efficiency-High Data Rate Personal Communication Wireless System. In *Proc. IEEE Vehicular Technology Conference (VTC)* (2000).

[64] JIANG, H., LIU, Z., WANG, Y., LEE, K., AND RHEE, I. Understanding Bufferbloat in Cellular Networks. In *Proc. ACM SIGCOMM IMC* (2012).

[65] KANNAN, J., JUNG, J., PAXSON, V., AND KOKSAL, C. Semi-Automated Discovery of Application Session Structure. In *Proc. ACM SIGCOMM IMC* (2006).

[66] KARAGIANNIS, T., PAPAGIANNAKI, K., AND FALOUTSOS, M. BLINC: Multilevel Traffic Classification in the Dark. In *Proc. ACM SIGCOMM* (2005).

[67] KATZ-BASSETT, E., JOHN, J. P., KRISHNAMURTHY, A., WETHERALL, D., ANDERSON, T., AND CHAWATHE, Y. Towards IP Geolocation Using Delay and Topology Measurements. In *Proc. ACM SIGCOMM IMC* (2006).

[68] KERALAPURA, R., NUCCI, A., ZHANG, Z., AND GAO, L. Profiling Users in A 3G Network Using Hourglass Co-Clustering. In *Proc. ACM MOBICOM* (2010).

[69] KOLEHMAINEN, N., PUTTONEN, J., KELA, P., RISTANIEMI, T., HENTTONEN, T., AND MOISIO, M. Channel Quality Indication Reporting Schemes for UTRAN Long Term Evolution Downlink. In *Proc. IEEE Vehicular Technology Conference (VTC)* (2008).

[70] Krishnamurthy, B., Naryshkin, K., and Wills, C. Privacy Leakage vs. Protection Measures: the Growing Disconnect. In *Proc. IEEE Workshop on Web 2.0 Security and Privacy (W2SP)* (2011).

[71] Krishnamurthy, B., and Wills, C. E. On the Leakage of Personally Identifiable Information via Online Social Networks. In *Proc. ACM Workshop on Online Social Networks (WOSN)* (2009).

[72] Kushner, H., and Whiting, P. Convergence of Proportional-Fair Sharing Algorithms under General Conditions. *IEEE Trans. Wirelss Communications* (2004).

[73] Lee, H., Chiang, T., and Zhang, Y. Scalable Rate Control for MPEG-4 Video. *IEEE Trans. Circuits and Systems for Video Technology* (2000).

[74] Li, Z., Pan, F., Lim, K., Lin, X., and Rahardja, S. Adaptive Rate Control for H. 264. In *Proc. IEEE ICIP* (2004).

[75] Liu, X., Sridharan, A., Machiraju, S., Seshadri, M., and Zang, H. Experiences in a 3G Network: Interplay between the Wireless Channel and Applications. In *Proc. ACM MOBICOM* (2008).

[76] Madhyastha, H., Isdal, T., Piatek, M., Dixon, C., Anderson, T., Krishnamurthy, A., and Venkataramani, A. iPlane: An Information Plane for Distributed Services. In *Proc. USENIX OSDI* (2006).

[77] Maier, G., Schneider, F., and Feldmann, A. A First Look at Mobile Hand-Held Device Traffic. In *Proc. International Conference on Passive and Active Network Measurement (PAM)* (2010).

[78] Manweiler, J., Agarwal, S., Zhang, M., Roy Choudhury, R., and Bahl, P. Switchboard: A Matchmaking System for Multiplayer Mobile Games. In *Proc. ACM MobiSys* (2011).

[79] Mao, Z. M., Cranor, C., Douglis, F., Rabinovich, M., Spatscheck, O., and Wang, J. A Precise and Efficient Evaluation of the Proximity between Web Clients and their Local DNS Servers. In *Proc. USENIX ATC* (2002).

[80] Mehrotra, S., Li, J., and Huang, Y.-Z. Optimizing FEC Transmission Strategy for Minimizing Delay in Lossless Sequential Streaming. *IEEE Trans. Multimedia* (2011).

[81] Mohomed, I., Cai, J., Chavoshi, S., and De Lara, E. Context-Aware Interactive Content Adaptation. In *Proc. ACM MobiSys* (2006).

[82] Moon, S., Skelly, P., and Towsley, D. Estimation and Removal of Clock Skew from Network Delay Measurements. In *Proc. IEEE INFOCOM* (1999).

[83] MULLINER, C. Privacy Leaks in Mobile Phone Internet Access. In *Proc. International Conference on Intelligence in Next Generation Networks (ICIN)* (2010).

[84] NATIONAL HURRICANE CENTER. National Hurricane Center. `http://www.nhc.noaa.gov/pdf/TAFB_Trifold.pdf`.

[85] NICHOLSON, A., CHAWATHE, Y., CHEN, M., NOBLE, B., AND WETHERALL, D. Improved Access Point Selection. In *Proc. ACM MobiSys* (2006).

[86] NICHOLSON, A., AND NOBLE, B. Breadcrumbs: Forecasting Mobile Connectivity. In *Proc. ACM MOBICOM* (2008).

[87] PADMANABHAN, V. N., AND SUBRAMANIAN, L. An Investigation of Geographic Mapping Techniques for Internet Hosts. In *Proc. ACM SIGCOMM* (2001).

[88] PANG, J., GREENSTEIN, B., KAMINSKY, M., MCCOY, D., AND SESHAN, S. WiFi-Reports: Improving Wireless Network Selection with Collaboration. In *Proc. ACM MobiSys* (2009).

[89] QIAN, F., WANG, Z., GERBER, A., MAO, Z., SEN, S., AND SPATSCHECK, O. Profiling Resource Usage for Mobile Applications: A Cross-Layer Approach. In *Proc. ACM MobiSys* (2011).

[90] QIAN, F., WANG, Z., GERBER, A., MAO, Z. M., SEN, S., AND SPATSCHECK, O. Characterizing Radio Resource Allocation for 3G Networks. In *Proc. ACM SIGCOMM IMC* (2010).

[91] QIAN, Z., WANG, Z., XU, Q., MAO, Z. M., ZHANG, M., AND WANG, Y.-M. You Can Run, but You Can't Hide: Exposing Network Location for Targeted DoS Attacks in 3G Networks. In *Proc. ISOC NDSS* (2012).

[92] QIU, L., PADMANABHAN, V. N., AND VOELKER, G. M. On the Placement of Web Server Replicas. In *Proc. IEEE INFOCOM* (2001).

[93] RIEDERER, C., ERRAMILLI, V., CHAINTREAU, A., KRISHNAMURTHY, B., AND RODRIGUEZ, P. For Sale: Your Data: By: You. In *Proc. Workshop on Hot Topics in Networks (HotNets)* (2011).

[94] RODRIGUEZ, P., CHAKRAVORTY, R., CHESTERFIELD, J., PRATT, I., AND BANERJEE, S. MAR: A Commuter Router Infrastructure for the Mobile Internet. In *Proc. ACM MobiSys* (2004).

[95] SCHUBERT, S., UYEDA, F., VASIC, N., CHERUKURI, N., AND KOSTIC, D. Bandwidth Adaptation in Streaming Overlays. In *Proc. International Conference on Communication Systems and NetworkS (COMSNETS)* (2010).

[96] SCHULMAN, A., NAVDA, V., RAMJEE, R., SPRING, N., DESHPANDE, P., GRUNEWALD, C., JAIN, K., AND PADMANABHAN, V. Bartendr: A Practical Approach to Energy-Aware Cellular Data Scheduling. In *Proc. ACM MOBICOM* (2010).

[97] SCHULZRINNE, H. RTP: A Transport Protocol for Real-Time Applications. *IETF, Request For Comments 3550* (2003).

[98] SEN, S., MADABHUSHI, N., AND BANERJEE, S. Scalable WiFi Media Delivery through Adaptive Broadcasts. In *Proc. USENIX NSDI* (2010).

[99] SEN, S., SPATSCHECK, O., AND WANG, D. Accurate, Scalable In-Network Identification of P2P Traffic Using Application Signatures. In *Proc. International Conference on World Wide Web (WWW)* (2004).

[100] SHAIKH, A., TEWARI, R., AND AGRAWAL, M. On the Effectiveness of DNS-based Server Selection. In *Proc. IEEE INFOCOM* (2001).

[101] SONG, L., DESHPANDE, U., KOZAT, U., KOTZ, D., AND JAIN, R. Predictability of WLAN Mobility and Its Effects on Bandwidth Provisioning. In *Proc. IEEE INFOCOM* (2006).

[102] SPRING, N., MAHAJAN, R., AND WETHERALL, D. Measuring ISP Topologies with Rocketfuel. In *Proc. ACM SIGCOMM* (2002).

[103] SPRING, N., WETHERALL, D., AND ANDERSON, T. Reverse-Engineering the Internet. In *Proc. Workshop on Hot Topics in Networks (HotNets)* (2002).

[104] SRIDHARAN, A., SUBBARAMAN, R., AND GUERIN, R. Distributed Uplink Scheduling in CDMA Networks. In *Proc. IFIP NETWORKING* (2007).

[105] SUBRAMANIAN, L., AGARWAL, S., REXFORD, J., AND KATZ, R. H. Characterizing the Internet Hierarchy from Multiple Vantage Points. In *Proc. IEEE INFOCOM* (2002).

[106] TAN, P.-N., STEINBACH, M., AND KUMAR, V. *Introduction to Data Mining*. Addison-Wesley, 2006.

[107] TAN, W., LAM, F., AND LAU, W. An Empirical Study on 3G Network Capacity and Performance. In *Proc. IEEE INFOCOM* (2007).

[108] TRESTIAN, I., RANJAN, S., KUZMANOVIC, A., AND NUCCI, A. Measuring Serendipity: Connecting People, Locations And Interests In A Mobile 3G Network. In *Proc. ACM SIGCOMM IMC* (2009).

[109] TSO, F., TENG, J., JIA, W., AND XUAN, D. Mobility: A Double-Edged Sword for HSPA Networks: A Large-Scale Test on Hong Kong Mobile HSPA Networks. In *Proc. ACM MobiHoc* (2010).

[110] WANG, Z., QIAN, Z., XU, Q., MAO, Z., AND ZHANG, M. An Untold Story of Middleboxes in Cellular Networks. In *Proc. ACM SIGCOMM* (2011).

[111] WEI, X., GOMEZ, L., NEAMTIU, I., AND FALOUTSOS, M. ProfileDroid: Multi-Layer Profiling of Android Applications. In *Proc. ACM MOBICOM* (2012).

[112] WIKIPEDIA. High-Speed Downlink Packet Access. `http://en.wikipedia.org/wiki/High-Speed_Downlink_Packet_Access`.

[113] WIKIPEDIA. High-Speed Uplink Packet Access. `http://en.wikipedia.org/wiki/High-Speed_Uplink_Packet_Access`.

[114] WOERNDL, W., SCHUELLER, C., AND WOJTECH, R. A Hybrid Recommender System for Context-aware Recommendations of Mobile Applications. In *Proc. IEEE ICDE* (2007).

[115] WOLSKI, R., SPRING, N., AND PETERSON, C. Implementing A Performance Forecasting System for Metacomputing The Network Weather Service. In *Proc. International Conference for High Performance Computing, Networking, Storage and Analysis (SC)* (1997).

[116] WONDRACEK, G., COMPARETTI, P., KRUEGEL, C., KIRDA, E., AND ANNA, S. Automatic Network Protocol Analysis. In *Proc. ISOC NDSS* (2008).

[117] WONG, B., STOYANOV, I., AND SIRER., E. G. Octant: A Comprehensive Framework for the Geolocalization of Internet Hosts. In *Proc. USENIX NSDI* (2007).

[118] XU, Q., ANDREWS, T., LIAO, Y., MISKOVIC, S., MAO, Z. M., BALDI, M., AND NUCCI, A. FLOWR: A Self-Learning System for Classification of Mobile App Traffic. In *Submission*.

[119] XU, Q., GERBER, A., MAO, Z. M., AND PANG, J. AccuLoc: Practical Localization of Peformance Measurement in 3G Networks. In *Proc. ACM MobiSys* (2011).

[120] XU, Q., HUANG, J., WANG, Z., QIAN, F., GERBER, A., AND MAO, Z. M. Cellular Data Network Infrastructure Characterization and Implication on Mobile Content Placement. In *Proc. ACM SIGMETRICS* (2011).

[121] XU, Q., MEHROTRA, S., MAO, Z. M., AND LI, J. PROTEUS: Network Performance Forecast for Real-Time, Interactive Mobile Applications. In *Proc. ACM MobiSys* (2013).

[122] XU, Q., PANG, E., GERBER, A., MAO, Z. M., PANG, J., AND VENKATARAMAN, S. Identify Diverse Usage Behaviors of Smartphone Apps. In *Proc. ACM SIGCOMM IMC* (2011).

[123] YAN, B., AND CHEN, G. AppJoy: Personalized Mobile Application Discovery. In *Proc. ACM MobiSys* (2011).

[124] ZHANG, L., TIWANA, B., QIAN, Z., WANG, Z., DICK, R. P., MAO, Z. M., AND YANG, L. Accurate Online Power Estimation and Automatic Battery Behavior Based Power Model Generation for Smartphones. In *Proc. International Conference on Hardware/Software Codesign and System Synthesis (CODES+ISSS)* (2010).

[125] ZHANG, M., ZHANG, C., PAI, V., PETERSON, L., AND WANG, R. PlanetSeer: Internet Path Failure Monitoring and Characterization in Wide-Area Services. In *Proc. USENIX OSDI* (2004).

[126] ZHUANG, Z., CHANG, T., SIVAKUMAR, R., AND VELAYUTHAM, A. A3: Application-Aware Acceleration for Wireless Data Networks. In *Proc. ACM MOBICOM* (2006).